

# UNIVERSITY OF LONDON THESIS

Degree PhD Year 2007 Name of Author THOMPSON, Hannah

# Development of the vertebrate visual system- the role of Slit and Robo and signalling from the lens

Hannah Thompson, B.Sc.

Supervisor; Dr. L.Erskine

**Submitted for the degree of Doctor of Philosophy, 2007**

Institute of Ophthalmology

University College London





ProQuest LLC
789 East Eisenhower Parkway
P.O. Box 1346
Ann Arbor, MI 48106-1346

## Abstract

Previous studies have shown that Slit and Robo proteins are key regulators of axon guidance at the developing optic chiasm. In addition to their expression around the chiasm *slit1* and *slit2* mRNAs are also expressed in the retina and along the border of the optic tract. *Robo2* mRNA expression has also been shown in the RGC layer in the retina suggesting these proteins may mediate RGC axon pathfinding in these regions. To investigate this I used immunohistochemistry and DiI-labelling during various stages in embryonic development to observe the RGC axons through the optic pathway.

Using this approach, I found that Slit1-2 and Robo2 are needed to direct correct pathfinding of RGC axons through the optic tract. In their absence, RGC axons project ectopically into the telencephalon and epithalamus and cross the dorsal midline. In the retina, I found roles for Slit1-2 and Robo2 in restricting RGC axons to the OFL and in directing the initial projection of axons away from the peripheral retina. These defects were region specific, occurring in different halves of the retina. I further examined the role of the lens, as a source of Slit2, in inhibiting RGC axon growth into the peripheral retina.

To study signalling from the lens further, I switched to chick as a model system which would enable in ovo manipulations and observations. This led to a study trying to elucidate signals from the lens that could influence coordinated growth of the retina and eye. In the absence of the lens, growth of the eye is dramatically reduced and the retina appears extensively folded. I have examined the expression of a range of molecules in the lens and looked further at the role of FGFs in regulating the coordinated growth of the eye and retina.

# Table of Contents

# List of Figures

# List of Tables

## Declaration

I declare that this thesis, submitted for the degree of Doctor of Philosophy, is of my own composition, and the data presented is my own original work, unless otherwise stated.

Hannah Thompson, B.Sc.

## Acknowledgements

There are so many people I need to thank for their help throughout my PhD and writing my thesis. Firstly Lynda, she encouraged me to start a PhD when I was contently passing away time as a research assistant pondering the best time to give up a salary and become a student again. She has been a great PhD supervisor and colleague, and I will really miss having her around in London. I would then like to thank Prof. Glen Jeffery, Dr. Christiana Ruhrberg, Dr. Quenten Schwarz, Prof. Ivor Mason, Dr. Mayan Semo, Bennett Alakakone, Dr. Juliet Parry and Dr. Olivier Camand for their help and advice at all other times, and for trying to answer my random questions.

Big thanks to Anthony, Aida, Sheona and Dave for a great nine month PhD "holiday". Thanks to my students; Chris, Niketa, Umbreen and Camila for doing the boring experiments and giving me the chance to practise supervising.

I would like to thank my friends and family for hopefully still being friends with me after I have ignored them for almost a year. I am looking forward to seeing your new houses (Dan, Claire, Jon, Paul, Mark, Dicky and Jayne) discussing weddings (Clare, Mark, Chris, Sian, Mark and M-C), and celebrating down the pub (everyone). I have a lot of catching up to do. Important thanks to Mum and Dad, who first explained to me what Philosophiae Doctor actually means.

Finally, the biggest thanks and love to my new husband Dan. He has been so supportive during the past three years, especially during the last year, where he cleverly planned the best way to keep my spirits up. Also, thanks for the teas, apple juices, snacks, wine, beer, jumpers and wheatbags and for doing all the cooking and cleaning. I don't think my housewife skills can really make it up to you.

## Abbreviations

| | |
|---|---|
| BCIP | 5-Bromo-4-chloro-3-indolyl phosphate |
| BMP | Bone morphogenic protein |
| CAM | Cell adhesion molecule |
| CSPG | Chondrotin sulphate proteoglycan |
| CXCR | Chemokine (CXC motif) receptor |
| DCC | Deleted in colorectal cancer |
| DiI | 1,1'-dioctadecyl-3,3,3',3'-tetramethylindocarbocyanine perchlorate |
| DMSO | Dimethyl sulphoxide |
| dTh | Dorsal thalamus |
| E(n) | Embryonic day n |
| ECM | Extracellular matrix |
| FGF | Fibroblast growth factor |
| FGFR | Fibroblast growth factor receptor |
| HSPG | Heparan sulphate proteoglycan |
| LGN | Lateral geniculate nucleus |
| MO | Morpholino |
| MTN | Medial terminal nucleus |
| NBL | Neuroblastic layer |

| | |
|---|---|
| NBT | Nitroblue tetrazolium |
| Nrp | Neuropillin |
| OFL | Optic fibre layer |
| P(n) | Post natal day n |
| PBS | Phosphate- buffered saline |
| PCR | Polymerase chain reaction |
| PFA | Paraformaldehyde |
| RGC | Retinal ganglion cell |
| RGCL | Retinal ganglion cell layer |
| RPE | Retinal pigment epithelium |
| SC | Superior colliculus |
| SCN | Suprachiasmatic nucleus |
| SDF | Stromal derived factor |
| Shh | Sonic hedgehog |
| TBS | Tris- buffered saline |
| WT | Wildtype |

# 1 Introduction

## 1.1 The developing visual system

### *1.1.1 Formation of the eye*

The eye is formed from bilateral outgrowths of the diencephalon called optic vesicles, which extend towards the overlying surface ectoderm (Figure 1.1A). Close contact between the ectoderm and the optic vesicles results in induction of a lens placode, seen as a thickening of the surface ectoderm (Figure 1.1B, Figure 1.2A). The lens placode then rounds up to form the lens vesicle which pinches off the surface ectoderm to be incorporated into the eye (Figure 1.1C, Figure 1.2B-D). The inner layer of the optic cup (closest to the lens) becomes the sensory neural retina, while the outer layer gives rise to the retinal pigment epithelium (RPE), and the tube leading from the brain to the eyecup, the optic stalk, later carries the optic nerve (Figure 1.1D). At the ventral-most side of the optic vesicle, the process of invagination forms a groove, the choroidal (or ventral) fissure which will eventually fuse (Figure 1.1E) (Reviewed by Chow and Lang, 2001).

At the point when the lens pit closes off from the surface ectoderm, the posterior cells closest to the presumptive retina begin to thicken as lens fiber cells differentiate, producing polarity within the lens (Figure 1.2C, D). Differentiation of the lens is characterised by fiber cell-specific crystallin expression: $\alpha$, $\beta$ and $\gamma$ - crystallins. The anterior-most cells form a monolayer of proliferating epithelial cells which overlie the terminally differentiated fiber cell mass (Figure 1.2E). Secondary lens fiber cells originate from the equatorial region of the lens in a process that continues throughout adulthood. This is followed by degradation of the organelles including the nucleus and mitochondria, which is essential for the production of a transparent lens (Reviewed by Chow and Lang, 2001).

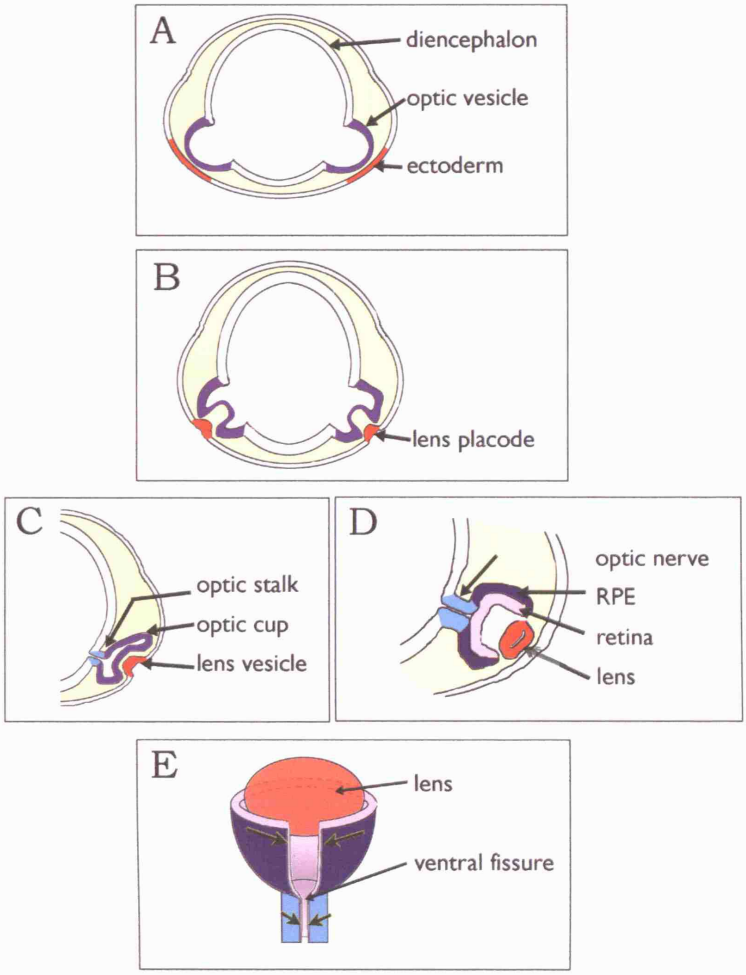


**Figure 1.1- Schematic representing the development of the eyes.**

(A) The diencephalon evaginates bilatateralerally. (B) Formation of the lens placode (red). (C) Formation of the optic cup (purple), optic stalk (blue) and lens vesicle (red). (D) A bi-layered structure is formed composed of the RPE (purple) and neural retina (pink). (E) The ventral fissure is a groove formed by the invagination of the optic cup, the edges grow towards each other. RPE, retinal pigment epithelium.

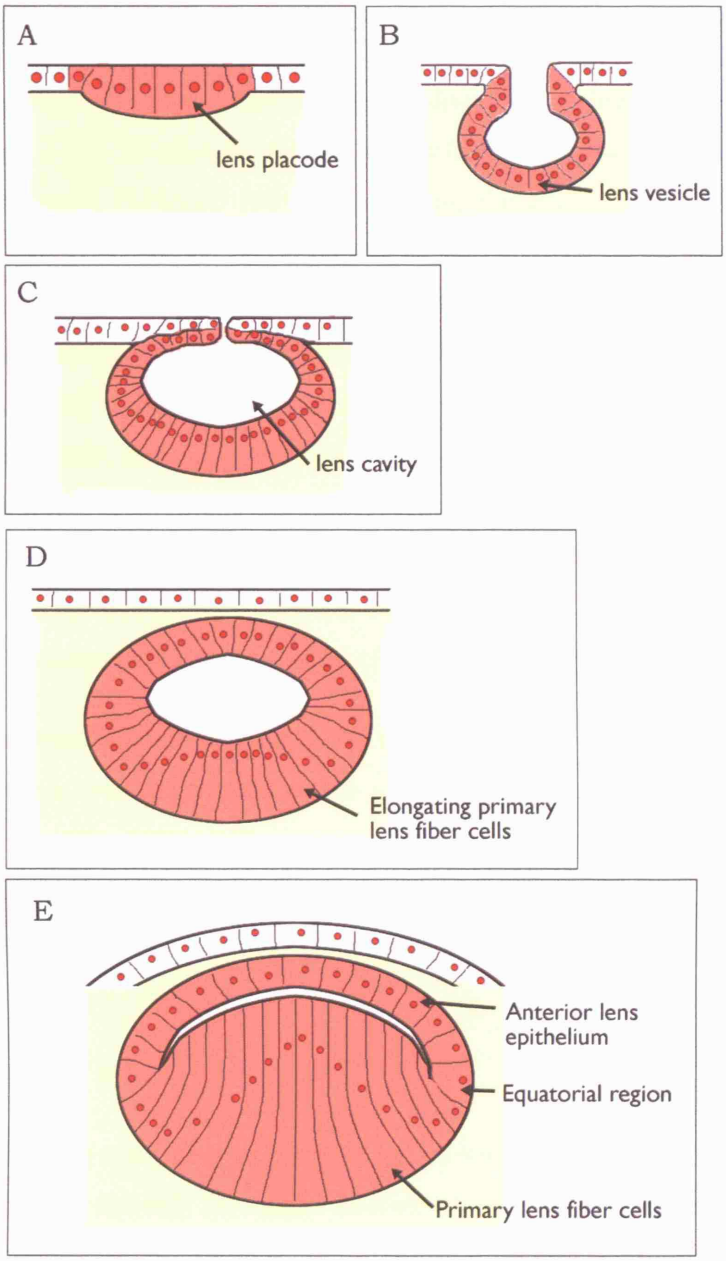


**Figure 1.2- Schematic representing the development of the lens.**

(A) The lens placode is a thickening of the ectoderm. (B, C) Invagination forms the lens vesicle. (D) The lens vesicle pinches off. (E) The primary lens fiber cells elongate.

### *1.1.2 Development of the retina*

In the mouse, the cells of the retina undergoing division are almost all located at the outer surface of the developing retina, the surface analogous to the ventricular surface of the brain (Sidman, 1961). Once born, the cells migrate to their final destination within the retina, with those at the inner surface of the retina forming first; the retinal ganglion cells (RGCs) and amacrine cells (Drager, 1985). In addition to the gradient of lamina formation seen in development, there is a central-to-peripheral gradient, with the cells located within the central retina, close to the developing optic disc, forming first (Figure 1.3A, B)(Sidman, 1961). The structure of the immature retina consists of three major layers; the OFL, the RGC layer and the neuroblastic layer where cells of the neuroepithelium are still in the cell cycle (Figure 1.3C). As development proceeds, further cells differentiate into layers forming the multilayered structure of the mature retina (Figure 1.3D)(Polyak, 1957).

After reaching their final destination in the retina, the RGCs then extend their axons towards the inner (vitreal) surface of the retina. Here they grow along the vitreal endfeet of surrounding neuroepithelial cells and later fasciculate with other axons to form the optic fibre layer (OFL) (Silver and Sidman, 1980). The growth of all RGC axons is in organised straight bundles projecting towards the centre of the retina, where they exit the eye via the optic disc.

### *1.1.3 Eye to optic tract*

RGC axons exit the eye and enter the optic nerve, here the axons project as a tightly fasciculated bundle towards the ventral midline of the diencephalon. At the chiasm, the axons diverge into the ipsilateral or contralateral optic tracts. Crossing of the axons into ipsilateral and contralateral optic tracts allows the appropriate bilateral connections that underlie normal binocular vision. Different animal species have varying degrees of crossed and uncrossed axons: in mice, the majority of axons (97%) cross at the chiasm; in humans, only 60% of axons cross at the chiasm; however in birds and fish all axons cross and they have no ipsilateral projection. In

humans those RGC axons which enter the ipsilateral optic tract are from RGCs found in the temporal retina, in mice the cells are restricted to the ventral-temporal part of the retina (Drager, 1985).

### *1.1.4 The optic tract*

Axons enter the optic tracts and project to their primary targets, the lateral geniculate nucleus (LGN) located in the diencephalon and superior colliculus (SC) (known as the tectum in fish and birds) in the midbrain (Figure 1.4). En route to the SC, a small proportion of axons branch away from the tract to innervate other targets such as the suprachiasmatic nucleus (SCN) in the hypothalamus, and the medial terminal nucleus (MTN) in the midbrain. As the axons extend through the diencephalon they grow adjacent to, but do not invade the telencephalon. They also display region-specific differences in their patterns of fasciculation. During their growth over the hypothalamus, they extend as a tightly fasciculated bundle, within the dorsal thalamus the axons defasciculate and spread out and into the thalamic tissue. At a later stage in development, a subset of RGC axons extends collateral branches to innervate relay neurons of the lateral geniculate nucleus (LGN). Leaving the dorsal thalamus, the axons then refasciculate and turn posteriorly away from the epithalamus, projecting again as a tight bundle as they approach the superior colliculus. In vitro, the hypothalamus and epithalamus, but not the dorsal thalamus, inhibit retinal axon outgrowth suggesting this pattern of fasciculation is due to the restricted expression within the diencephalon of inhibitory guidance molecules (Tuttle et al., 1998). Little is known of the molecular nature of these signals. This fact will be addressed later.

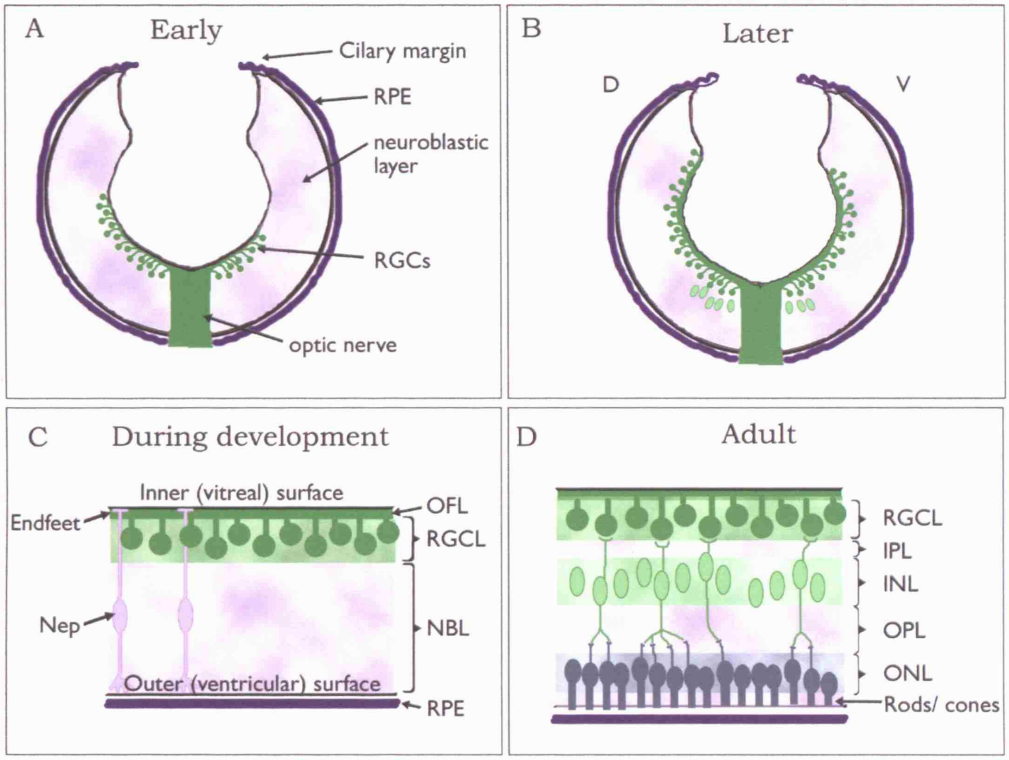


**Figure 1.3- Schematic representing the development of the retina.**

(A-B) Whole retina images. (A) Early in retinal development, the first retinal ganglion cells are born within the central retina, (B), later in retinal development, retinal ganglion cells are born in more peripheral locations. (C-D) Cross-sections of retina. (C) Early in development the retina is composed of three layers, the OFL (optic fibre layer), the RGCL (retinal ganglion cell layer), and the NBL (neuroblastic layer). Neuroepithelial cells (Nep) extend across the retina with their endfeet at the vitreal surface. (D) The adult retina is composed of many layers, the RGCL, the IPL (inner plexiform layer), the INL (inner nuclear layer) composed of amacrine cell, displaced RGCs, bipolar and horizontal cells, the OPL (outer plexiform layer), the ONL (outer nuclear layer) composed of the cell bodies of the photoreceptor cells and the photoreceptor segment layer composed of the outer segments of the rods and cones.

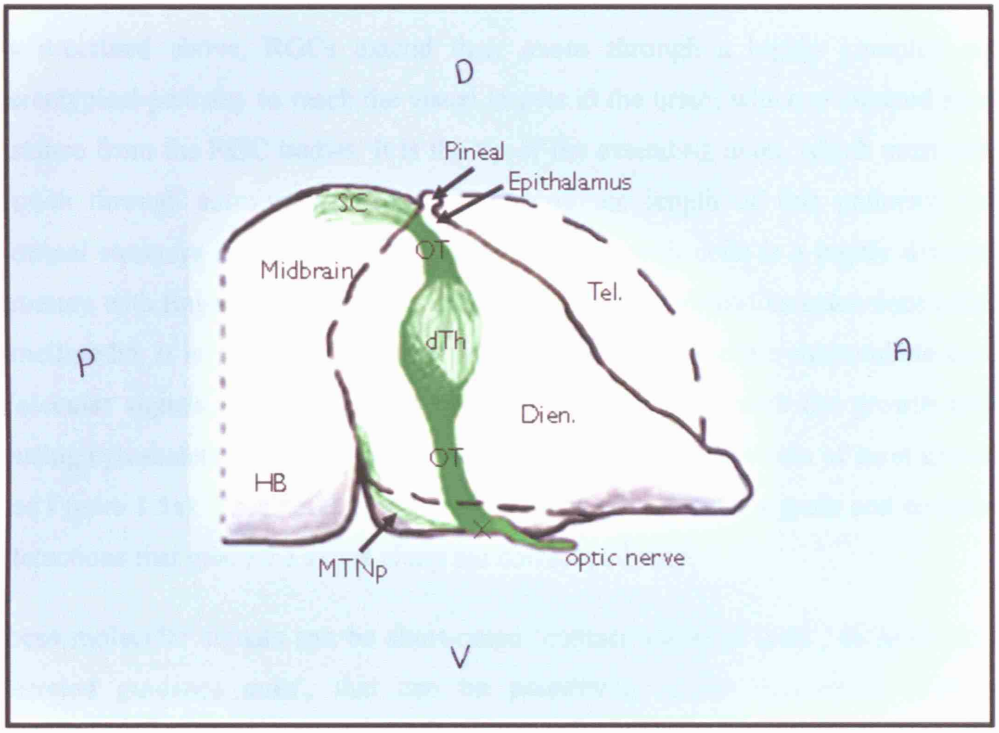


**Figure 1.4- Schematic representing the path of the optic tract.**

Diagram of a mouse brain viewed laterally after removal of the telencephalon. RGC axons cross to the contralateral side of the brain at the chiasm on the ventral midline. They then join the optic tract and project dorsally as a tight bundle of fibres, until they reach the dorsal thalamus (dTh) where they defasciculate over the surface. Exiting the dorsal thalamus they refasciculate and project posteriorly into the superior colliculus (SC). Epi., epithalamus; Tel., telencephalon; OT, optic tract; HB, hind brain; Dien., diencephalon; X, chiasm; MTNp, medial terminal nucleus projection.

## 1.2 Axon guidance

As described above, RGCs extend their axons through a highly complex and stereotypical pathway to reach the visual targets in the brain, which are situated some distance from the RGC bodies. It is the tip of the extending axon, which must steer growth through surrounding tissues and along the length of this pathway; this terminal structure is called a growth cone. The growth cone is a highly dynamic structure with finger-like projections called filopodia and sheet-like extensions called lamellipodia; it is composed of actin filaments extending from a microtubule core. Molecular signals along the length of the pathway interact with the growth cone causing cytoskeletal rearrangements, which can change the direction of axon growth (see Figure 1.5a). These events rely on a number of molecular signals and complex interactions that guide the axons along the correct pathway.

These molecular signals can be short-range 'contact guidance cues', or long-range 'secreted guidance cues', that can be permissive or non-permissive to axon extension, and can either attract or repel growth cones (see Figure 1.5b).

### *1.2.1 Short-range, contact guidance molecules*

The first axon guidance molecules to be discovered were short-range 'contact guidance cues'; these include extracellular matrix (ECM) molecules, cell adhesion molecules and Ephrins. Growth cones can interact with molecules of the extracellular matrix such as laminin and fibronectin via the cell surface receptor integrin (Hall et al., 1987) and have been shown to affect axon extension *in vitro* (Baron-Van Evercooren et al., 1982; Hall et al., 1987). Laminin is thought to have a role in guiding RGC axons along the optic pathway, as it is only expressed in this region at a time when axons are extending along it (Cohen et al., 1987). Other extracellular matrix molecules that have been shown to have a role in axon guidance are the proteoglycans (Bovolenta and Fernaud-Espinosa, 2000). Chrondroitin sulphate proteoglycans (CSPGs) and heparin sulphate proteoglycans (HSPGs) have been

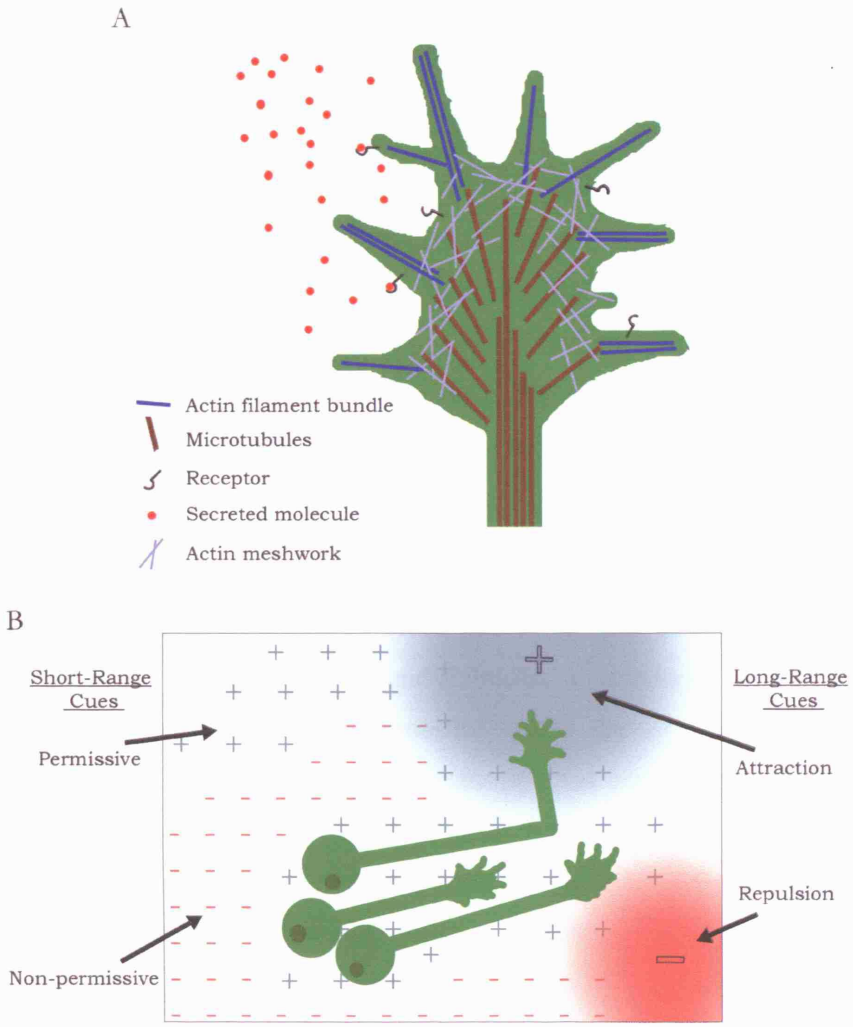


**Figure 1.5- Summary diagram showing the growth cone structure and types of axon guidance cues.**

(A) The growth cone is composed of a microtubule core (brown) and actin filaments (blue) extending into filopodia, or as a mesh in the lamellipodia. The growth cone displays receptors for axon guidance molecules (red). (B) The growth cone receives a mixture of signals, either short-range or long-range that can attract (blue) or repel (red) growth cones and/or are permissive or non-permissive to outgrowth. The growth cone can respond by turning away or towards these signals.

shown to influence RGC axon guidance (Brittis et al., 1992; Brittis and Silver, 1995; Pratt et al., 2006), however, whether this is by altering the distribution of guidance ligands (Johnson et al., 2004; Steigemann et al., 2004) or a direct effect on the axon is not known.

Surrounding cells, axons and growth cones can also express molecules which influence axon guidance and extension, including the cell adhesion molecules N-CAM, L1-CAM and cadherin which bind together via homophilic interactions. It is thought that these molecules are important for axons to grow together as bundles, as disruption results in axon defasciculation which can lead to misprojection (Pollerberg and Beck-Sickinger, 1993; Brittis et al., 1995).

The most well known group of short-range guidance molecule are the large family of membrane-bound proteins the Ephrins (reviewed by O'Leary et al., 1999). There are two types of Ephrin ligands; EphrinAs and EphrinBs. EphrinAs are bound to the cell membrane by a glycosylphosphatidylinositol (GPI) anchor and bind to EphA receptors. EphrinBs have a transmembrane domain and bind EphB tyrosine kinase receptors. They have a well known role in RGC axon guidance: Ephrins and Eph-receptors are expressed in gradients across the tectum (SC) and retina respectively and have been shown to be involved in patterning the precise retinotectal topographic map (Figure 1.6). Interestingly, evidence demonstrates that Ephrin-Eph interactions can involve bi-directional signalling (Holland et al., 1996; Rashid et al., 2005), with the receptor acting as a ligand and vice-versa.

### *1.2.2 Long-range, secreted guidance molecules*

The three classical secreted guidance molecules and their receptor were characterised in the 1990s, and are well conserved across species; these include, Netrin/DCC, Slit/Robo and Semaphorin/Plexin/Neuropilin. The ligands from each family are attractants or repellents, depending on the type of axon population being affected and the context the growth cone is found. Netrin1 (unc-6 in *Caenorhabditis elegans*) and its receptor Deleted in Colorectal Cancer (DCC/Unc-40) are best known for their role

in attracting commissural axons from the dorsal spinal cord towards the floor plate at the ventral midline (Kennedy et al., 1994; Serafini et al., 1994; Keino-Masu et al., 1996). However, they have also been shown to have a role in guiding RGC axons at specific points along the optic pathway (Deiner et al., 1997; Deiner and Sretavan, 1999). Interestingly, Netrin1 can act as an attractant through its receptor DCC (Keino-Masu et al., 1996), and also as a repellent through another Netrin receptor; Unc-5 (Colamarino and Tessier-Lavigne, 1995; Leonardo et al., 1997).

Slits and their receptors Roundabout (Robo) were first discovered in mutagenesis studies looking for axon guidance molecules in the ventral nerve cord of *Drosophila melanogaster* (Rothberg et al., 1990; Seeger et al., 1993). Slit is secreted from midline glia and repels axons expressing Robo (Kidd et al., 1999). The roles of these molecules are looked at in more detail later.

Semaphorins, original known as Collapsin in chick (Luo et al., 1993), are a large family of membrane-bound and secreted molecules. Of the eight classes of Semaphorins, it is the class-three secreted Semaphorins (Sema3A-G) which are the most studied as axon guidance molecules. Semaphorins have been shown to induce collapse of growth cones ( Fan and Raper , 1995) and drive the growth cone to turn away from a graded source *in vitro* (Fan and Raper, 1995). The receptors for Semaphorins are the Plexins and Neuropilins (Chen et al., 1997; He and Tessier-Lavigne, 1997; Tamagnone et al., 1999). A number of class three Semaphorins have been shown to have a role in RGC axons guidance (Campbell et al., 2001; Steinbach et al., 2002; Liu et al., 2004).

Growth factors have been implicated in axon guidance for a long time. For example, *in vitro* a gradient of brain-derived trophic factor (BDNF) or neurotrophin 3 (NT-3) attracts the growth cone of *Xenopus* spinal neurons (Song et al., 1997). However, whether these are true axon guidance molecules or are just acting as growth factors is unclear. It may depend on what defines an axon guidance molecule.

In the last decade, molecules that were traditionally thought of as morphogens have also been shown to have a role in axon guidance, these include; Bone-morphogenic

proteins (Bmps), Sonic hedgehog (Shh), Wnts and Fibroblast growth factors (FGFs). Confirming these molecules are not just patterning tissues has been important in proving their role in acting directly as axon guidance molecules. Shh and FGFs have been shown to act as attractants to commissural axons (Charron et al., 2003) and trochlear motor axons (Irving et al., 2002) respectively, and as repellents to RGC axons (Trousse et al., 2001; Webber et al., 2003), showing a direct role for these molecules as secreted axon guidance cues. A role in regulating commissural axon guidance has been shown for Bmps and Wnts: Bmp7 and a related molecule, Growth differentiating factor 7 (Gdf7), are the candidate molecules for the roof plate repellent of commissural axons (Augsburger et al., 1999). Wnt5 has been shown to repel commissural axons (Yoshikawa et al., 2003), while Wnt4 acts as an attractant to post-crossing commissural axons (Lyuksyutova et al., 2003). A role for Wnt3 in topographic mapping has been shown in chick, where a decreasing medial-lateral (dorsal-ventral) gradient is present in the tectum (Schmitt et al., 2006). Wnt3 repels RGC axons expressing the repulsive Wnt receptor Ryk, which is expressed in a decreasing ventral-dorsal gradient in the retina (Schmitt et al., 2006) (Figure 1.6).

### *1.2.3 Cytoplasmic signal transduction*

How axon guidance molecules directly affect growth cone collapse, extension or turning has been the focus of much study in the last 20 years. Binding of a ligand to the cell surface receptor is thought to induce an intracellular signalling cascade resulting in cytoskeletal rearrangements. A role for the cyclic nucleotide, cAMP as a possible second messenger in this signalling cascade, to mediate growth cone turning, was first shown by Lohof and colleagues (1992). Growth cones of *Xenopus* neural tube explants turned towards a source of dB-cAMP (membrane permeable-cAMP) but not dB-cGMP (Lohof et al., 1992). Later it was shown that Netrin1- or BDNF- induced attraction and Semaphorin- induced repulsion involve cAMP (Ming et al., 1997; Song et al., 1997; Song et al., 1998), strongly linking this molecule to the process of growth cone turning.

In addition to asymmetric distribution of cAMP, the intracellular mediator $Ca^{2+}$ has been shown to be important in mediating the turning response. When extracellular calcium levels are reduced to lower than normal levels, no growth cone turning is seen in response to the attractive cues Netrin1 and BDNF (Ming et al., 1997; Song et al., 1997). It is a calcium influx through the plasma membrane calcium channels and calcium release from internal stores that is required for Netrin1-induced attraction (Hong et al., 2000). Additionally, localised increases in intracellular calcium on one side of the growth cone by focal laser-induced photolysis (FLIP) induces turning to the side of the growth cone with elevated calcium (Zheng, 2000). This highlights the requirement for changes to cytoplasmic calcium levels for the growth cone turning response.

The Rho family of small GTPases, including Rho, Rac and Cdc42 are thought to play a role in axon guidance by regulating cytoskeletal rearrangements (Hall, 1998). Specifically, Cdc42 and Rac have been shown to be involved in the production of filopodia and/or lamellipodia, while RhoA causes growth cone collapse (Kozma et al., 1997). It is thought that signalling molecules binding to their cell-surface receptors, cause activation of these molecules resulting in cytoskeletal rearrangements and growth cone turning. Direct evidence for this has been shown in *Drosophila* with the Semaphorin receptor Plexin B, which inhibits Rac and enhances RhoA signalling (Hu et al., 2001).

More recently, a role for local protein synthesis in regulating axon guidance responses to Netrin1, Sema3A and Slit has also been shown in *Xenopus* retinal axons (Campbell and Holt, 2001; Piper et al., 2006). Rapid local changes in protein levels within the growth cone, when isolated from their cell bodies, has been shown in response to signalling molecules and is required for growth cone turning. One of the proteins shown to be synthesised in this way is β-actin, which becomes asymmetrically localised following exposure of the growth cone to a signalling gradient (Leung et al., 2006; Yao et al., 2006).

### *1.2.4 Attraction or repulsion? Combining axon guidance signals*

The reaction of a particular growth cone to a guidance molecule can be attractive or repulsive depending on the level of cyclic nucleotides within the growth cone. Combinations of secreted and short-range molecules change the levels of cyclic nucleotides and therefore modulate the growth cone response. For example, the repulsive effect of Sema3 on *Xenopus* spinal neurons in culture can be converted to an attractive response following activation of the cGMP pathway (Song et al., 1998). Additionally, attraction of retinal axons towards a source of Netrin1 is converted to repulsion when the axons were grown in the presence of laminin1 (Hopker et al., 1999), or a membrane-permeable competitive analogue of cAMP (Ming et al., 1997). The chemokine stromal cell-derived factor1 (SDF1) has been shown to attenuate the repellent activities of Slit2 on cultured RGC axons, of Sema3A on DRG axons and of Sema3C on sympathetic axons. This modulation functions by elevating cAMP levels in the growth cone via the chemokine (CXC motif) receptor 4 (CXCR4) (Chalasani et al., 2003). Another level of modulation is seen externally, when Netrin1 stimulation of rat embryonic dorsal spinal cord explant axon outgrowth is potentiated by IC-3. IC-3 is a metalloproteinase inhibitor, which also blocked shedding of DCC ectodomains. The metalloproteinases in culture are prevented from cleaving the ectodomains of DCC increasing the number of functional receptors and therefore enhancing outgrowth (Galko and Tessier-Lavigne, 2000). It is thought *in vivo* metalloproteinases would function to modulate axon guidance possibly by terminating ligand/receptor interactions (McFarlane, 2003). Furthermore, there is a hierarchy seen within signalling system, for example, in *Xenopus*, activation of Robo silences the attractive effect of Netrin1 by interaction of the cytoplasmic domains of Robo and DCC (Stein and Tessier-Lavigne, 2001). This suggests it is an integration of signalling molecules acting on the growth cone that allows an axon to continue growing along its correct pathway, passing through a changing extracellular environment. It may also explain why axons are not halted at a source of attractive signals but can move away from them and continue growing.

### *1.2.5 Transcription factors and axon guidance*

To date, research has focused on the extracellular cues, their receptors and the intracellular mechanisms which are involved in controlling axon guidance. However, the signals needed to specify how a particular neuron will respond to axon guidance cues are only more recently being elucidated. Transcription factors regulate which molecules are present on the growth cones and therefore, specify its specific response to the extracellular cues.

An example of how transcription factors may influence axon guidance can be seen in the regulation of the ipsilateral projection in formation of the optic chiasm. The decision to cross to the contralateral optic tract or remain on the ipsilateral side of the brain has been shown to involve Eph-Ephrin interactions. The EphrinB ligands are expressed by midline glia at the chiasm and EphB receptors are expressed by RGCs in the ventral-temporal (VT) retina. These molecules inhibit subsets of axons from crossing the midline and when absent the ipsilateral projection is lost (Nakagawa et al., 2000; Williams et al., 2003). Two transcription factors have been suggested as regulators of *ephB* expression, *zic2* (Herrera et al., 2003) and *foxd1* (Herrera et al., 2004). Both these factors are expressed in the VT retina by those RGCs which project ipsilaterally, and when their expression is reduced or absent in knockout mice a reduction is seen in the number of axons projecting to the ipsilateral side of the brain (Herrera et al., 2003; Herrera et al., 2004). Another level of transcriptional regulation has been shown to involve the transcription factor *islet-2*, which is expressed in RGC that only project contralaterally and is thought to restrict *zic2* and *ephB1* to the subset of axons which project ipsilaterally at the optic chiasm (Pak et al., 2004). An example of how transcription factors regulate axon guidance in the optic tract is seen with *foxg1*. When expression of this molecule is lost in mice a subset of RGC axons are seen projecting ectopically into the ventral telencephalon, a region normally expressing *foxg1* (Pratt et al., 2002). It is possible that *foxg1* regulates the expression of a RGC axon inhibitor, normally preventing extension of these axons into this region. Interestingly, thalamocortical axons which are normally able to project into this region, are excluded in *foxg1* mutants, suggesting this

transcription factor may not only regulate expression of inhibitory factors, but also attractive ones (Pratt et al., 2002). *Foxg1* has also been shown to regulate normal crossing of RGC axons at the chiasm, most likely due to expression at the chiasm which regulates the balance of factors controlling the decision to cross (Pratt et al., 2004). These are by no means the only examples of transcriptional control seen to regulate axon guidance. More recently, a novel role for transcription factors showing a direct role in axon guidance has been discovered: the transcription factor Engrailed2 (en2) acts as a diffusible signal attracting nasal RGC axons and repelling temporal RGC axons when applied exogenously *in vitro* (Brunet et al., 2005).

## 1.3 RGC axon guidance

Axon guidance of RGC axons in the visual system has mainly focused on retinotectal mapping in the midbrain. The organisation of RGCs in the retina is represented in the optic tectum/superior colliculus (SC), which can be simplified as the temporal-nasal axis of the retina onto the anterior-posterior axis in the midbrain targets, and the dorsal-ventral axis of the retina along the medial-lateral axis of the midbrain targets. This mapping was analysed first in the 1960s in the regenerating retinotectal system of goldfish and frogs; even if the eye was rotated 180°, the regenerating axons grew back to their usual destinations. The molecular basis of this mapping only began to be discovered in the 1990s, with the discovery of Ephs and Ephrins and their graded expression patterns in the retina and tectum/SC (Figure 1.6). The mapping of temporal-nasal axis of RGC axons along the anterior-posterior axis of the tectum involves EphrinA-EphA signalling, whereas mapping of the dorsal-ventral axis of RGC axons along the medial-lateral axis of the tectum involves EphrinB-EphB signalling and Wnt3/Ryk/Frz signalling (Reviewed by O'Leary et al., 1999; Zou and Lyuksyutova, 2007). Little is known about what other factors maybe controlling retinotectal mapping, but the transcription factor *vax2* may control expression of molecules involved with anterior lateral-medial patterning (Reviewed by McLaughlin and O'Leary, 2005). Other transcription factors thought to regulate the development of the retinotectal map include the genes *en1* and *en2*. The En

proteins are distributed in a high posterior low anterior gradient, and retroviral overexpression disrupted the topographic targeting (Gardner et al., 1988; Friedman and O'Leary, 1996). It is likely a number of other molecules involved with the retinotectal mapping have yet to be discovered.

Projecting along the optic nerve, the RGC axons extend in a highly fasciculated bundle; one molecule shown to influence this restriction is Semaphorin5A. Sema5A is expressed by neuroepithelium cells surrounding RGC axons in the optic nerve (Oster et al., 2003). If signalling by this molecule is disrupted, axons are able to stray away from the optic nerve suggesting its role is an inhibitory sheath surrounding the path of RGC axons through the optic nerve.

A number of guidance molecules involved in regulating chiasm formation are beginning to be revealed. Slit/Robo (Figure 1.7B) (Erskine et al., 2000; Niclou et al., 2000; Fricke et al., 2001; Plump et al., 2002), EphAs (Marcus et al., 2000), Netrin1/DCC (Figure 1.7C) (Deiner and Sretavan, 1999) and the extracellular matrix molecules; CSPGs (Figure 1.7D) (Chung et al., 2000a; Chung et al., 2000b) and HSPGs (Pratt et al., 2006) are all involved in restricting the position of axon crossing at the ventral midline. If any of these molecules are disrupted axons cross the midline in a more disorganised fashion spreading more anterior or posterior to the true chiasm, axons remain at the midline or misproject into the contralateral optic nerve. Slit/Robo signalling has been shown to channel RGC axons across the midline through an inhibitory corridor of expression (Erskine et al., 2000; Plump et al., 2002). This guidance may be modulated by differential sulfation of HSPG. Heparan sulphate sulfotransferase (hst) mutants lack enzymes which modify HSPGs and have axon guidance defects at the optic chiasm similar to *Slit1/2* -/-; expression of these molecules largely coincides with regions of *Slit* expression, suggesting they possibly function together at the chiasm (Pratt et al., 2006). Netrin1/DCC signalling is an attractant for commissural axons at the ventral midline in more caudal regions of the embryo (Kennedy et al., 1994; Serafini et al., 1994). However, Netrin1 is not expressed at the midline at the optic chiasm and does not appear to function as an attractant here, but does affect the trajectory of RGC axons as they cross the midline

(Deiner and Sretavan, 1999). The control of which axons cross the midline however appears to be controlled by a number of other molecules. For example, EphrinB2 is expressed by radial glia at the ventral midline in the region of the optic chiasm and is inhibitory to EphB1 expressing RGC axons preventing them from crossing the midline. EphB1 is only expressed by RGCs in the ventrotemporal retina, a region of the retina that gives rise to the ipsilateral projection (Williams et al., 2003).

Less is known about axon guidance in the optic tract and retina, this will be the focus of chapter 3 and 4, and therefore will be discussed later.

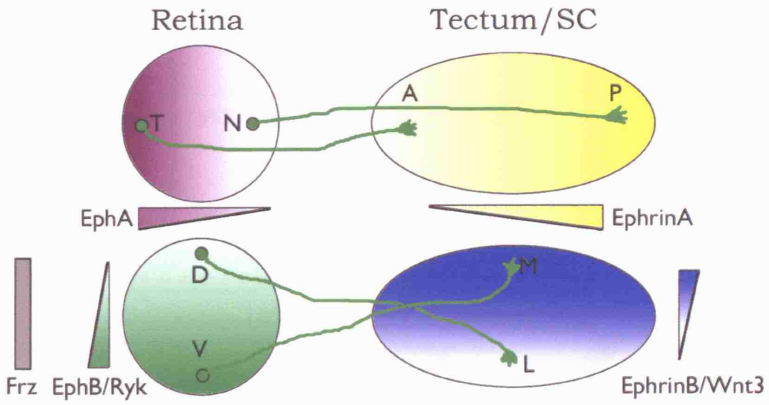


**Figure 1.6- Retinotectal mapping of RGC axons require gradients of receptors in the retina and their ligands in the tectum/SC.**

Axons from the temporal (T) retina express high levels of the EphA receptor (purple) and project to the anterior (A) regions of the tectum/SC. Whereas, axons from the nasal (N) retina project to the posterior (P) regions of the tectum/ SC which expresses high levels of the inhibitory molecule EphrinA (yellow). Axons from the ventral (V) retina express high levels of the EphB receptor and Ryk receptor (green) and are attracted to high levels of EphrinB (blue) in the medial (M) regions of the tectum/SC. Axons from the dorsal (D) retina express low levels of Ryk receptor (green) and the Frizzled receptor (grey) and are attracted to low levels of Wnt3 (blue) in the lateral (L) regions of the tectum/SC.

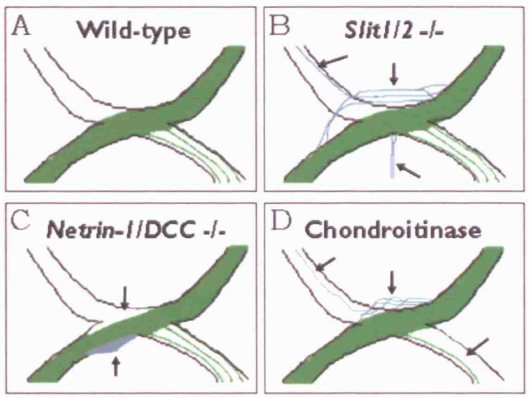


**Figure 1.7- Diagrammatic examples of axon guidance defects at the optic chiasm.**

A-D, looking at ventral view of chiasm, showing RGC axons (green) from the left eye and ectopic RGC projections (blue). A, wild-type. B, ectopic projections in *slit1/2 -/-* mice (Plump et al., 2002). C, chiasm shape is affected in netrin-1 or DCC- deficient mice (Deiner and Sretavan, 1999). D, ectopic projections following treatment with chondroitinase ABC (Chung et al., 2000b)

## 1.4 Slit and robo

*Slit* and *robo* (*roundabout*) were initially identified through genetic studies in *Drosophila* in the search for mutants with commissural axon guidance defects. In these *robo* mutants, ipsilateral and commissural axons cross and re-cross the midline (Seeger et al., 1993; Kidd et al., 1998b). Mutations in the *Drosophila* Slit gene (*sli*) result in collapse of all nerve cord axons into the midline. This was thought originally to be caused by a defect in the development of the midline glia, and not linked to Robo (Rothberg et al., 1988; Rothberg et al., 1990). However later, Slit was characterised and found to be a secreted midline repellent for CNS axons and the ligand for Robo, in *Drosophila* and in vertebrates. (Brose et al., 1999; Kidd et al., 1999; Li et al., 1999). Since their discovery, two further *robo* genes have been found in *Drosophila*; *robo2* and *robo3,* but no further *Drosophila slit* genes. The *robo/robo2* double mutant has the same phenotype as *slit* mutants (Rajagopalan et al., 2000b), linking these genes to the same genetic pathway

In the *Drosophila* nerve cord axons grow towards the midline due to attraction by Netrins (Kennedy et al., 1994), however it does not appear to control which axons cross the midline, and which remain in the ipsilateral longitudinal tracts. This appears to be controlled by the midline repellent Slit, through its receptor Robo, which is expressed in high levels by ipsilateral axons preventing them from crossing the midline (Kidd et al., 1998b; Kidd et al., 1999). Commissural axons are able to cross the midline, but are prevented from recrossing by dynamic expression of Robo. Commissural growth cones express very low levels of Robo protein as they cross the midline, but this is dramatically upregulated once they reach the opposite side (Kidd et al., 1998b; Kidd et al., 1998a). It is thought that whether or not Robo is expressed on the cell surface of commissural axons is due to expression of another gene discovered at the same time as *robo*; *commissureless* (*comm*)(Seeger et al., 1993). *Comm* mutants have no axons crossing the midline and the *comm/robo* double mutant has the same phenotype as the robo mutant, linking these genes in the same pathway (Seeger et al., 1993). Comm is a transmembrane protein expressed by

midline cells and commissural axons, and is thought to antagonise Robo reducing surface expression on commissural growth cones during midline crossing (Tear et al., 1996; Georgiou and Tear, 2002; Keleman et al., 2002; Keleman et al., 2005). How Comm functions is appearing difficult to determine. Comm protein is found in midline glia and commissural axons, and mRNA expression, although originally thought to be confined to midline glia (Tear et al., 1996), is now known to be expressed by crossing commissural axons and midline glia, and is needed by both in order to permit crossing to the contralateral side (Georgiou and Tear, 2002; Keleman et al., 2002; McGovern and Seeger, 2003). There are at present two models to explain how Robo/Comm functions to permit midine crossing. The first includes Comm function at the midline and autonomously by commissural axons; interactions between Comm on the surface leads to removal of Comm/Robo complex from the plasma membrane and targeted towards a degradation pathway (Georgiou and Tear, 2002; Myat et al., 2002; Georgiou and Tear, 2003). The second suggests Comm functions only in commissural axons where it sorts Robo directly from the Golgi to lysosomes while axons cross the midline, but allows Robo transport to the plasma membrane in ipsilateral and post-crossing commissural axons (Keleman et al., 2002). The different models arise from different analysis techniques and clearly more work is needed to clarify this matter. Whether contralateral or ipsilateral, the axons in the nerve cord join one of three longitudinal tracts at a defined lateral distance from the midline. This lateral position is defined by a combinatorial code of the three robo receptors and a presumptive Slit gradient (Rajagopalan et al., 2000b; Rajagopalan et al., 2000a; Simpson et al., 2000a; Simpson et al., 2000b).

Slit-Robo signalling mediates repulsion in part using downstream signalling through enabled, abelson kinase, DOCK, Pak and Cross GAP possibly by altering the local actin cytoskeleton (Bashaw et al., 2000; Fan et al., 2003; Hu et al., 2005).

### *1.4.1 Slit and Robo in vertebrates*

Slit and Robo are evolutionarily conserved molecules and to date, three mammalian homologs of *Drosophila slt*; *slit1*, *slit2* and *slit3*, and four homologs of *robo*; *robo1*,

*robo2*, *robo3* (*rig1*) and *robo4* (*magic roundabout*) have been identified (Kidd et al., 1998b; Yuan et al., 1999a; Huminiecki and Bicknell, 2000; Simpson et al., 2000b) (Holmes et al., 1998; Itoh et al., 1998). Characterisation of the Slit proteins (Figure 1.8) revealed large, secreted, glycosylated molecules containing four tandem leucine rich repeats (LRRs) near the N-terminus, 9 EGF-like motif repeats, an agrin-laminin-perlecan (ALPs) motif and a cysteine-rich knot at the carboxy-terminal (Brose et al., 1999; Li et al., 1999). Robo proteins (Figure 1.8) are a transmembrane protein containing five Immunoglobulin-like (Ig) domains, three fibronectin (FN) type III repeats and a long cytoplasmic tail containing highly conserved regions (Kidd et al., 1998b). Robo 4 is different from the other Robos; it is smaller with only 2 Ig- and FN III-domains and is thought to be vascular specific (Huminiecki and Bicknell, 2000; Huminiecki et al., 2002).

Biochemical and genetic evidence have shown that Robo is the receptor for Slit, and studies using deletion constructs have identified the LRRs in Slit and the Ig domains in Robo as those regions essential for Robo-Slit binding (Battye et al., 1999; Brose et al., 1999; Li et al., 1999; Chen et al., 2001; Nguyen Ba-Charvet et al., 2001). The EGF domains are important for controlling the diffusion of Slit and the conserved cytoplasmic motifs in Robo share redundant roles determining the intracellular effect of Slit (Bashaw et al., 2000).

Slit and Robo have been shown to have a conserved role in axon guidance at the vertebrate midline as in the *Drosophila* nerve cord. In the spinal cord, commissural axons first project ventrally toward the floor plate and either turn and project adjacent to the midline or cross and join longitudinal tracts on the contralateral side. *Robo1* and *robo2* are expressed by commissural neurons, and all three *slits* are expressed at the midline (Itoh et al., 1998; Kidd et al., 1998b; Brose et al., 1999; Li et al., 1999). *Robo1 and robo2* expression appears to specify which lateral position in the longitudinal tracts the axons will extend, as in *Drosophila* (Long et al., 2004). Interestingly, the role of *robo3* (*rig1*) appears to be different to that in the fly, as expression of Robo3 is reverse of what would be expected, with high expression before crossing and low afterwards. Furthermore, loss of *robo3* results in the absence

of commissural axons, similar to *commissureless (comm)* in *Drosophila*, seemingly through repression of Slit signalling (Sabatier et al., 2004). How Robo3 represses Slit function is not known. Further evidence for the unique function of Robo3 comes from analysis of the human syndrome horizontal gaze palsy with progressive scoliosis (HGPPS). In these patients' corticospinal and somatosensory axons do not appear to cross the midline, and all patients studied have mutations in the *robo3* gene (Jen et al., 2004). Another interesting difference in vertebrates is the apparent lack of a homologue to *Drosophila comm.* However, Robo3 appears to fill this function, acting as a negative regulator of Slit/Robo signalling, but functioning in a different way to comm (Sabatier et al., 2004).

### *1.4.2 Other functions of Slit in vertebrates*

Along with its role in axon guidance at the midline in vertebrates, Slit has been shown to repel the axons of a number of other neuronal cell types including; spinal motor axons, central projection of sensory neurons, hippocampal axons, olfactory bulb axons, corpus callosal axons and retinal ganglion cell axons *in vivo* and/ or *in vitro* (Brose et al., 1999; Li et al., 1999; Nguyen Ba-Charvet et al., 1999; Erskine et al., 2000; Niclou et al., 2000; Ringstedt et al., 2000; Bagri et al., 2002; Nguyen-Ba-Charvet et al., 2002; Plump et al., 2002; Campbell et al., 2007). In olfactory development, axons from the olfactory bulb project ipsilaterally to the olfactory areas in the cortical telencephalon, these axons turn away from the midline, forming the lateral olfactory tracts. Slit1 and Slit2 have shown to be a chemorepellent secreted by the septum, at the midline, preventing axons from crossing and therefore play an important role in olfactory bulb axon guidance (Li et al., 1999; Nguyen-Ba-Charvet et al., 2002). Interestingly, along with its role in axon repulsion, Slit has also been

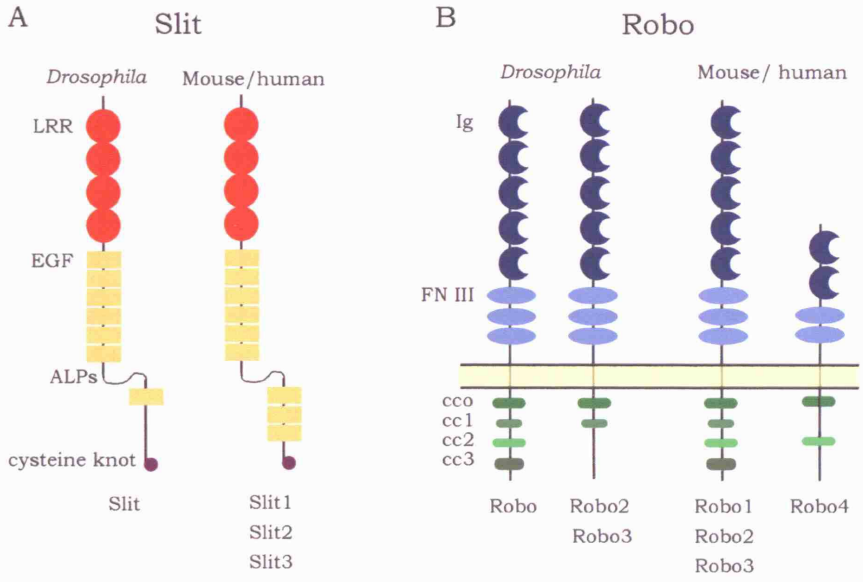


**Figure 1.8- Schematic diagram illustrating the domain structures of Slit and Robo**

(A) Slit contains 4 tandem leucine rich repeats (LRR) and multiple EGF-like repeats (7 in *Drosophila*, and 9 in mouse and human), an agrin-laminin-perlecan (ALPs) motif and a cysteine rich knot (Brose et al., 1999; Li et al., 1999). (B) Robo contains 5 immunoglobulin-like (Ig) domains (Robo4 has only 2), 3 fibronectin type (FN) III repeats (Robo4 has only 2) and a long cytoplasmic tail containing conserved regions (dRobo; CC0, CC1, CC2, CC3, dRobo2/3; CC0, CC1, mouse/human Robo1-2; CC0, CC1, CC2, CC3 and Robo4; CCO, CC2) (Kidd et al., 1998b; Huminiecki et al., 2002; Park et al., 2003).

shown to function in a contradictory fashion, as an elongation and branching factor in some cell types (Wang et al., 1999; Ozdinler and Erzurumlu, 2002; Piper et al., 2002; Sang et al., 2002; Whitford et al., 2002). The first example of this was in 1999 (Wang et al., 1999), when rat NGF-sensitive DRG cells were cultured in the presence of purified calf brain extract. These DRG axons were shown to elongate and branch, suggesting a factor in the calf brain extract acts as a regulator for DRG axon collateral formation. This factor was then isolated and found to be Slit2 (Wang et al., 1999). Since then, Slit has been shown to induce branching and arborisation in a number of cell types *in vitro,* and on trigeminal peripheral axons *in vivo* (Yeo et al., 2004; Ma and Tessier-Lavigne, 2007), and even act on the same cell in both an inhibitory and later attractive manner (Sang et al., 2002). Recently, Robo2 and Slit1a have been shown to inhibit arborisation and synaptogenesis of RGC axons in the tectum of zebrafish (Campbell et al., 2007), revealing another inhibitory function for Slit/Robo signalling in axon guidance.

In addition to its role in axon guidance Slit has also been shown to have a role in cell migration within the central nervous system (Hu, 1999; Wu et al., 1999; Zhu et al., 1999), and with a number of processes outside the nervous system including, kidney development, tracheal branch development, mesoderm cell-migration, neural crest migration and leukocyte chemotaxis (Kramer et al., 2001; Wu et al., 2001; Englund et al., 2002; De Bellard et al., 2003; Grieshammer et al., 2004). Furthermore, Slit and Robo have been shown to have angiogenic function, promoting vascularisation in cancerous tumours (Wang et al., 2003).

### *1.4.3 Slit and Robo and other molecules*

A number of molecules have been shown to interact with Slit and Robo affecting Slit distribution and directly or indirectly influencing the response of growth cones. The group of extracellular matrix molecules; heparan sulphate proteoglycans (HSPG) interact with Slits and have been shown to be regulators of Slit localisation and function (Liang et al., 1999; Hu, 2001; Johnson et al., 2004; Steigemann et al., 2004). If the syndecan group of HSPGs are disrupted in *Drosophila* the distribution of Slit

in regions surrounding the midline is altered and Robo-positive axons are able to cross the midline (Johnson et al., 2004). An interaction between Syndecan, Slit and Robo has been suggested with genetic and biochemical evidence (Johnson et al., 2004; Steigemann et al., 2004) and direct evidence for a ternary complex, which stablises Slit/Robo interactions has now been shown (Hussain et al., 2006). These data all suggest HSPGs are needed for midline axon guidance in *Drosophila,* bind Slit and Robo, and affect Slit localisation. Furthermore, evidence has shown HSPGs are needed for the Slit2 induced repulsion of murine olfactory interneuron precursors, olfactory bulb axons (Hu, 2001) and *Xenopus* RGC axons (Hussain et al., 2006; Piper et al., 2006). *In vivo* evidence linking HSPGs to the ability of RGC axons to respond to Slit has been shown in mice, and differential post-translational modifications of HSPGs are required for Slit-mediated RGC axon guidance at the optic chiasm (Inatani et al., 2003). It also appears that the fine structure of HSPGs modulate specific aspects of RGC axon guidance at the chiasm and RGC axons avoid regions expressing particular HSPG modification enzymes, which also coincide with Slit expression (Pratt et al., 2006). This highlights the complexity of interactions needed for correct axon navigation.

In addition to HSPGs/Slit/Robo interactions, there is evidence to suggest Slit/Robo interactions between the cell adhesion molecules, N-Cadherin and β-integrin modulating growth cones responses to guidance cues (Rhee et al., 2002; Stevens and Jacobs, 2002), functioning through Abl tyrosine kinase and the adaptor protein Cables (Rhee et al., 2007). Slit inactivates N-cadherin-mediated adhesion, presumably to enhance repulsion of Robo expressing axons while promoting growth of Robo negative axons through the same environment. The Slit/Robo pathway can also interact with other signalling systems for example, in *Xenopus,* activation of Robo silences the attractive effect of Netrin1 by interaction of the cytoplasmic domains of Robo and DCC (Stein and Tessier-Lavigne, 2001). This would allow a hierarchical signalling response of an axon in reaction to the detection of opposing signals at the growth cone. Another example of a pathway interacting with Slit/Robo signalling is the stromal cell-derived factor-1/ chemokine receptor-4 (SDF1/

CXCR4) pathway. SDF1 attenuates the repulsive action of Slit in culture assays by elevating intracellular cAMP levels (Chalasani et al., 2003), and morpholino knockdown rescues the axon defects seen with partial loss of *robo2* in zebrafish *in vivo* (Chalasani et al., 2007). Whether SDF1 is acting by reducing responses to repellents or actually as an attractant is unclear. RGC axons have been shown to be attracted towards a source of ectopic SDF1 in zebrafish (Li et al., 2005), however as morpholino knockdowns will rescue only partial *robo2* mutants not null mutants it is thought a cooperation between signalling system is needed (Chalasani et al., 2007). Regardless of how these molecules function together, expression of SDF1 in the optic stalk helps RGC axons to extend past the surrounding inhibitory environment, highlighting the importance of integration of signals at the growth cone.

In addition to the examples where Slit and Robo interact with other molecules to modify a growth cones response to axon guidance, evidence also indicates a role for Robo/Robo interactions (Hivert et al., 2002). Robo-positive RGCs grown in culture over Robo expressing 3T3 cells extend longer neurites than when grown over control cells, but , Robo-negative cerebellar neurons do not. What's more, Robo1 and Robo2 can homophilically bind together in an interaction thought to be similar to CAMs (Hivert et al., 2002). This brings out the possibility that Robo acts like CAMs to promote axon growth via homophilic binding. Studies in *C.elegans,* where there is only one *slit* (*slt1)* gene and one *robo* (*sax3)* gene, show a number of axon guidance defects when these genes are knocked out (Zallen et al., 1998; Hao et al., 2001). Most of the defects are the same in the *sax3* mutants as in the *slt1* mutants, however *slt1* mutants do not show the nerve ring axon guidance defects seen in *sax3* mutants, suggesting a non-Slit ligand function of Robo. This could be a Robo/Robo interaction, or due to an unknown Robo ligand. In support of this theory, analysis of major forebrain axon tracts and cortical interneuron migration in *robo1-* (Andrews et al., 2006), compared to *slit1/2-* deficient mice (Bagri et al., 2002; Marin et al., 2003) reveal phenotypic differences suggestive of additional ligand or receptor molecules in the Slit/Robo signalling pathway. However, more detailed analysis in triple *slit* knockout and triple *robo* knockouts maybe needed to prove this.

More recently the suggestion that Slit may have a non-Robo function was proposed following analysis of RGC arborisation in zebrafish *astray/slit1a*MO mutants (Campbell et al., 2007). Campbell et al. show *robo2* is the only *robo* expressed by RGCs during tectal arborisation, and *slit1a* is the only *slit* expressed in the tectum, and when both genes' function are disrupted there is an enhancement of the *robo2* null phenotype. They suggest this is due to a Robo2-independent Slit pathway, and as Robo2 is the only Robo expressed by RGCs at this time it must mean a non-Robo receptor of Slit (Campbell et al., 2007). However, as *robo3* expression was seen at low levels one day prior to this analysis (Lee et al., 2001), further work is needed to prove the existence of this non-Robo receptor of Slit.

### *1.4.4 Slit in the visual system*

In mammals, of the three *slit* and four *robo* genes; *slit1*, *slit2*, *robo1* and *robo2* are thought to be important for RGC axon guidance due to expression patterns and *in vitro* and/or *in vivo* evidence (Erskine et al., 2000; Niclou et al., 2000; Ringstedt et al., 2000). In rodents, from the time that the first RGCs are generated, both *robo2* and *slit1* are expressed in the RGC layer. Slightly later in development, *slit2* and *robo1* are also expressed within the RGC and presumptive inner nuclear layers, however *robo1* is only expressed in a scattered population of cells, not by every cell in the RGC layer (Erskine et al., 1998; Niclou et al., 2000; Ringstedt et al., 2000; Plump et al., 2002). *In vitro,* both Slit1 and Slit2 are inhibitors of RGC axon outgrowth (Tuttle et al., 1998; Erskine et al., 2000; Plump et al., 2002). Slits control RGC axon guidance at the optic chiasm based on patterns of expression, their ability to inhibit RGC axon outgrowth and *in vivo* data. Loss of both Slit1 and 2 result in RGC axons crossing the midline at an ectopic chiasm, which is more anterior to the true chiasm. Additionally, ectopic axons are seen projecting into the contralateral optic nerve and a number of projections extend caudally and dorsally away from the chiasm. Slits are thought to tunnel the tightly fasciculated tract through the chiasm defining its position on the ventral midline and restricting RGC axons to the optic pathway (Erskine et al., 2000; Plump et al., 2002). This supports what was seen previously in zebrafish: the robo2 (*astray)* mutants show anterior/posterior RGC

axon pathfinding defects, excessive midline crossing and defasciculation (Karlstrom et al., 1996; Fricke et al., 2001). Futhermore, Robo2 may function at the midline to correct occasional naturally occurring pathfinding errors made by wildtype growth cones (Hutson and Chien, 2002). Together these data show that Robo2/Slit signalling has an important role in multiple aspects of RGC axon guidance.

## 1.5 Aims

- To elucidate the role of Slit and Robo as axon guidance molecules in the mouse optic tract.

- To elucidate the role of Slit and Robo as intraretinal guidance molecules, in the mouse.

In the course of my studies I identified the lens as a potential signalling centre controlling axon outgrowth and eye development.

- To investigate the signals from the lens which coordinate growth of the eye.

# 2 Materials and Methods

## 2.1 Preparation of Commonly used solutions

**BCIP:** 50mg/ml in 100% dimethylformamide

**Collagen Gel:** 180µl Bovine dermis collagen (BD Biosciences, Oxford, UK), 180µl Rat tail collagen (BD Biosciences), 40µl 10X Dulbecco's Modified Eagle's Medium (DMEM; Gibco/Invitrogen, Paisley, UK) and 0.8M $NaHCO_3$ until colour change is seen and the pH is neutral. Keeping solution on ice stops it from setting.

**Colour reaction:** 4.5µl NBT and 3.5µl BCIP (Roche, Lewes, UK) in 1ml NTMT (Roche).

**Hybridisation buffer:** 25ml Formamide, 12.5ml 20X SSC (pH4.5), 0.25ml tRNA (20mg/ml; Sigma, Poole, UK), 0.5g SDS, 0.25ml heparin (10mg/ml; Sigma) to a volume of 50ml with distilled water. Working solution: 50% formamide, 5X SSC, 50µg/ml tRNA 1% SDS, 50µg/ml heparin.

**LB agar plates:** 10g of tryptone, 5g of yeast extract, 5g of NaCl, 1ml 1N NaOH and 15g of agar is made up to a volume of 1 litre with distilled water and autoclaved. Following autoclaving, cool the solution to 55°C and add 10µg/ml ampicillin (Sigma), mix and pour approximately 25ml into 10cm diameter Petri dishes. Cool and store at 4°C.

**Luria Base media (LB):** 10g of tryptone, 5g of yeast extract, 5g of NaCl and 1ml 1N NaOH is made up to a volume of 1 litre with distilled water and autoclaved.

**MABT pH 7.5:** Make 100mM maleic acid and 150mM NaCl then autoclave. Finally add Tween-20 to make 1%.

**NBT:** 75mg/ml in 70% dimethylformamide

**NTMT:** Add 2ml 5M NaCl, 10ml 1M Tris-HCl (pH 9.5), 5ml 1M $MgCl_2$, and 1ml Tween-20 to a volume of 100ml of distilled water. Working solution: 100mM NaCl, 100mM Tris-HCl (pH 9.5), 50mM $MgCl_2$, and 1% Tween-20.

**4% Paraformaldehyde (PFA) in PBS:** 40g paraformaldehyde, 900ml $dH_2O$ and 2 drops of 10M NaOH heat until dissolved. Add 100mls 10X PBS. Freeze until use.

**PBST:** PBS plus 1% Tween-20

**PBT:** PBS plus 0.1% Tween-20

**Phosphate Buffered Saline (PBS) 10X:** 82g NaCl, 4.3g $NaH_2PO_4.2H_2O$ and 17.4g $Na_2HPO_4$, top up to 1L with distilled water ($dH_2O$). Dilute 1:10 with $dH_2O$ to use. Working solution: 140 mM NaCl, 15 mM Phosphate buffer, pH 7.5.

**Tris EDTA buffer (TE):** 10mM Tris-chloride, pH8 and 1mM EDTA, pH8.

**Tris buffered saline (TBS) pH7.2:** 12.1g of Tris base and 9g of NaCl made to a volume of 1L with distilled water and pH adjusted with HCl. Working solution: 0.1M Tris, 0.9% NaCl.

**TBST:** TBS plus 1% Tween-20

**Solution 1:** 25ml Formamide, 12.5ml 20X SSC (pH4.5) and 2.5ml SDS to a volume of 50ml with distilled water. Working solution: 50% formamide, 5X SSC and 1% SDS.

**Solution 3:** 25ml Formamide and 5ml 20X SSC (pH4.5) to a volume of 50ml with distilled water. Working solution: 50% formamide and 2X SSC.

**20X SSC:** 175g of NaCl and 88g of $Na_3.C_6H_5O_7.2H_2O$ to a volume of 1L with distilled water and pH adjusted with citric acid. Working solution: 3M NaCl, 0.3M $Na_3.C_6H_5O_7.2H_2O$.

**Wholemount in situ hybridisation buffer:** 25ml Formamide, 3.25ml 20X SSC (pH4.5), 0.5ml 0.5M EDTA (pH8), 125µl tRNA (20mg/ml), 100µl heparin

(50mg/ml), 100µl Tween-20, 2.5ml 10% CHAPS (Roche) to a volume of 50ml with distilled water. Working solution: 50% formamide, 1.3X SSC, 5mM EDTA, 50µg/ml tRNA, 100µg/ml heparin, 0.2% Tween-20, 0.5% CHAPS.

## 2.2 Animals

### *2.2.1 Mice*

All conditions and all experimental procedures were in accordance with the UK Animals (Scientific Procedures) Act 1986 and associated guidelines. Experiments were performed using C57bl/6J and *slit1*- and/or *slit2*- deficient mice (Plump et al., 2002) (gift from Dr. M. Tessier-Lavigne) and *robo1*- or *robo2*-deficient mice were a gift from Dr. W. Andrews and Professor J. Parnavelas (Department Anatomy and Developmental Biology, University College London) (Andrews et al., 2006; Lu et al., 2007). The C57bl/6J and *slit*-deficient mice were maintained in in-house timed-pregnancy breeding colonies. Noon on the day that the vaginal plug was found was considered embryonic day 0.5 (E0.5). Pregnant mothers were killed by a rising gradient of $CO_2$ followed by cervical dislocation and the embryos collected in DMEM/F12 for culture or in PBS and fixed in 4% PFA in PBS either overnight for immunohistochemistry or 2 days for lipophilic dye, 1,1'-dioctadecyl-3,3,3',3'-tetramethylindocarbocyanine perchlorate (DiI; Molecular Probes, Eugene, OR) labelling or *in situ* hybridisation.

For postnatal mice, the day of birth was recorded as postnatal day 0 (P0). These were administered an overdose of the inhalation anaesthetic Isoflurorane-Vet (Merial Animal Health, Essex, UK), followed by exsanguination and fixed as above.

### *2.2.2 Genotyping*

The *slit*-deficient mice were genotyped by extracting genomic DNA from either tail snips, ear punches, or embryonic neck folds, which were first digested overnight at 55°C in 500µl lysis buffer (100mM Tris-HCl, pH 8.5, 5mM EDTA, pH 8.0, 200mM NaCl, 0.2 % SDS) with 100µg/ml proteinase K (Sigma). The DNA was isolated

using ethanol precipitation, and then genotyped by PCR (Figure 2.1) using the primers designed against the *slit* genes or the knocked-out regions (Sigma-Genosys Biotechnologies, Cambridge, UK; Table 2.1).

PCR was carried out for *slit1* in Green Buffer (Tris-HCl, pH 8.8- 67mM, $MgCl_2$-6.7mM, BSA- 170μg/ml, Ammonium Sulphate- 16.6mM), 400μM dNTPs (Bioline, London, UK), 1 Unit Biotaq (Bioline), with slit1 primers (Table 2.1) at a final concentration of 0.2μM, using the following programme: 95°C for 5 minutes, then 30 cycles of 95°C for 30 seconds, 60°C for 30 seconds, 72°C for 30 seconds, followed by 72°C for 5 minutes. *Slit2* PCRs were set up in MegaMix Blue (Helena Biosciences, Sunderland, UK), with slit2 primers (Table 2.1) at a final concentration of 0.2μM, using the following programme: 94°C for 5 minutes, then 34 cycles of 94°C for 40 seconds, 55°C for 1 minute, 72°C for 1 minute 30 seconds, followed by 72°C for 5 minutes. The *robo1*- and *robo2*-deficient mice were provided and genotyped by Dr. W. Andrews and Professor J. Parnavelas (Department Anatomy and Developmental Biology, University College London).

### *2.2.3 Chick*

Experiments were performed using fertile white leghorn chicken eggs (Henry Stewart and co. Ltd, Lincolnshire, UK) or Rhode Island hens eggs (Needle Farm, Enfield, UK), incubated on their sides at 37°C in a humidified incubator. For collection, embryos were collected in PBS, staged according to Hamburger and Hamilton (1951; Hamburger and Hamilton, 1992) and the extra-embryonic membranes removed before fixing in 4% PFA in PBS either overnight for immunohistochemisty or 2 days for *in situ* hybridisation.

**Table 2.1- Genotyping primers**

| Gene | Allele | Direction | Primer | Product length |
|---|---|---|---|---|
| Slit1 | wildtype | forward | 5'-AAGATGCCTCCTCTGACTTC-3' | 250bp |
| | | reverse | 5'-ACCCTTAGCTTCTACCAACC-3' | |
| | mutant | forward | 5'-TCTCCTTTGATCTGAGACCG-3' | 400bp |
| | | reverse | 5'-AGGTTTCTCGAGCGTCATAG-3' | |
| Slit2 | wildtype | forward | 5'-AAGACCTGTGCTTCTGTCAG-3' | 400bp |
| | | reverse | 5'-AAACAGGTTTCTACCGCACG-3' | |
| | mutant | forward | 5'-AAGACCTGTGCTTCTGTCAG-3' | 250bp |
| | | reverse | 5'- AAGTCTAGTAGAGTCGAGCG-3' | |

(Sigma-Genosys Biotechnologies, Cambridge, UK).

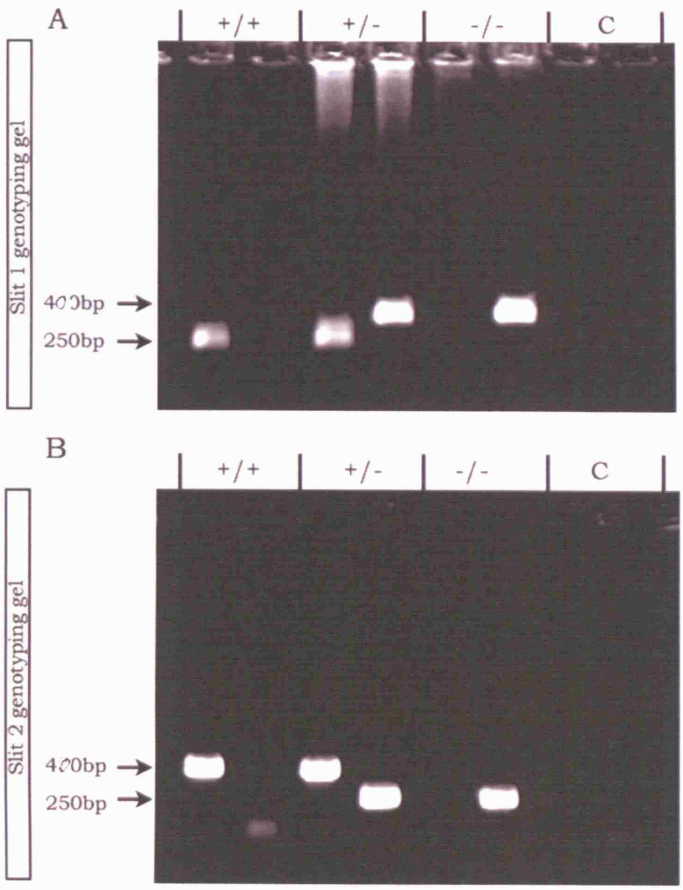


**Figure 2.1- Agarose gel electrophoresis of PCR reaction used to establish genotype of *slit*-deficient mice.**

(A) A sample result for *slit1* genotyping. The wildtype allele marker in the left-hand lane of each pair is 250bp. The mutant allele marker on the right is 400bp. (B) A sample result for *slit2* genotyping. The wildtype allele marker in the left-hand lane of each pair is 400bp. The mutant allele marker on the right is 250bp. +/+ is wildtype, +/- is heterozygote and -/- is homozygous mutant. C is the no DNA control.

## 2.3 Imaging

### *2.3.1 Image acquisition and preparation*

Images were taken with a Nikon SMZ1500 dissecting microscope with Nikon digital camera DXM1200 and Nikon ACT-1 imaging software, an Olympus BX50 fluorescent compound microscope, using digital camera and software as above, or with a Zeiss LSM 510 confocal microscope. The images were prepared using Adobe Photoshop.

## 2.4 DiI labelling

### *2.4.1 Anterograde DiI Labelling*

The skin, cornea, lens and neural retina were removed from one eye and, using a fine glass pipette, a crystal of DiI was positioned covering the optic nerve. The embryonic mice were stored at 37°C for 4 days at E14.5, 10 days at E16.5, 14 days at E18.5, 3 weeks at P0 or 4 weeks at P2 in PBS containing 0.01% sodium azide. The labelled brains were removed from the skulls and viewed intact or after the removal of the telencephalon, using a Nikon SMZ1500 fluorescent dissecting microscope with Nikon digital camera DXM1200 and Nikon ACT-1 imaging software. The brains were sectioned coronally or sagitally in agarose (see 2.5.2). The sections were imaged with a compound or confocal microscope (see 2.3.1).

### *2.4.2 Retrograde DiI labelling*

E18.5 mouse embryos were dissected to reveal the superior colliculus and small DiI crystals placed just under the surface of the anterior colliculus to label all entering axons. The embryos were stored at 37°C for 16 days in PBS containing 0.01% sodium azide. The labelled brains were removed and imaged intact with a dissecting microscope and the neural retinas were removed and flat mounted, using Vectashield

(Vector Labs, Peterborough, UK) and imaged with a compound microscope (see 2.3.1).

### *2.4.3 Focal DiI*

E16.5 neural retinas were isolated after carefully marking the orientation, and a small crystal of DiI placed in either the dorsal or ventral peripheral retina. After 6 hours of incubation at 37°C the retinas were flat mounted, using Vectashield and imaged with a compound microscope.

## 2.5 Sectioning of tissues

### *2.5.1 Cryosectioning*

Embryonic heads (mouse E17.5 or E18.5; chick stage 22-36) were cryoprotected with an increasing concentration of sucrose (5% sucrose, 1 hour; 15% sucrose, overnight; 25% sucrose, until sunk) then 1:1 in 25% sucrose/Cryo-m-bed, (Bright Instruments, Huntington, UK), embedded in Cryo-m-bed, and frozen using dry ice. Sections were cut coronally at 14μm unless otherwise stated, on a cryostat and mounted onto Superfrost Plus slides (VWR, Poole, UK).

### *2.5.2 Vibratome sectioning*

Mouse embryonic heads, brains or retinas (E13.5-E18.5) were dried on filter paper, before embedding in 3% agarose/PBS. Chick embryonic heads (E5-E6) were placed in 20% gelatine/PBS and left to infiltrate for 1 hour at 55°C, embedded at room temperature and left on ice for 30 minutes before fixing overnight in ice-cold 4% PFA/PBS. Sections were cut horizontally, coronally or sagitally at 100μm on a vibrotome and mounted on slides (VWR) using Vectashield, or mounted on Superfrost Plus slides for *in situ* hybridisation.

## 2.6 Immunohistochemistry

### *2.6.1 Standard Immunohistochemistry*

Cryosectioned tissue was blocked with 10% goat serum (Sigma)/0.2% Triton X-100 (Sigma)/PBS for 90 minutes, followed by overnight incubation in a primary antibody (Table 2.2) in the same blocking solution. The sections were washed with PBS and incubated for 2 hours in an appropriate secondary antibody (Table 2.3) in 1% goat serum/PBS. Tissue sections were then washed in PBS, mounted using Vectashield and imaged using a compound or confocal microscope. Control sections from wildtype animals or from which the primary antibody was omitted, showed no staining.

### *2.6.2 Robo antibody staining*

Lightly fixed (4 hours) E16.5 mouse brains were cyrosectioned at 15μm and treated with 0.3% $H_2O_2$ (Sigma) for 45 minutes then washed 3 times in PBS. Sections were blocked in TSA Tetramethylrhodamine system blocking reagent (Perkin-Elmer, Bucks, UK)/ 0.3% Triton for 2 hours before incubating in commercially available (R&D systems, Abingdon, UK) or Murakami anti-Robo antibodies (gift from Dr. F. Murakami, Osaka University, Japan) (Table 2.2) in the same blocking solution for two nights, followed by the appropriate biotinylated secondary antibody (Table 2.3) in the same blocking solution for two hours. The signal was then amplified using Avidin-Biotinylated enzyme complex from the Vectorstain Elite ABC kit (Vector Labs) for two hours. The the sections were washed five times in PBS and colour developed with the addition of the enzyme substrate DAB (Sigma). The sections were dehydrated in ethanol (75%-100%) and washed in Histoclear (National Diagnostics/Fisher, UK) for 5 minutes, then mounted with DPX.

### *2.6.3 Flatmounting and sectioning mouse retinas for imaging and analysis*

Prior to removing whole mouse retinas for labelling, a cut was made in the ventral pole to enable orientation and the lens and RPE removed. Retinas were blocked and

incubated in anti-TUJI (which labels neuronal β-tubulin, a cytoskeletal protein, to visualise cell bodies and axons; Table 2.2) in the same blocking solution for two nights followed by the appropriate secondary antibody (Table 2.3) in the same blocking solution for 2 hours. Labelled retinas were flatmounted, OFL-side up, or sectioned coronally in agarose at 100μm on a vibratome and imaged using a compound or confocal microscope.

## 2.7 In situ hybridisation

### *2.7.1 Subcloning*

Mouse robo4 EST (Clone ID: 3978776; Invitrogen) homologous to nucleotides 1-1766 was subcloned into pBluescript KS+ (pBS). Firstly, by digesting 5-10μg DNA with Xho1 (NEB, Hitchin, UK) and HindIII (NEB) in 3μl 10X restriction buffer, 5 units restriction enzyme, 0.3μl of BSA and distilled water to a volume of 30μl and incubated at 37°C for 2 hours. 1-2μg of this DNA product was run against uncut DNA on a 1% agarose gel, the band exised and the DNA purified using the QIAquick Gel extraction kit (Qiagen, Crawley, UK). Between 50 and 200ng of vector DNA was ligated with a 1:2 molar ratio of insert DNA, using 3 units of T4 DNA ligase (Promega, Southampton, UK) and 5μl of 2X Rapid Ligation Buffer (Promega) in a volume of 10μl. This was carried out for 20 minutes at room temperature. The ligated DNA was transformed into DH5 α-T1R chemically competent cells (Invitrogen). Frozen aliquots of chemically competent cells (Invitrogen) were thawed on ice and 50μl of cells were mixed with 3μl ligation mix or 1μl plasmid. This was mixed gently and stored on ice for 30 minutes followed by a heat-shock at 42°C for 30 seconds, then returned to ice for 2 minutes. 250μl of LB was added and the bacteria incubated at 37°C for 1 hour, rocking at 225rpm on their side. 20μl to 200μl of the bacteria were plated onto LB agar plates containing 50μg/ml ampicillin, inverted and incubated at 37°C overnight. Individual colonies were selected, amplified overnight and the DNA isolated using Qiagen miniprep kit

**Table 2.2- Primary antibodies**

| Name | Conc. | Company |
|---|---|---|
| Polyclonal serum rabbit anti-GFP | 1:500 | Molecular probes, Eugene, OR |
| Monoclonal mouse IgG, anti-neuron-specific-β-tublin (TUJI) | 1:1000 | Covance Research, Cambridge Bioscience Ltd, UK |
| Monoclonal mouse IgG anti-Islet 1 homeobox (39.4D5) | 1:50 | [T.M.Jessell] DSHB, Iowa City, USA * |
| Monoclonal rabbit IgG anti-phospho histone H3 (Ser 10) | 1:100 | Upstate Biotechnology, Lake Placid, NY |
| Polyclonal serum rabbit anti-calretinin | 1:10 000 | Swant, Bellinzona, Switzerland |
| Monoclonal mouse IgG1 anti-neurofilment-associated antigen (3A10) | 1:20 | [T.M.Jessell/ J.Dodd] DSHB * |
| Polyclonal goat IgG anti-robo1 | 1:100 | R&D systems, Abingdon, UK |
| Polyclonal goat IgG anti-robo2 | 1:100 | R&D systems, Abingdon, UK |
| Rabbit anti-robo1 | 1:2000 | Prepared by Dr. Murakami |
| Rabbit anti-robo2 | 1:2000 | Prepared by Dr. Murakami |

* DSHB (Developmental Studies Hybridoma Bank) developed under the auspices of the NICHD and maintained by the University of Iowa, Iowa City, USA.

(Qiagen). The robo4 DNA was confirmed by sequencing the insert using the M13 forward and reverse primer sites located within pBluescript (Table 2.4). 1μg of robo4 plasmid DNA was mixed with 12.8 pmol of each primer and sent to Advanced Biotechnology Centre, Imperial College London. The returned sequences were Blasted on NCBI.

### *2.7.2 Preparation of riboprobes*

Riboprobe templates were produced by PCR by taking advantage of the M13 forward and reverse primer sites in pBS (Table 2.4). PCR was carried out in $NH_4$ buffer (Bioline, London, UK), 2.5mM $MgCl_2$ (Bioline), 200μM dNTP (Bioline) and 1 unit taq using the following programme: 95°C for 5 minutes, then 25 cycles of 95°C for 2 minutes, 55°C for 30 seconds, 72°C for 3 minutes, followed by 72°C for 5 minutes. Following the PCR, in vitro transcription was performed as follows; 30 units of RNA polymerase was added to 2μl of 10X transcription buffer (Roche, Lewes, UK), 1μl digoxigenin- (DIG) labelled nucleotide mix (Roche), 4μl PCR product DNA, 20 units RNAsin (Promega) in a volume of 20μl and incubated for 2 hours at 37°C. After synthesis probes were treated with 2μl DNAse1 (Roche) for 10 minutes at 37°C. Unincorporated nucleotides were removed by precipitating twice with 80μl TES (Tris-EDTA plus 0.1% SDS), 8μl 5M LiCl, 300μl ice cold ethanol and 1μl glycogen at -20°C for 30 minutes, and finally resuspended in 100μl TES.

### *2.7.3 In situ hybridization on vibratome sections*

Embryonic heads (mouse E16.5) were vibratome sectioned coronally at 100μm in agarose. The sections were dehydrated and rehydrated in 25%-100% methanol in PBT (PBS + 0.1% Tween-20) and bleached with 6% $H_2O_2$ in PBT for 1 hour. The sections were then treated with 5 μg/ml Proteinase K in PBT for 10 minutes, which was inactivated with fresh 2mg/ml glycine in PBT for 10 minutes, washed twice in PBT and postfixed with 4% PFA in PBT for 20 minutes and washed twice in PBT. The sections were incubated at 65°C in hybridisation buffer (50% Formamide, 5x

**Table 2.3- Secondary antibodies**

| Name | Conc. | Company |
|---|---|---|
| Goat anti-rabbit IgG Cy3 | 1:500 | Jackson ImmunoResearch, Soham, UK |
| Goat anti-mouse IgG Cy3 | 1:500 | Jackson ImmunoResearch |
| AlexaFluor 488 goat anti-mouse IgG | 1:200 | Molecular Probes/ Invitrogen, Paisley, UK |
| Rabbit anti-goat IgG-Biotin | 1:200 | Vector Labs, Peterborough, UK |
| Goat anti-rabbit IgG-Biotin | 1:200 | Vector Labs, Peterborough, UK |

**Table 2.4- M13 PCR primers**

| Gene | Direction | Primer |
|---|---|---|
| M13 | forward | 5'- GTAAAACGACGGCCAGT-3' |
| | reverse | 5'- CAGGAAACAGCTATGAC -3' |

SSC, 50 µg/ml tRNA, 1% SDS, 50 µg/ml Heparin) for 1 hour, followed by overnight at 65°C in digoxigenin-labelled riboprobes against *slit1-3* or *robo1-4* (Table 2.5), diluted 15µl in 1ml hybridisation buffer. The sections were washed three times with 50% formamide, 5 x SSC, 1% SDS at 65°C then with 50% formamide, 2 x SSC at 60°C, blocked with 10% sheep serum/TBST (TBS + 1% Tween-20) and incubated overnight in anti-DIG-alkaline phosphatase (AP) antibody (Roche) diluted 1:2000 in 1% sheep serum/TBST. To activate the colour reaction, the sections were washed extensively with TBST and the alkaline phosphatase activity detected using NBT (337.5 µg/ml) and BCIP (175 µg/ml) in NTMT (100 mM NaCl, 100 mM Tris-HCl, pH 9.5, 50 mM $MgCl_2$, 1% Tween-20). Sections were mounted in 90% glycerol/PBS and imaged using a dissecting microscope.

### *2.7.4 In situ hybridization on cryosections*

Cryosectioned embryonic heads (chick E4, E5 or E6) were treated with 5 µg/ml Proteinase K in PBT for 10 minutes, postfixed with 4% PFA in PBT for 20 minutes, then washed twice in PBT. The sections were incubated at 65°C in hybridisation buffer (50% Formamide, 5x SSC, 50 µg/ml tRNA, 1% SDS, 50 µg/ml Heparin) for 60 minutes, followed by overnight at 65°C in digoxigenin-labelled riboprobes against *fgf4, fgf8, shh, tbx5, bmp2, bmp4, ephrinB2* and *ephrinB3* (Table 2.5), diluted 15µl in 1ml hybridisation buffer. The sections were washed three times with 50% formamide, 5 x SSC, 1% SDS at 65°C then with 50% formamide, 2 x SSC at 60°C, blocked with 10% sheep serum/TBST (TBS + 1% Tween-20) and incubated overnight in anti-DIG-AP antibody diluted 1:2000 in 1% sheep serum/TBST. To activate the colour reaction, the sections were washed extensively with TBST and the alkaline phosphatase activity detected using NBT (337.5 µg/ml) and BCIP (175 µg/ml) in reaction buffer (100 mM NaCl, 100 mM Tris-HCl, pH 9.5, 50 mM MgCl2, 1% Tween-20). Sections were mounted in 90% glycerol/PBS and imaged using dissecting microscope.

### *2.7.5 Wholemount in situ hybridization*

Embryonic chicken (E3) and mouse limbs (E14.5) were fixed in 4% PFA for 2 days and washed twice in PBST. The embryos were dehydrated in 25%-100% methanol in PBST (PBS + 1% Tween-20), bleached with 6% $H_2O_2$ in methanol for 1 hour, rehydrated in 75%-25% methanol and treated with 10 µg/ml Proteinase K in PBST for 20 minutes, which was then inactivated and postfixed with 4% PFA/ 0.1% gluteraldehyde for 20 minutes then washed twice in PBST. The embryos were incubated at 70°C in wholemount-hybridisation buffer (50% formamide, 1.3X SSC, 5mM EDTA, 50µg/ml tRNA, 100µg/ml heparin, 0.2% Tween-20, 0.5% CHAPS) for 1 hour, followed by overnight at 70°C in digoxigenin-labelled riboprobes against *pyst1* or *robo4* (Table 2.5), diluted 10µl in 1ml wholemount-hybridisation buffer. The embryos were washed four times with wholemount-hybridisation buffer at 70°C, then three times 30 minutes with MABT (100mM maleic acid, 150mM NaCl, 1% Tween-20; pH7.5), and blocked with 2% BBR (Roche) /20% goat serum/MABT and incubated overnight in anti-DIG-AP antibody diluted 1:2000 in the same block. To activate the colour reaction, the sections were washed extensively with MABT and the alkaline phosphatase activity detected using NBT (337.5 µg/ml) and BCIP (175 µg/ml) in NTMT. The reaction was stopped by washing in MABT and fixing in 4% PFA. Embryos were imaged using a dissecting microscope.

## 2.8 RT-PCR

### *2.8.1 Reverse Transcription- (RT-) PCR from total RNA extraction*

Lenses (E4 or E6 chick) and limbs (as a positive control) collected in Tri-reagent (Sigma) were homogenised with a syringe and increasing gauge needles and centrifuged to remove insoluble material. Chloroform was added, mixed, phase separated and the aqueous phase (RNA) mixed with isopropanol to precipitate. The precipitate was washed with 75% ethanol before redissolving in clean water. Invitrogen SuperScript III first Strand synthesis system (Invitrogen) was used to

**Table 2.5- Riboprobes**

| Probe | RNA polymerase for antisense/sense probe | Source | Animal |
|---|---|---|---|
| Robo1 | T7 | (Brose et al., 2000) | Mouse |
| Robo2 | T7 | (Brose et al., 2000) | Mouse |
| Robo3/ Rig1 | T7 | (Brose et al., 2000) | Mouse |
| Robo4 | T7 | Made from EST | Mouse |
| Slit1 | T7 | (Brose et al., 2000) | Mouse |
| Slit2 | T7 | (Brose et al., 2000) | Mouse |
| Slit3 | T7 | (Niswander et al., 1994) | Mouse |
| FGF4 | T7 | (Vogel et al., 1996) | Chick |
| FGF8 | T3 | (Francis et al., 1994) | Chick |
| Pyst1 | T7 | S. Keyse | Chick |
| BMP2 | T3 | (Francis et al., 1994) | Chick |
| BMP4 | T3 | (Riddle et al., 1993) | Chick |
| Shh | T3 | (Logan et al., 1998) | Chick |
| EphrinB2 | T7 | Gift from Claudio Stern | Chick |
| EphrinB3 | T7 | Gift from Claudio Stern | Chick |
| Tbx5 | T7 | (Mohammadi et al., 1997) | Chick |

make cDNA by combining 1μg of RNA with the kit ingredients; Oligo-dT primers (5μM) and dNTPs (1mM) and incubating at 65°C for 5 minutes, then on ice for 1 minute. This was then added to the kit ingredients; RT buffer, 5mM $MgCl_2$, 1mM DTT, RNaseOUT (40 Units) and SuperScript III RT (200 Units) and incubated for 50 minutes at 50°C, followed by 85°C for 5 minutes, then RNase H is added for 20 minutes at 37°C. GAPDH was used as a positive primer control and limb tissue as a positive for tissue expression. PCR was performed using MegaMix Blue, with forward and reverse primers (Table 2.6) on 2μl of cDNA, using the following programme: 94°C for 5 minutes, then 34 cycles of 94°C for 40 seconds, 55°C for 1 minute, 72°C for 1 minute 30 seconds, followed by 72°C for 5 minutes.

## 2.9 Co-culture

### *2.9.1 Coculture*

E15.5 wildtype embryos were collected in DMEM/F12 and the retinas isolated keeping the left and right retinas separated and orientated with a small cut on the nasal side and stored on ice. Explants prepared from the peripheral third of ventro-temporal or dorso-temporal retinas were cultured in a 50:50 mix of bovine dermis and rat tail collagen gels (Fahrenheit lab supplies, Rotherham, UK) either alone or with lenses taken from E15.5 wild-type or *slit1-/-, slit1-/-; slit2+/-, or Slit1/2 -/-* at a distance of 100-300μm (Figure 2.2). After 24 hours at 37°C in 5% $CO_2$, the cultures were fixed with 4% PFA in PBS, and stained with TUJ1 followed by AlexaFluor 488 goat anti-mouse IgG (see 2.6.1) to reveal the extent of RGC axon outgrowth. Labelled cultures were imaged using a dissecting microscope and the extent of outgrowth was quantified using the public domain NIH Image program (developed at the U.S. National Institutes of Health and available on the Internet at http://rsb.info.nih.gov/nih-image/). The measurement takes into account both the length and the number of RGC axons. Because outgrowth was not radial, with most growth from the central-most side, care was taken to ensure the correct orientation of the explants when positioning around the lens. The cultures were set up and

analysed blind to the genotype of the lenses and the results presented are the mean (± s.e.m) of four independent experiments.

## 2.10 Chick embryology

### *2.10.1 Lentectomy*

On embryonic day four the lenses were removed from chick using a method adapted from Coulombre and Coulombre, 1964. Eggs were removed from the incubator and turned 180° and left for 30 minutes prior to experiment to loosen the embryo. A hole was made in the blunt end of the egg and ~2ml of albumin removed. Selotape was stuck to the upper surface of the egg and a "window" approximately 1cm by 2cm was cut to reveal the embryo developing on the upper surface of the yolk. An opening was made in the chorion and aminion directly above the eye and an incision made at the edge of the RPE opposite the ventral fissure (Figure 2.3B). The lens was grasped by the capsule, and rocked gently to separate the capsule from its zonular connections and from the margin of the optic cup (Figure 2.3C). In most cases this allowed the removal of the intact lens without significantly damaging or removing adjacent tissues (Figure 2.3D), these are referred to as aphakic eyes. Those that were damaged were immediately discarded. For controls either, a sham operation was performed, where an incision was made but the lens was not removed (controls), or the lens was removed and then replaced (referred to as replaced-lens or controls). The eggs were sealed with selotape and re-incubated either for 2 hours, 24 hours (E5), 2 days (E6), 3 days (E7) or 6 days (E10) before staging and collecting. Those used for total cell counts (see below) were used immediately but those for in situ or collection were fixed in 4% PFA in PBS overnight. Embryos were imaged using a dissecting microscope and eye diameters measured using NIH image software.

**Table 2.6- RT-PCR primers and product length for chick genes**

| Gene | Name | Primer | Product length |
|---|---|---|---|
| FGF2 | Reverse | 5'-GGCTTGTACTGTCCAGTCCT-3' | 318bp |
| | Forward | 5'-AGCGGCTCTACTGCAAGAAC-3' | |
| FGF4 | Reverse | 5'-TTCTTCCGTTTTTGCTCAGG-3' | 306bp |
| | Forward | 5'-GTCTCTATTGCAACGTGGGC-3' | |
| FGF8 | Reverse | 5'-AGCACGATCTCGGTGAAGAC-3' | 315bp |
| | Forward | 5'-AGCAGAGCCTGGTGACAGAT-3' | |
| GAPDH | Reverse | 5'-CTTCTGTGTGGCTGTGATGG-3' | 401bp |
| | Forward | 5'-GGACAGTTCAAGGGCACGT-3' | |

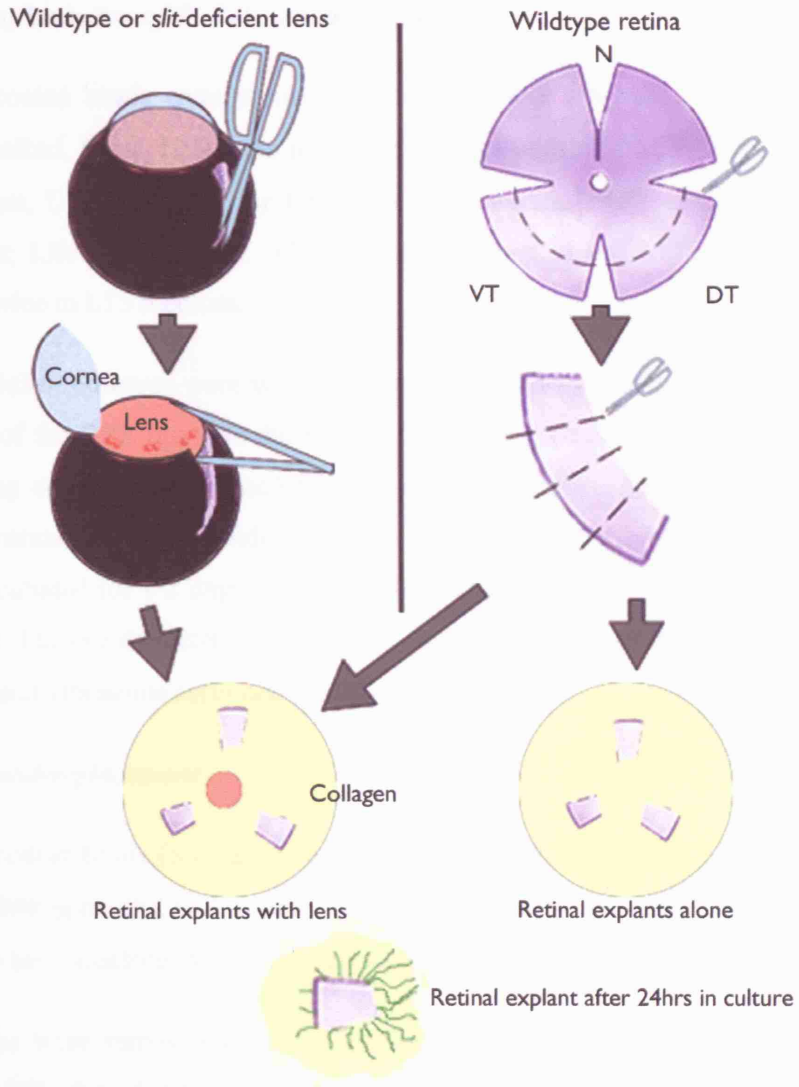


**Figure 2.2- Collagen gel culture of retinal explants with or without lens**

To remove the lens, an incision is made through the RPE and retina and the cornea is carefully cut away. The lens is removed using forceps and cleaned of any attached tissues. To produce retinal explants, a cut is made on the nasal side and the neural retina is removed and flattened. The peripheral third of VT and DT retina is isolated and cut into explants. Retinal explants are then cultured alone or with wild-type or slit-deficient lenses for 24hrs at 37°C.

### *2.10.2 Implantation of SU5402-coated beads*

SU5402-coated beads were prepared as follows: AG 1-X2 anion exchange resin beads (BioRad, Herts, UK) were incubated in 20µl of 10mM SU5402 (Calbiochem, Nottingham, UK) in DMSO for 1 hour followed by washing twice in L15 medium (Leibovitz; Life technologies). Controls were incubated in DMSO for 1 hour then washed twice in L15 medium.

Day 4 chicken embryos were windowed as above (2.10.1), and an incision made at the edge of the RPE opposite the ventral fissure (Figure 2.3B). Between 6 and 10 (depending on size of the bead) SU5402-coated or control beads were transferred into the vitreal cavity surrounding the lens using fine forceps. The eggs were sealed and re-incubated for 1-2 days (E5, E6) before staging and fixing in 4% PFA in PBS overnight. The eye diameter was measured as above and the tissue embedded in 20% gelatine, and vibratome sectioned at 100µm.

### *2.10.3 Bead-replacement*

Heparin-coated beads (Sigma) were prepared by washing twice in L15 medium and then incubating in 10µl of 25µg/ml FGF8 (R&D systems, Abingdon, UK) in PBS for 1 hour on ice. Controls were washed twice in L15 medium and then left in PBS.

The lenses were removed from E4 chicken embryos as described above (2.10.1; Figure 2.4A), then 6-10 (depending on size) FGF8-coated or control beads were transferred into the position of the removed lens using fine forceps (Figure 2.4B). The eggs were sealed with selotape and re-incubated for 1 day (E5) before staging and fixing in 4% PFA in PBS overnight. The tissue was then embedded in gelatine and sectioned at 100µm, or cryoprotected and cryosectioned at 25µm.

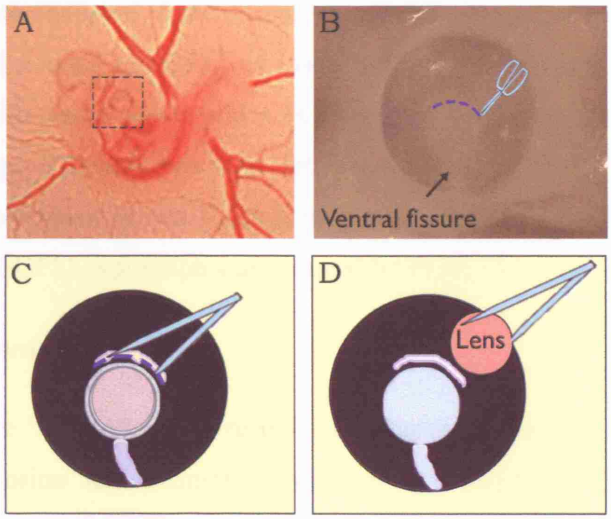


**Figure 2.3- Procedure for lentectomy.**

(A) Day 4 chicken embryos were "windowed" and the embryo revealed. (B) An incision was made opposite the ventral fissure, (C) forceps were used to grasp the lens, (D) the lens was gently removed from the eye.

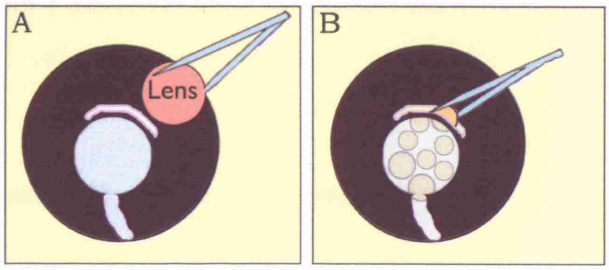


**Figure 2.4- FGF8- bead lens replacement**

(A) The lens was removed as above, (B) FGF8 or control beads were transferred into the position of the removed lens.

### *2.10.4 Implantation of FGF8-coated beads into flank*

This method was adapted from Brent et al. (2003). E3 Chicken eggs were "windowed" and a small incision was made in the flank between the limbs with a tungsten flame-sharpened needle and a FGF8-coated bead was pushed into the hole using fine forceps. The embryos were left for 6 hours and then fixed in 4% PFA overnight. Wholemount *in situ* hybridisation was performed to determine if p*yst1* (downstream of FGF8) expression was induced by FGF8 (Eblaghie et al., 2003).

### *2.10.5 Electroporation*

Day 4 eggs were "windowed" to reveal the developing embryo. An opening was made in the chorion and aminion above the eye. Platinum/Iridium (Pt80/Ir20) 0.25mm-diameter wire electrodes were positioned either side of the eye, with the positive electrode on the dorsal side (Figure 2.5A). A finely-pulled glass capillary (Harvard apparatus, Edenbridge, UK) was used to inject chicken-β-actin green-fluorescent-protein (cβA-GFP; gift from Prof. I. Mason) plasmid DNA with Fast green (VWR) into the vitreal cavity. A current was passed through the eye with a potential difference of 20V repeated 6 times (Figure 2.5B). This allows uptake of the plasmid DNA into the cells of the neural retina. The eggs were sealed with selotape and re-incubated for 1 day (E5) before staging and fixing in 4% PFA overnight.

## 2.11 Analysis

### *2.11.1 Quantification of axons in outer regions of the retina*

Ectopic axon bundles were counted from flatmounted E16.5 mouse retinas from dorsal and ventral halves. A branched bundle was counted as two bundles. Assuming all axons projected with a general peripheral to central direction the bundle was categorized as dorsal or ventral depending on its site of origin. The average number of bundles was determined for each genotype and analysed for significance using student's paired or unpaired t-test as appropriate.

### *2.11.2 Determining proportion of looping/unordered axons in the peripheral OFL*

The radii of E13.5- E18.5 flatmounted mouse retinas were obtained using the public domain NIH Image software, with measurements taken from the centre of the optic disk to the edge of the OFL. The extent of the OFL containing looping and unordered axons was determined as a proportion of the total radius.

### *2.11.3 Total retinal cell counts*

E4 and E6 chick eyes were isolated from control or operated embryos in HBSS without calcium/magnesium (Invitrogen). The neural retinas were isolated by first incubating in HBSS at 37°C for 30 minutes to allow the RPE to be easily removed. The cells were dissociated by firstly incubating with Worthington's trypsin (Invitrogen; 10mg/ml) at 37°C for 15 minutes at E4 or 20 minutes E6 followed by drawing through a series of narrowing flame-sharpened glass pipettes to produce a single-cell suspension. Cell counts were performed on unoperated retinas, aphakic retinas and replaced-lens (control) retinas using a haemocytometer and the total number of cells per retina was determined.

### *2.11.4 Counting number of mitotic cells*

Wildtype, *slit1-/-*, *slit1-/-; slit2+/-* or *slit1/2 -/-* mouse embryos (E16.5) were cryosectioned coronally. Consecutive sections were collected onto slides. The slide with the most central eye sections was determined as the section containing the optic disk, and was stained using anti-phospho histone H3 and goat anti-rabbit IgG Cy3 (2.6.1, Table 2.2, Table 2.3) as above. In addition to this central slide, the slide 3-slides prior to the central slide, and 3-slides after the central slide were also stained, in order to label mitotic cells throughout the neural retina. The number of mitotic cells per 100μm was determined by imaging each retina and using NIH Image software to measure the length of the outer retina and count the number of labelled cells.

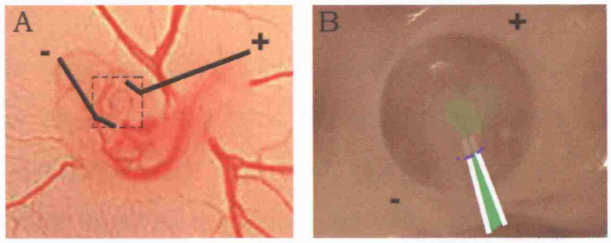


**Figure 2.5- Electroporation into the chicken retina**

Day 4 chicken embryos were "windowed" and the embryo revealed. (A) Electrodes were placed on opposite sides of the right eye, (B) cβA-GFP plasmid DNA with Fast green was injected into the vitreal cavity using a fine glass capillary and a current was passed through to allow uptake of the plasmid DNA into the cells of the dorsal neural retina.

# 3 The role of Slit and Robo in the developing optic tract

## 3.1 Introduction

### *3.1.1 Axon guidance in the optic tract*

In contrast to the large amount of research which is focused on the guidance molecules in other regions of the optic pathway; at the chiasm, in the retina and establishing the topographically organised retinotectal projection, much less is known about the cues involved in guiding the RGC axons through the optic tracts. Research to date has found a role for FGFs (McFarlane et al., 1995; McFarlane et al., 1996), β1-integrin, N-cadherin (Stone and Sakaguchi, 1996), metalloproteinases (Webber et al., 2002; Hehr et al., 2005) and HSPGs (Walz et al., 1997) in *Xenopus laevis*; GAP43 in mice (Zhang et al., 2000); CSPGs in chick (Ichijo and Kawabata, 2001) and *robo2* in zebrafish (Fricke et al., 2001; Hutson and Chien, 2002), in correct pathfinding of RGC axons through the optic tract. If these molecules are disrupted a number of guidance errors are seen at different points along the whole length of the optic tract. These include one or a combination of the following; defasciculation of axons, misprojection into aberrant regions such as the telencephalon and across the dorsal midline, and failure to enter the tectum/SC.

Two adhesion molecules that together are needed along the whole length of the optic tract are the extracellular matrix receptor β1-integrin and the calcium-dependent cell adhesion molecule N-cadherin. If their function is blocked individually in *Xenopus* using function blocking antibodies no obvious pathfinding errors are seen. However, when injected together, the antibodies caused ectopically projecting axons within the optic tract including, aberrant projections into the telencephalon and towards the hypothalamus, RGC axon defasciculation and failure to enter the tectum (Stone and Sakaguchi, 1996) (Figure 3.1B). Entry of RGC axons into the optic tectum has been reported to involve bFGF (FGF2) and FGFRs (McFarlane et al., 1995; McFarlane et al., 1996). RGCs express FGFRs, and FGF2 is expressed at a high level along the

length of the optic tract and at low levels in the tectum (McFarlane et al., 1995). It is thought to be the change in FGF levels at the optic tract/tectum boundary that allows axons to enter. If FGF2 is overexpressed along the length of the tract in *Xenopus,* or if RGCs are transfected with a dominant negative FGFR, preventing FGF signalling, RGC axons are unable to enter the optic tectum (Figure 3.1C-D) (McFarlane et al., 1995; McFarlane et al., 1996). Furthermore, expression of HS sidechains which can preferentially bind FGF2 matches expression patterns of FGF2, and overexpression, or heparitinase treatment causes the same tectal bypass, suggesting FGF2 axon guidance may require HS function (Walz et al., 1997). Another role of FGF2 and HS(FGF2) is in the elongation of RGC axons along the optic tract. Heparitinase treatment reduces axon extension and causes ectopic projection into the telencephalon. However this reduction in extension, but not the ectopic projections can be restored by the addition of FGF2, indicating FGF/HS function is needed for axons to extend along the optic tracts at the correct speed (Walz et al., 1997).

Another group of extracellular matrix molecules the CSPGs are important for intraretinal pathfinding and guidance at the optic chiasm (Snow et al., 1991; Chung et al., 2000b) but their role in guiding RGC axons through the optic tracts appears limited to preventing expansion over the diencephalic/telencephalic border (Ichijo and Kawabata, 2001). Enzymatic removal of CSPGs results in an anterior enlargement of the optic tract in chick but not in *Xenopus* (Ichijo and Kawabata, 2001; Walz et al., 2002). However conflicting evidence is seen in CS overexpression experiments which result in tectal bypass (Walz et al., 2002), suggesting a possible link for these molecules along the length of the optic tract.

A family of proteolytic enzymes, the metalloproteinases, regulates ligand/receptor interactions by cleavage of either guidance cues or their receptors (McFarlane, 2003). A role for these enzymes in axon extension and guidance is emerging, and they have been shown to have a role *in vivo* in RGC axon guidance (Webber et al., 2002; Hehr et al., 2005). Treatment of exposed *Xenopus* brain preparations with a broad spectrum metalloproteinase inhibitor causes tectal bypass defects similar to those seen when FGF signalling is disrupted (Webber et al., 2002). This is likely to be due

to metalloproteinase activity interacting with guidance cue signalling, possibly the FGF signalling pathway, but this has yet to be determined.

Defasciculation of RGC axons and the formation of ectopic projections into the telencephalon and across the midline were seen following disruption of *robo2* (*astray)* in zebrafish (Figure 3.1E-F) (Karlstrom et al., 1996; Fricke et al., 2001). This was the first time *in vivo* that Robo was shown to be involved with RGC axon guidance and suggested an involvement of Slit/Robo signalling in the optic tract.

Murine models have shown Slit1 and Slit2 (but not Slit 3) are important for RGC axon guidance in the visual system (Erskine et al., 2000; Niclou et al., 2000; Ringstedt et al., 2000; Plump et al., 2002), and have been shown to inhibit both ipsilateral and contralateral RGC axon outgrowth and promote fasciculation *in vitro* (Erskine et al., 2000; Niclou et al., 2000; Ringstedt et al., 2000; Plump et al., 2002). The Slit receptors *robo1* and *robo2* are expressed by cells in the RGC layer at the time when RGC axons are extending through the optic tract (Erskine et al., 2000; Niclou et al., 2000; Ringstedt et al., 2000; Sundaresan et al., 2004). *In vitro,* the hypothalamus and epithalamus, but not the dorsal thalamus, inhibit RGC axon outgrowth, suggesting that the bundling together of RGC axons is due to the restricted expression within the diencephalon of inhibitory guidance molecules (Tuttle et al., 1998). Little is known of the molecular nature of these signals, but , Ringstedt et al. (2000) postulated they could be Slits. Within the diencephalon, expression patterns of *slit1* and *slit2* correlate with fasciculation and innervation patterns. Expression is seen in the ventral diencephalon and epithalamus surrounding the path of the tightly fasciculated axons, but not in the dorsal thalamus where RGC axons defasciculate away from the surface (Erskine et al., 2000; Niclou et al., 2000; Ringstedt et al., 2000; Marillat et al., 2002; Piper et al., 2006). Furthermore, *in vivo* evidence has shown Slit and Robo are critical for the formation of the optic chiasm and function to maintain fasciculation and restrict the RGC axons to the optic pathway (Fricke et al., 2001; Hutson and Chien, 2002; Plump et al., 2002). The optic tract develops abnormally in zebrafish *astray/robo2* mutants, with growth across the dorsal midline and into the contralateral tectum, defasciculation

and RGC axons extending away from the optic tracts into the telencephalon and posterior into the hindbrain (Karlstrom et al., 1996; Fricke et al., 2001). In *Slit1/2* double knockout mice, the chiasm appears defasciculated and RGC axons cross the midline in an ectopic commissure (Plump et al., 2002). These data together show Slits are important for RGC axon guidance at the chiasm and suggest they may be important for guidance not just at the midline, but also of post-crossing axons along the length of the optic tract, functioning to provide a channel along which Robo-expressing RGC axons grow, promoting fasciculation and preventing aberrant growth into ectopic regions.

To determine directly the role of Slit and Robo in regulating optic tract development, I analysed mice lacking *slit1* and/or *slit2* (Plump et al., 2002), *robo1* (Andrews et al., 2006) or *robo2* (Lu et al., 2007). The results demonstrate that Slit/Robo signalling does not play a significant role in regulating the fasciculation of the optic tract but is an important component of the guidance mechanism that restricts RGC axons to the optic pathway and prevents them crossing the diencephalic/telecephalic boundary and extending into the epithalamus. This provides direct evidence that, in addition to their function at the optic chiasm, Slits and Robos are also required for the guidance of post-crossing RGC axons.

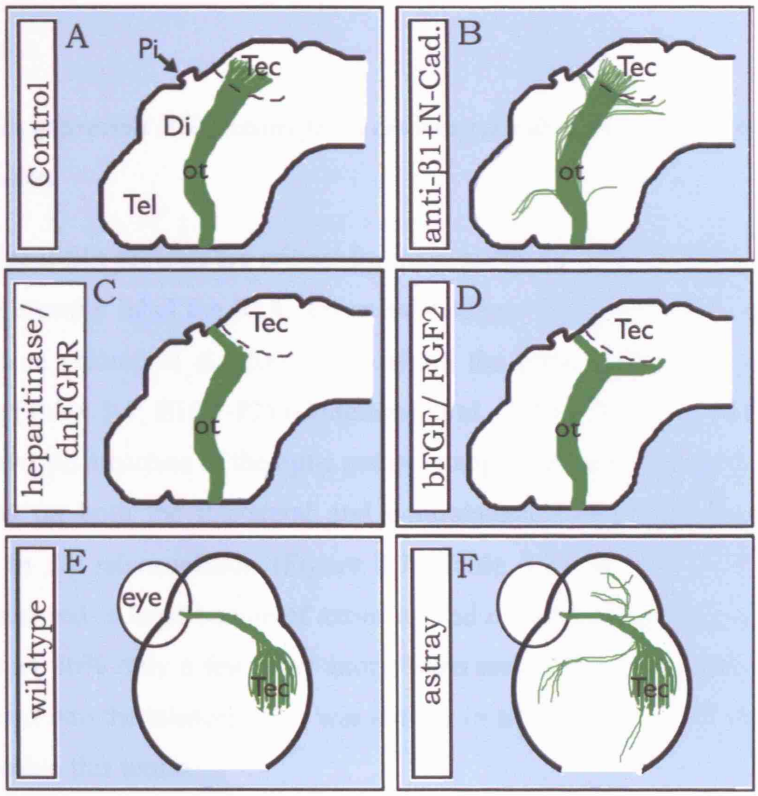


**Figure 3.1- Diagrammatic examples of axon guidance defects in the optic tract.**

(A-D) Lateral view of the optic tract in *Xenopus*. Dorsal is up, rostral is left. *(*A) The normal optic tract of the *Xenopus* projects dorso-caudally along the surface of the diencephalon towards the optic tectum. (B) Following injections of function-blocking antibodies against β1-integrin and N-cadherin, RGC axons project anteriorly and posteriorly away from the optic tract, bypassing the tectum ventrally and anteriorly and appear defasciculated. (C) Following treatment with heparitinase to remove endogenous heparan sulphate or transfection of RGCs with dominant-negative FGF receptor (dnFGFR), RGC axons bypass the tectum and project across the dorsal midline. (D) Following treatment with exogenous bFGF, RGC axons bypass the tectum ventrally and cross the dorsal midline. (E-F) A dorsal view of the optic tract in zebrafish, anterior is up. (E) The normal optic tract of zebrafish projects dorso-caudally along the surface of the diencephalon towards the tectum. (F) In *astray/robo2* mutants, RGC axons project across the dorsal midline and into the opposite tectum, anteriorly into the telencephalon, and posteriorly into the hindbrain. Axons also appear defasciculated. Tec, tectum; Di, diencephalon; Tel, telencephalon; ot, optic tract; Pi, pineal.

## 3.2 Results

### *3.2.1 Slits help prevent RGC axons from crossing the diencephalic/ telencephalic boundary*

To determine if Slit proteins are critical for axon guidance in the optic tracts, DiI was used to unilaterally label the RGC axons in wildtype (WT) and *slit1*- and/or *slit2*-deficient mice (Plump et al., 2002) throughout the period when the optic tract is developing (Table 3.1; E16.5-P2) (Godement et al., 1984). In *slit1*-/-; *slit2* +/- mice, whilst the overall structure of the optic pathway appeared grossly normal, a subset of RGC axons on both the ipsilateral and contralateral side of the brain extended aberrantly in the telencephalon (Figure 3.2; Table 3.2). In 70% (7/10) of E16.5 embryos analysed, a large bundle of axons extend into the telencephalon whereas in the remaining 30% only a few stray axons were seen. The site at which the RGC axons crossed into the telencephalon was similar in all embryos, as was the path they followed within this tissue.

Similar defects also occurred in all E18.5 (n=6) and P2 (n=2) *slit1* -/-; *slit2* +/- animals with the number of RGC axons in both ipsilateral and contralateral telencephalon becoming more substantial as development proceeds (Figure 3.3C-D). This increase in the number of aberrantly located axons could occur because a subset of both young and old RGC axons are dependent on Slits for their guidance or, indirectly, as a result of later generated axons following lost pioneer axons. Irrespective of the underlying mechanism, this demonstrates that, at least by early postnatal stages, these guidance errors are not corrected. In embryos lacking *slit1* or *slit2* individually or, surprisingly, in *slit1/2* -/- mice in which significant projection errors occur at the optic chiasm (Plump et al., 2002) (Figure 3.2F, Figure 3.3E), RGC axons did not extend into the ventral telencephalon in significant numbers (Figure 3.2C, D, F, Figure 3.3E; Table 3.2). At best, only a few stray axons were seen (Figure 3.2G).

To visualise the entire path of the optic tract, the telencephalon was removed and the brains viewed laterally (Figure 3.4). In wildtype embryos, RGC axons extended through the proximal region of the optic tract as a single, tightly grouped bundle (Figure 3.4B). In all *slit1* -/-; *slit2* +/- and *slit1/2* -/-, but not the single mutant mice, a large branch developed at a point just ventral to the dorsal thalamus (Table 3.2). This branch always developed from the side of the optic tract closest to the telencephalon, was composed of axons that were tightly bundled and, unlike the endogenous tract, was not integrated into the diencephalon (Figure 3.4C, D). Labelled RGC axons were also present on the medial surface of the telencephalic tissue removed from *slit1* -/-; *slit2* +/- and *slit1/2* -/-, but not wildtype embryos, demonstrating that this branch extended across the diencephalic/telencephalic boundary (Figure 3.4E-G).

### *3.2.2 RGC axons are restricted to the surface of the telencephalon*

To determine if in the *slit*-deficient mice, RGC axons make additional pathfinding errors not evident from the wholemount views, the DiI-labelled brains were sectioned coronally. In wildtype animals, the RGC axons were restricted to the diencephalon (Figure 3.5A, B, E). In only 11% (2/19) of embryos were 1 or 2 RGC axons seen that crossed into the telencephalon. It is likely these are axons that have made pathfinding errors, which may later be corrected (Hutson and Chien, 2002). RGC axons also were restricted predominately to the diencephalon in *slit1* and *slit2* single knockout mice, although the extension of small number of RGC axons into the telencephalon occurred more frequently than in wildtype mice (*slit1*, 25%, *slit2*, 14% of embryos). However, in *slit1* -/-; *slit2* +/- embryos, two distinct projection errors were found: In 72% (13/18) of embryos, a subset of RGC axons projected over the ventral surface of the telencephalon (Figure 3.5C). In the remaining 28% of embryos, fewer axons extended into the ventral telencephalon and, additionally, a subset of axons extended into the medial telencephalon (Figure 3.5F). This medial projection often appeared as a distinct branch extending along the outer surface of the telencephalon (Figure 3.5G, H). Extension of RGC axons into and along the medial,

**Table 3.1- Number of wildtype and *slit*-deficient mice (E16.5-P2) analysed.**

| **Genotype** | **Wholemounts** | | **Sectioned** |
|---|---|---|---|
| | **Intact** | **Telencephalon removed** | |
| **Wildtype** | 12 | 8 | 19 |
| ***Slit1* +/-** | 4 | 12 | 8 |
| ***Slit1* -/-** | 8 | 12 | 8 |
| ***Slit2* +/-** | 6 | 5 | 6 |
| ***Slit2* -/-** | 3 | 11 | 7 |
| ***Slit1* -/-; *Slit2* +/-** | 17 | 18 | 21 |
| ***Slit1* -/-; *Slit2* -/-** | 10 | 7 | 10 |

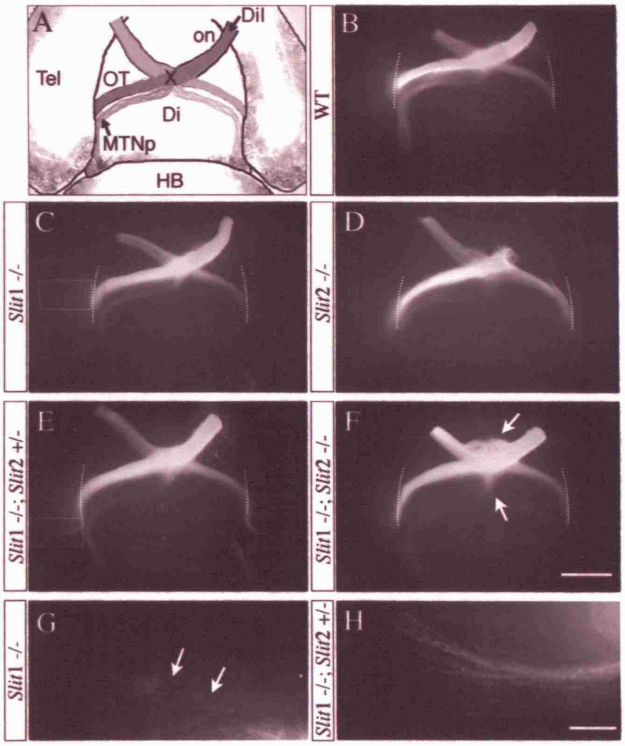


**Figure 3.2- RGC axons extend into the telencephalon in *slit*-deficient mice.**

(A) Schematic diagram of the path followed by RGC axons over the surface of the diencephalon in wildtype mice, Di, diencephalon, HB, hindbrain, MTNp, medial terminal nucleus projection, on, optic nerve, OT, optic tract, Tel, telencephalon, X, optic chiasm. (B-F) Unilateral DiI labelling of the proximal optic pathway in E16.5 embryos. In each image the edges of the telencephalon are indicated by the lines. In wildtype embryos (B), RGC axons extend from the chiasm into the optic tracts and, as they grow over the surface of the diencephalon, become obscured from view by the overlying telencephalic vesicles. In *slit1 -/-* (C, G), *slit2 -/-* (D) and *slit1/2 -/-* (F) embryos, RGC axons are restricted predominately to the diencephalon. However, in *slit1 -/-*; *slit2 +/-* mice (E), a subset of RGC axons grows into and along the ventral surface of the telencephalon. Arrows in (F) indicate RGC axons extending aberrantly at the optic chiasm. Boxed regions in (C) and (E) are shown at higher power in (G) and (H) respectively. (G) Arrows indicate small number of DiI labelled RGC axons extending into the telencephalon in the absence of *slit1* alone. (H) In *slit1 -/-*; *slit2 +/-* embryos significantly more RGC axons grow into this region. Bar, 800μm (B-F), 200μm (G-H).

**Table 3.2- Percentage of wildtype and *slit*-deficient mice (E16.5-P2) with RGC axons extending aberrantly into the telencephalon**

| **Genotype** | **Axons on ventral surface of telencephalon (Figure 3.2E)** | | **Ectopic branch from optic tract (Figure 3.4C)** |
|---|---|---|---|
| | **Few axons (eg. Figure 3.2G)** | **Large bundle (eg. Figure 3.2H)** | |
| Wildtype | 0% (12) | 0% (12) | 0% (8) |
| *Slit1* -/- | 13% (8) | 13% (8) | 0% (12) |
| *Slit2* -/- | 0% (3) | 0% (3) | 0% (11) |
| *Slit1* -/-; *Slit2* +/- | 28% (18) | 72% (18) | 100% (8) |
| *Slit1* -/-; *Slit2* -/- | 25% (10) | 0% (10) | 100% (7) |

(n) = number analysed.

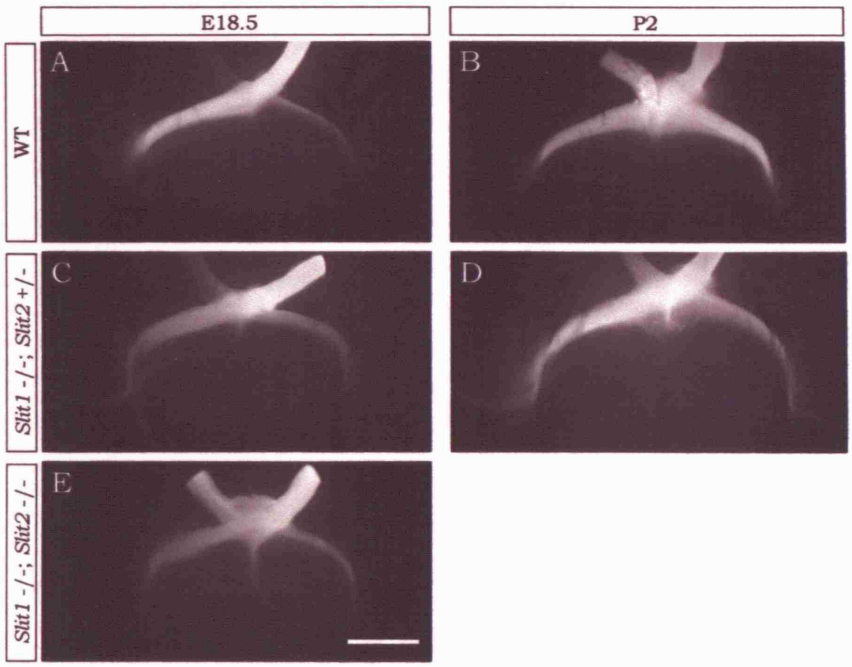


**Figure 3.3- Growth of RGC axons into the telencephalon of *slit*-deficient mice is maintained after birth.**

Unilateral DiI labelling of RGC axons in E18.5 (A, C, E) or P2 (B, D), wildtype (A, B), *slit1 -/-*; *slit2 +/-* (C, D) or *slit1/2 -/-* (E) mice. In *slit1 -/-*; *slit2 +/-* (C, D) but not *slit1/2 -/-* mice (E) a subset of RGC axons grow over the surface of the telencephalon. Bar, 800μm.

but not the ventral, surface of the telencephalon also was seen in all (10/10) *slit1/2* -/- embryos (Figure 3.5D, I).

Sectioning the embryos sagitally revealed no additional defects (Figure 3.6) and, in all genotypes, RGC axons did not extend away from the pial surface into deeper regions of the telencephalon. The ectopic ventral projection in *slit1* -/-; *slit2* +/- embryos can be seen projecting ventrally away from the optic tract onto the ventral surface of the telencephalon (Figure 3.6D, E). The ectopic medial projection can be seen projecting in a dorso-anterior direction in the *slit1/2* -/- embryos into the telencephalon (Figure 3.6G, H).

### *3.2.3 In slit1/2 -/- embryos a subset of RGC axons extends into the epithalamus but many RGC axons are still able to reach the SC successfully.*

In *slit1/2* -/- mice (7/7) but none of the other genotypes, RGC axons also made guidance errors in more dorsal regions of the optic tract. As they approached the dorsal midline, the RGC axons followed a more anterior trajectory than in wildtype animals, and a subset extended away from the tract into the epithalamus, including the pineal, and across the dorsal midline (Figure 3.7)(Figure 3.6C, F, I). These axons are not restricted to the surface; they invade deep into the diencephalon (Figure 3.7B, D, F). They appear to defasciculate over the surface of the epithalamus away from the optic tract (Figure 3.7H). However, many RGC axons reached the SC. Since the *slit1/2* -/- mice die at birth (Plump et al., 2002), this was determined at E18.5, using three different methods. Firstly, the RGC axons were anterogradely labelled with DiI and viewed either as wholemounts or in sections. Using this approach, labelled axons were always detected within the SC (Figure 3.8A, B). Secondly, an anti-calretinin antibody was used to label the entire optic projection. RGC axons within the brachium of the SC were labelled as were a subset of cells within the SC (Figure 3.8C-F), Finally, small crystals of DiI were placed in the SC and resulted in retrogradely labelled RGC axons throughout the optic pathway (Figure 3.8G, H) and within the retina (Figure 3.8I, J). These data all confirm that many RGC axons reach their primary target.

### *3.2.4 RGC axon path-finding defects occur in regions where slits are expressed normally*

When the *slit*-deficient mice were generated, *tau*-GFP was knocked into the gene locus under control of the slit promoters (Yuan et al., 1999b; Erskine et al., 2000; Niclou et al., 2000; Ringstedt et al., 2000; Plump et al., 2002). Consequently, any cells that normally express *slit1* or *slit2* now express GFP in their cell bodies and processes. In *slit1* +/- and *slit2* +/- tissue, strong expression of GFP was found in the diencephalon and telencephalon in patterns that correlate with the RGC axons guidance errors (Figure 3.9). In *slit1* +/- embryos, anti-GFP staining was seen in the hypothalamus, with high expression around the chiasm, and in the epithalamus and telencephalon, regions into which RGC axons extend in the absence of Slits. By contrast, no anti-GFP staining was detected in the dorsal thalamus or SC (Figure 3.9A-D). In *slit2* +/- animals, GFP was expressed strongly along the length of the midline and in the epithalamus and hypothalamus. Staining also was seen on the medial and ventral surfaces of the telencephalon, corresponding to the position where RGC axons grow in the *slit*-deficient mice. Strong expression of GFP also was found at the dorsal midline and in the pineal (Figure 3.9E-H). *In situ* hybridisation using riboprobes for *slit1-3* revealed essentially identical patterns of expression and demonstrated that, within the telencephalon, *slit3* is expressed in a pattern complementary to that of *slit1* and *slit2* (Figure 3.9I-K). Whereas *slit1* and *slit2* are expressed in regions of the telencephalon directly adjacent to the diencephalon (Figure 3.9I, J), *slit3* is present in a more dorsal domain and was not detected within the ventral region of the telencephalon (Figure 3.9K).

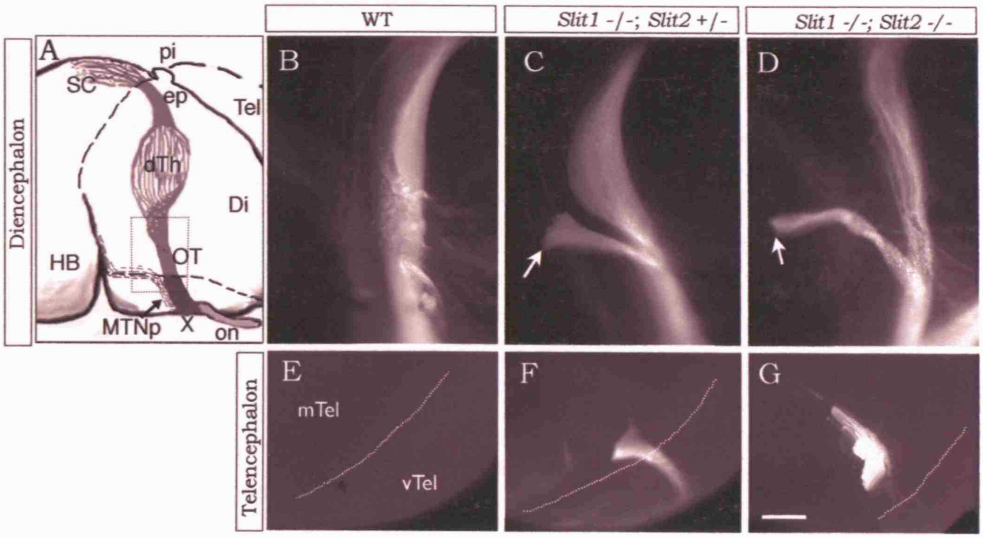


**Figure 3.4- A branch develops from the optic tract in *slit*-deficient embryos and extends into the telencephalon.**

(A) Schematic diagram of the path followed by the RGC axons as they extend from the optic chiasm towards their targets. Boxed region indicates areas shown in panels B-D. dTh, dorsal thalamus, ep, epithalamus, mTel, medial telencephalon, pi, pineal. (B-D) DiI-labelled RGC axons within the proximal region of the optic tract of E16.5 embryos viewed following removal of the telencephalon. In wildtype embryos (B), RGC axons are tightly bundled together as they extend through the proximal region of the optic tract. In *slit1 -/-; slit2 +/-* (C) and *slit1/2 -/-* (D) embryos, RGC axons remain tightly bundled. However, a large branch (arrows) extends laterally away from the surface of the diencephalon. (E-G) Medial view of the telencephalic tissue removed from the embryos shown in panels (B-D). The dotted line indicates the approximate boundary between medial and ventral telencephalon. In *slit1 -/-; slit2 +/-* (F) and *slit1/2* (G) but not wildtype (E) embryos RGC axons extend over the medial surface of the telencephalon. Bar, 200μm (B-D), 300μm (E-G).

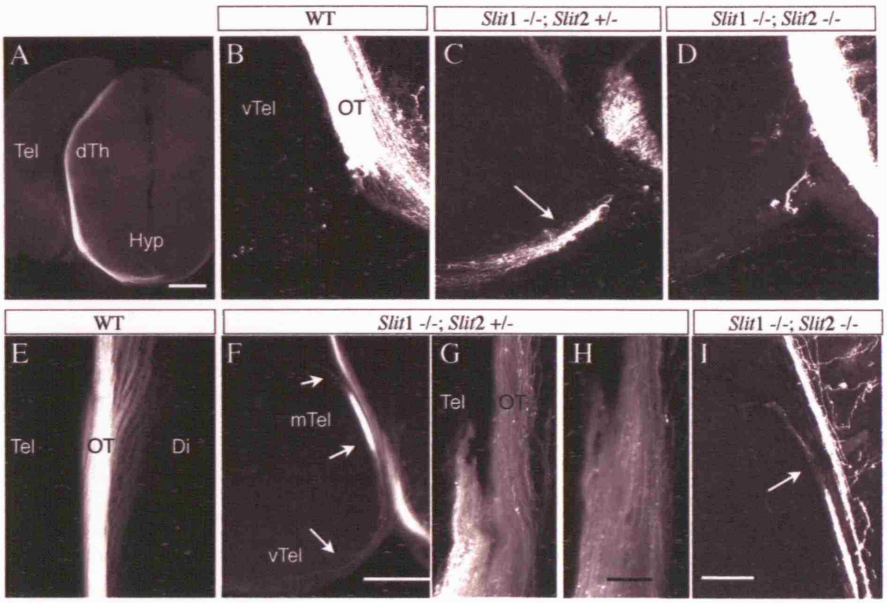


**Figure 3.5- In the telencephalon, RGC axons are restricted to the pial surface.**

Coronal sections of DiI-labelled E16.5 wildtype (A, B, E), *slit1 -/-; slit2 +/-* (C, F, G, H) and *slit1/2* (D, I) brains. (A) Path followed by the RGC axons as they extend through the optic tracts in wildtype embryos. (B-I) Confocal images of ventral (B-D) or medial (E-I) telencephalon. In wildtype embryos (B, E) RGC axons are restricted to the diencephalon. In s*lit1 -/-; slit2 +/-* embryos, a subset of RGC axons extend into the ventral (arrow in panel C) or ventral and medial (arrows in panel F) telencephalon. Extension of RGC axons on the medial surface of the telencephalon also occurs (G, H). In *slit1/2 -/-* embryos, a subset of RGC axons extends into medial (arrow in panel I) but not ventral telencephalon (D). In all embryos, RGC axons within the telencephalon are restricted to the pial surface (C, F-I). Hyp, hypothalamus, vTel, ventral telencephalon. Bar, 500μm (A), 300μm (B-E, I), 100μm (F), 50μm (G, H)

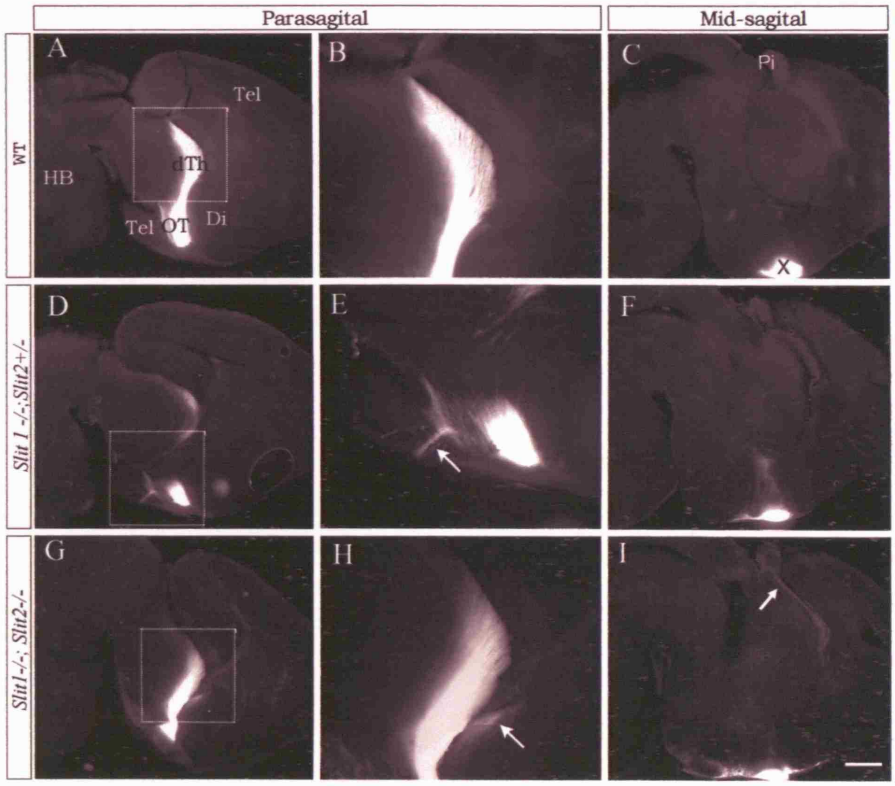


**Figure 3.6- Sagital sectioning reveals no further ectopic projections.**

(A-B, D-E, G-H) Parasagital sections and (C, F, I) mid sagital sections of E16.5 wildtype (A-C), *slit1* -/-; *slit2* +/- (D-F) and *slit1/2* -/- DiI-labelled brains. The boxed regions in panel A, D and G are shown at higher power in B, E and H respectively. In wildtype embryos (A-C), RGC axons are restricted to the diencephalon. In *slit1* -/-; *slit2* +/- embryos (D-F), a subset of RGC axons leaves the optic tract and project ventrally into the telencephalon (arrow in E). In *slit1/2* -/- embryos (G-I) RGC axons leave the optic tract and project more dorsally into the telencephalon (arrow in H), and axons are seen at the dorsal midline projecting towards the pineal (arrow in I), axons are not seen at the dorsal midline in other genotypes (C, F). Bar, 500μm (A, C-D, F-G, I), 200μm (B, E, H).

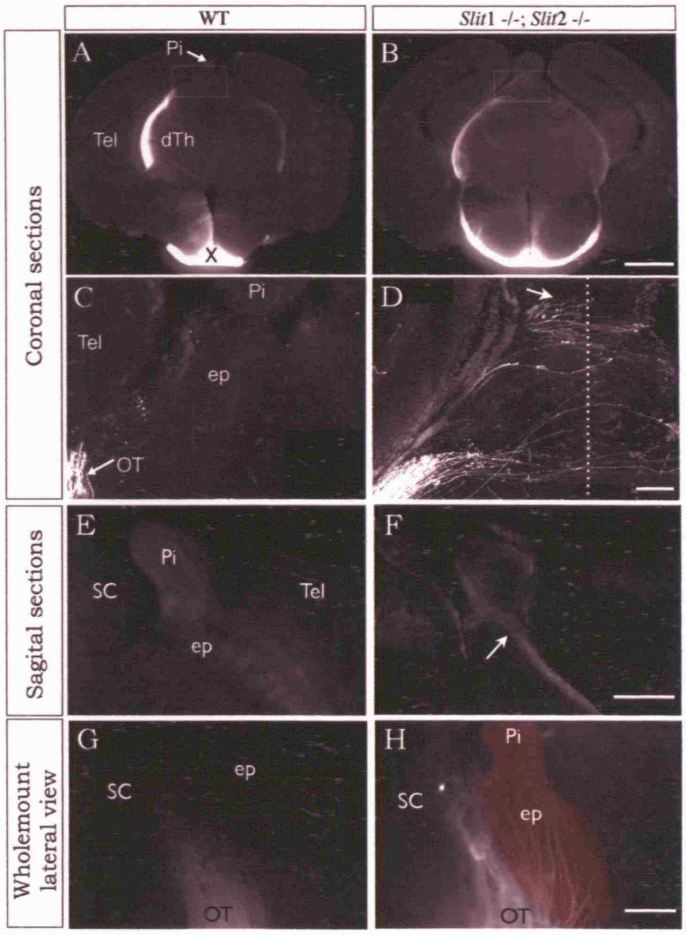


**Figure 3.7- RGC axons make guidance errors in more dorsal regions of the optic tract.**

(A-F) Coronal (A, B) or sagital sections (E, F) of E16.5 wildtype (A, E) and *slit1/2 -/-* (B, F) DiI-labelled brains. Confocal images of the boxed regions in panels A and B are shown at higher power in panels C and D respectively. (G, H) Lateral view of dorsal optic tract following removal of the telencephalon in wildtype (G) and *slit1/2 -/-* (H) DiI-labelled brains. In wildtype embryos (A, C, E, G), RGC axons avoid the epithalamus and turn posteriorly away from this region towards the SC, no axons are seen entering this region. In *slit1/2 -/-* embryos (B, D, F, H), a subset of RGC axons leave the optic tract and grow into the epithalamus (red region in panel H) where they extend across the dorsal midline of the nervous system (dotted line in panel D) and into the pineal (arrow in panels D and F). Arrows in panels A and C indicate the pineal (Pi) and optic tract (OT) respectively. Bar, 700μm (A, B), 100μm (C, D), 250μm (E, F), 200μm (G, H).

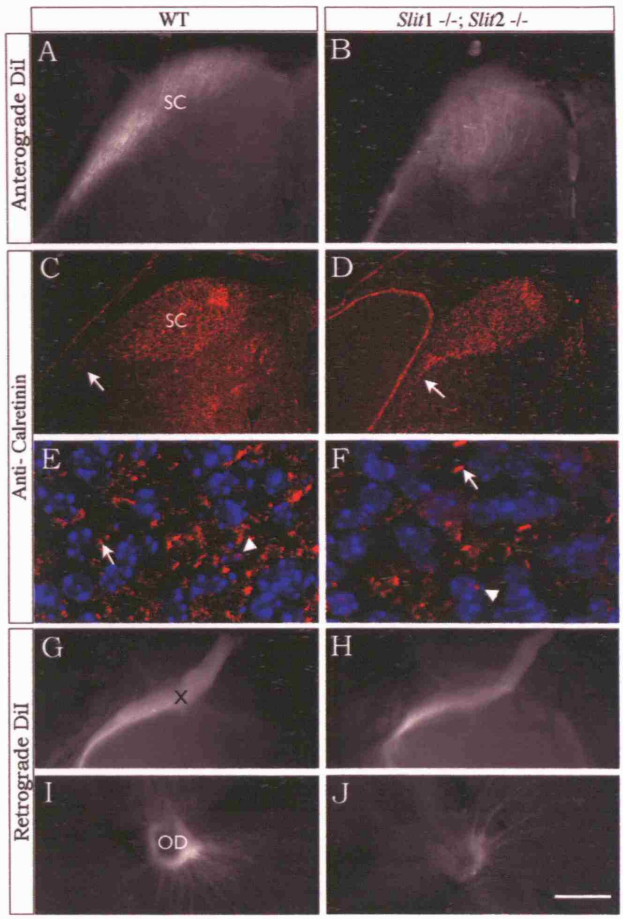


**Figure 3.8- In the absence of Slits, many RGC axons reach the SC.**

(A-F) Coronal sections through the SC of E18.5 wildtype (A, C, E) or *slit1/2* -/- (B, D, F) brains following anterograde labelling of the RGC axons with DiI (A, B) or stained with an anti-calretinin antibody (red) and DAPI (blue) to label the RGC axons and cells of the SC respectively (C-F). DiI-labelled (A, B) and calretinin-positive RGC axons (C-F) are present within the brachium of the SC (arrows in panels C, D) and the main body of the SC of both wildtype (A, C, E) and *slit1/2* -/- (B, D, F) embryos. In addition to RGC axons (arrows in panels E, F), calretinin also labels a subset of SC cells (arrowheads) in both wildtype (E) and *slit1/2* -/- (F) embryos. (G-J) Ventral view of E18.5 wholemount brains (G-H) or E18.5 flatmount retinas (I-J) following retrograde labelling of RGC axons with DiI from the SC. DiI-labelled RGC axons are present within the chiasm and retina in both wildtype and *slit1/2* -/- embryos. Bar, 300μm (A-D), 50μm (E, F), 800μm (G, H), 250μm (I, J).

### *3.2.5 The Slit receptors, robo1 and robo2, are expressed by RGCs*

*In situ* hybridisation has shown previously that *robo1* and *robo2* are expressed in the developing murine retina (Yuan et al., 1999b; Erskine et al., 2000; Niclou et al., 2000; Ringstedt et al., 2000; Marillat et al., 2002). I decided to repeat the *in situ* hybridisation looking at mouse retinas at E16.5, at the same time as establishing the expression in the retina of the other Robo family members (*robo3* and *robo4)* (Huminiecki et al., 2002; Park et al., 2003). *Robo1,* at this age appears to be expressed in a subset of cells in the inner layers of the retina (Figure 3.10B), while r*obo2* is expressed by the vast majority of cells in the RGC layer (Figure 3.10C). However, *robo3 (rig1)* is not expressed in the neural retina (Figure 3.10D). Expression of *robo4* (*magic roundabout*) has previously been shown to be vascular-specific (Huminiecki and Bicknell, 2000; Huminiecki et al., 2002). To confirm it is not expressed by RGCs during development a riboprobe against *robo4* was created and expression was examined. At E16.5 no specific expression of *robo4* was seen in the RGC layer (Figure 3.10E). As a positive control, expression of *robo4* in E14.5 limbs and in E16.5 sectioned brain was analysed; *robo4* is expressed in a specific manner within both these tissues (Figure 3.10F-G). This expression is in a pattern similar to the developing vasculature.

Antibody staining using two different antibodies against Robo1 and Robo2 were used to determine protein expression of these molecules within the retina at E16.5. Robo1 and Robo2 expression was seen in the RGC layer, OFL and optic nerve head (Figure 3.10H-K); Robo2 expression was stronger than Robo1, which only appeared to be expressed by a subset of cells, confirming the *in situ* hybridisation data. To confirm RGCs express Robo1 and Robo2, protein expression at the optic chiasm was examined; this region contains only RGC axons and was found to express both Robo1 and Robo2 (Figure 3.10L-O). Together with the *in situ* hybridisation results, these data demonstrate that Robo1 and Robo2, but not Robo3 (Rig1) and Robo4, are expressed by RGCs. The functional significance of Robo1 and Robo2, in terms of RGC axons guidance was therefore examined.

### *3.2.6 Robo2, but not Robo1, is essential for axon guidance within the developing optic tract*

A detailed analysis of optic tract development in *robo1*- and *robo2*-deficient mice has been performed by others, which revealed additional pathfinding errors not seen in the *slit* mutants (Dr. W. Andrews and Prof. J. Parnavelas; Department Anatomy and Developmental Biology, University College London, personal communication). To establish if this disparity is due to differences in the analysis method, DiI was used to unilaterally label the RGC axons in E16.5 wildtype and *robo1*- or *robo2*-deficient embryos (Figure 3.11) (Andrews et al., 2006; Lu et al., 2007). Labelled brains were viewed as wholemounts and laterally following telencephalon removal (Table 3.3). The development of the chiasm and optic tract of *robo1*-deficient and *robo2* +/- mice was largely normal, and the overall fasciculation was unchanged (Figure 3.11 B-C, H-I). However, at the ventral midline of *robo2*-deficient mice, errors were seen which resemble those seen in the *slit1/2*-deficient mice (Plump et al., 2002) (Figure 3.2 F). These include, the development of an ectopic commissure in the pre-optic area, axons projecting into the contralateral optic nerve and axons projecting caudally along the ventral midline (n=6, 100%; Figure 3.11F, Figure 3.13D). Following removal of the telencephalon; an ectopic branch could be seen leaving the optic tract in *robo2* -/- embryos (n=4, 100%; Figure 3.11L), but not in other genotypes (Figure 3.11H-K).

In order to look in more detail at the developing optic tract, the embryonic brains were sectioned coronally (Figure 3.12, Figure 3.13; Table 3.4). In *robo1*-deficient embryos RGC axons are restricted to the developing optic tract and no axons project into the telencephalon (Figure 3.12F, G) or into other aberrant regions of the brain (Figure 3.12C, D, I, J). However, in agreement with the previous study (Andrews and Parnevelas; Personal communication) several defects in axon pathfinding were seen in *robo2*-deficient embryos, showing similarity to the axon guidance defects in *slit1/2*, with the addition of a further pathfinding error unique to the total loss of *robo2*. In *robo2*-deficient mice, axons cross the diencephalic/telencephalic boundary and project along the surface of both the medial and ventral telencephalon (Figure

3.13G), and also extend into the epithalamus and across the dorsal midline (Figure 3.13J). Interestingly, in 40% (n=5) of *robo2* +/- embryos a small number of RGC axons are seen projecting aberrantly into the ventral telencephalon (Figure 3.13F) and epithalamus (Figure 3.13I). In these cases the number of aberrant axons was always fewer than seen in *robo2* -/- embryos. In addition to these pathfinding errors which are also seen in *slit1/2*-deficient mice, in *robo2-/-* mice a unique pathfinding error was seen; a subset of RGC axons cross into the telencephalon and project away from the surface towards the cortex (Figure 3.13M).

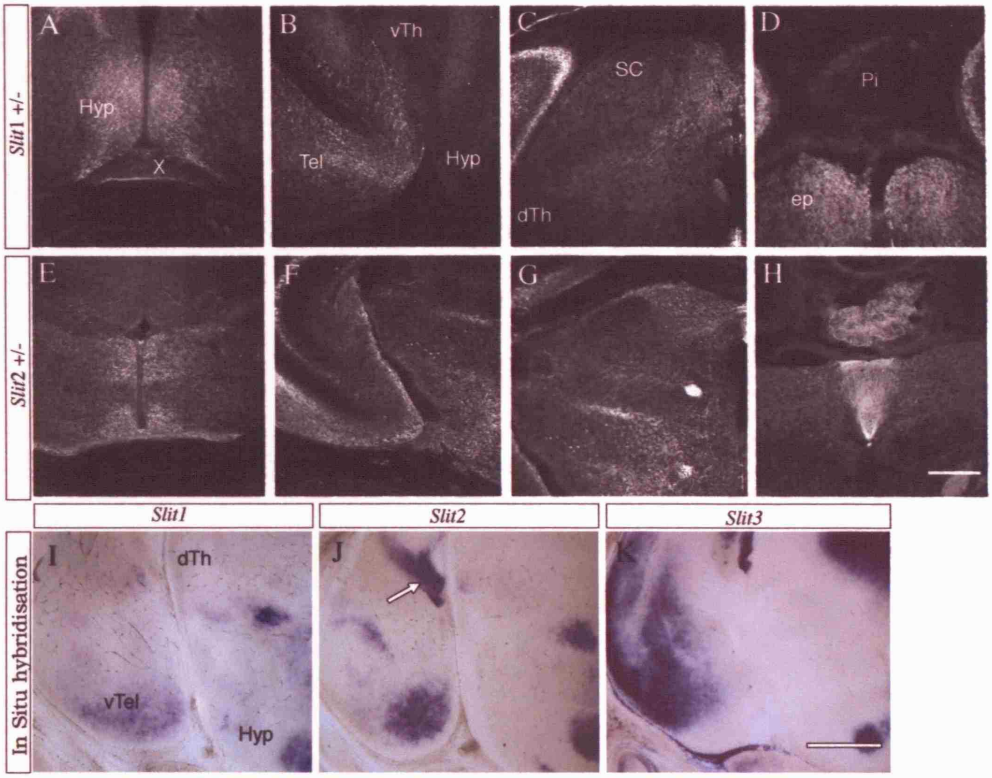


**Figure 3.9- Determination of *slit* expression in the region of the developing optic tract.**

(A-H) Coronal sections of E17.5 *slit1* +/- (A-D) or *slit2* +/- (E-H) embryos at the level of the hypothalamus (A, B, E, F), SC (C, G) and pineal (D, H). In both *slit1* +/- and *slit2* +/- embryos, tau-GFP is expressed in the hypothalamus surrounding the developing optic chiasm (A, E), in the ventral region of the telencephalon (B, F) and in regions bordering the SC (C, G) including the epithalamus (D, H). In *slit2* +/- but not *slit1* +/- tissue, tau-GFP also is strongly expressed in the roof-plate and the pineal (D, H). Bar, 300μm (A-C, E-G), 150μm (D,H). (I-K) In situ hybridization using riboprobes for *slit1* (I), *slit2* (J) or *slit3* (K). *slit1* and *slit2* are expressed within the ventral region of the telencephalon adjacent to the diencephalon, whereas *slit3* is expressed more dorsally and laterally. Arrow in panel J indicates strong expression of *slit2* within the medial region of the telencephalon. Bar, 300μm

**Figure 3.10- Determination of robo expression in the developing visual system.**

(A) Schematic diagram illustrating the structure of the retina. (B-E) Coronal sections of E16.5 WT embryos following *in situ* hybridisation using digoxigenin-labelled riboprobes for *robo1* (B), *robo2* (C), *robo3 (rig1;* D) or *robo4* (E). Expression of *robo1* and *robo2* is seen in the RGC layer. *Robo3* and *robo4* are not expressed by RGCs. (F) Dorsal view of E14.5 WT limb following *in situ* hybridisation using digoxigenin-labelled riboprobes for *robo4.* (G) Coronal section of an E16.5 WT embryo following *in situ* hybridisation using digoxigenin-labelled riboprobes for *robo4,* showing telencephalon at dorsal midline. (F-G) *robo4* shows specific expression in the limb at E14.5 and in the telencephalon of E16.5. (H-M) Horizontal and (N-O) coronal sections of E16.5 WT embryos stained with commercial antibodies (H-I, L-M) or Murakami antibodies (J-K, N-O) against Robo1 (H, J, L, N) or Robo2 (I, K, M, O) showing the retina (H-K) and chiasm (L-O). Robo1 is expressed by a subset of cells in the RGC layer (H, J) and by RGC axons at the chiasm (L, N). Robo2 is expressed by cells in the RGCs (I, K) and by RGC axons at the chiasm (M, O). RPE, retinal pigment epithelium; OFL, optic fibre layer; X, chiasm. Bar, 200μm (B-E, H-K), 350μm (F), 150μm (G), 250μm (L-O).

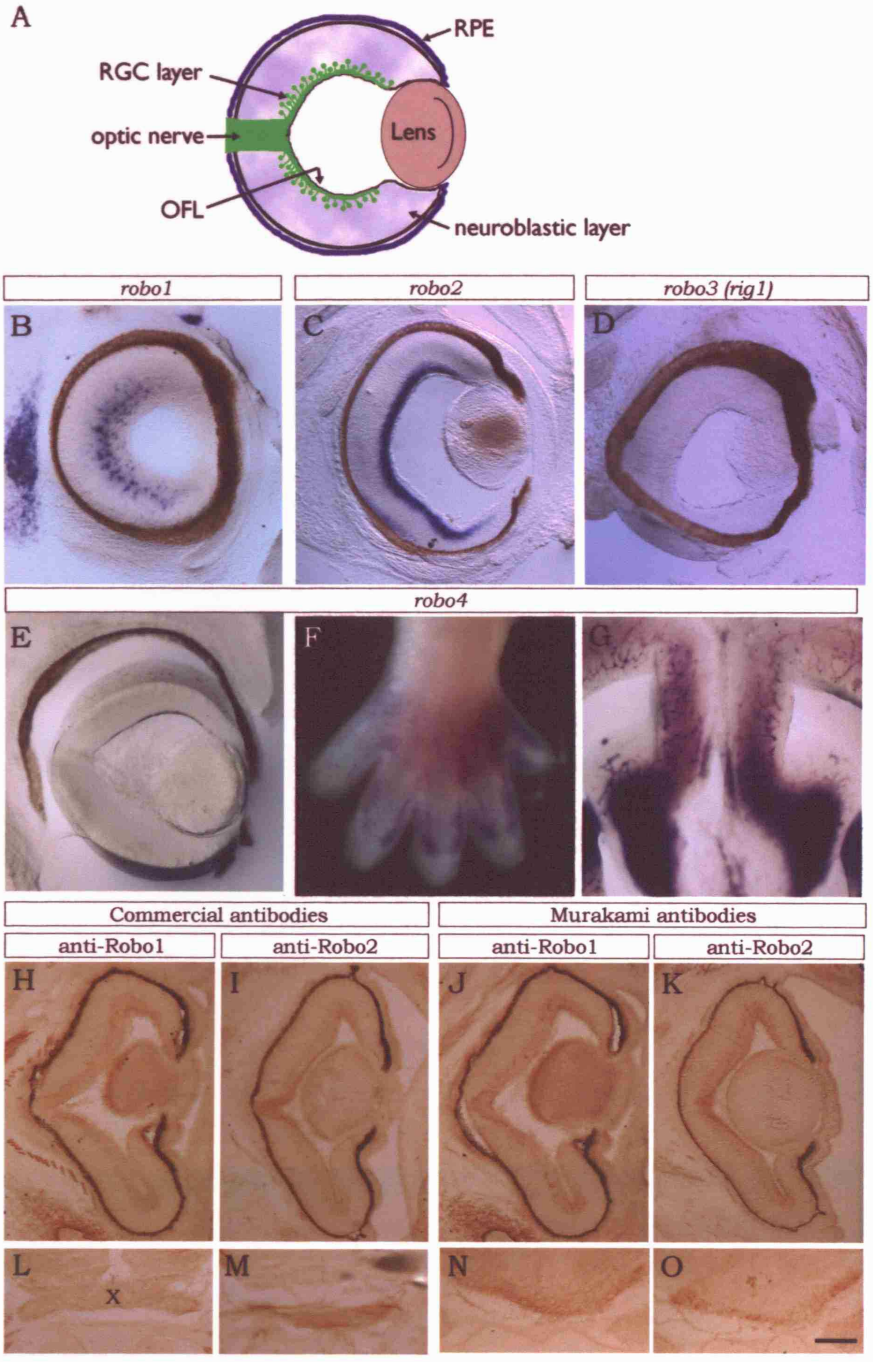
A
RPE
RGC layer
Lens
optic nerve
OFL
neuroblastic layer
robo1
robo2
robo3 (rig1)
B
C
D
robo4
E
F
G
Commercial antibodies
Murakami antibodies
anti-Robo1
anti-Robo2
anti-Robo1
anti-Robo2
H
I
J
K
L
M
N
O
X

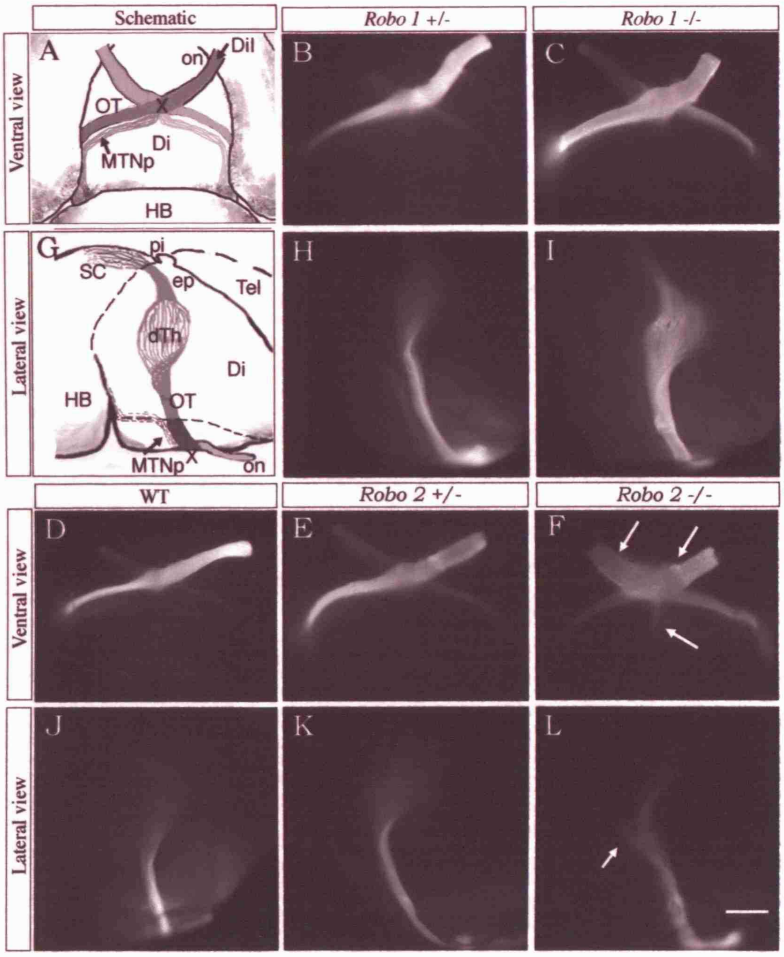


**Figure 3.11- Axon guidance errors are seen in *robo2*-, but not *robo1*- deficient mice.**

(A, G) Schematic diagrams of the path followed by RGC axons over the surface of the diencephalon in wildtype mice. Ventral view (B-F) and lateral view (H-L). Unilateral DiI labelling of the proximal optic pathway in E16.5 embryos. In *robo1* +/- (B, H) *robo1* -/- (C, I), and *robo2* +/- (E, K) RGC axons follow the same path as wildtype embryos. However, in *robo2* -/- (F, L), RGC axons project into the preoptic area and caudally along the ventral midline (arrows in panel F) and a large branch (arrows in panel L) extends laterally away from the optic tract. Bar, 500μm.

**Table 3.3- Number of *robo*-deficient mice (E16.5) analysed.**

| Genotype | Wholemounts | | Sectioned |
|---|---|---|---|
| | Intact | Telencephalon removed | |
| ***Robo1*** **+/-** | 6 | 2 | 3 |
| ***Robo1*** **-/-** | 6 | 2 | 6 |
| ***Robo2*** **+/-** | 7 | 2 | 5 |
| ***Robo2*** **-/-** | 9 | 4 | 5 |

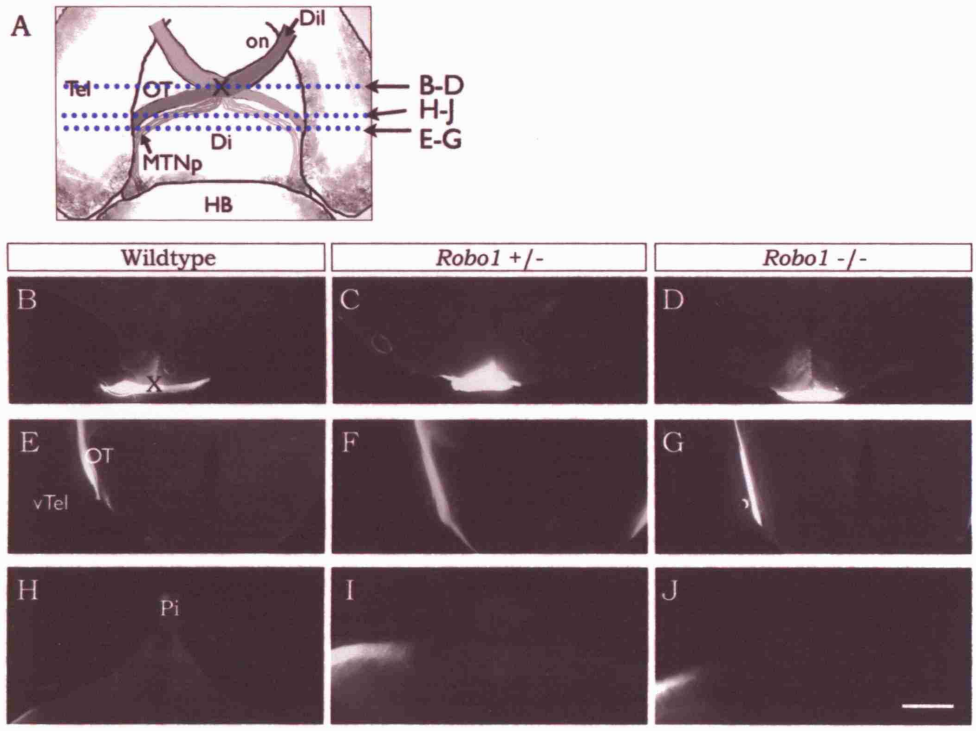


**Figure 3.12- RGC axons project normally in *robo1*-deficient mice.**

(A) Schematic diagram of the optic tract showing where sections were taken, as seen below. (B-J) Coronal sections of DiI-labelled E16.5 wildtype (B, E, H), *robo1* +/- (C, F, I) and *robo1* -/- (D, G, J) at the level of the chiasm (B-D), the optic tract (E-G) and the pineal (H-J). In *robo1*-deficient mice RGC axons were seen to project normally at the chiasm, and did not enter the ventral telencephalon or pineal. RGC axons remain in a tightly fasciculated bundle, as seen in the wildtype mice. Bar, 700μm (B-G) and 200μm (H-J).

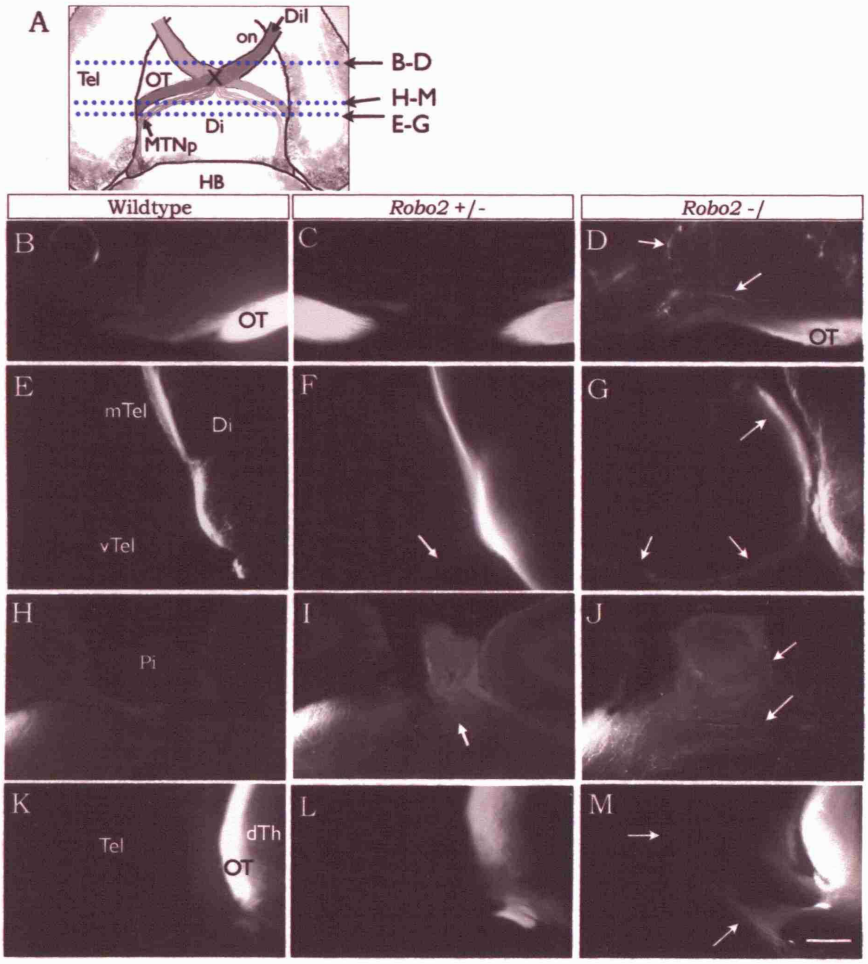


**Figure 3.13- RGC axons project aberrantly in *robo2*-deficient mice.**

(A) Schematic diagram of the optic tract showing where sections were taken, as seen below. Coronal sections of DiI-labelled E16.5 wildtype (B, E, H, K), *robo2* +/- (C, F, I, L) and *robo2* -/- (D, G, J, M) at the level of the preoptic region (B-D), the ventral optic tract (E-G), the pineal (H-J) and the medial optic tract (K-M). In *robo2* -/- mice RGC axons were seen projecting into the preoptic region (arrows in D), into the telencephalon along the ventral and medial surface (arrows in G), crossing the dorsal midline and entering the pineal (J) and additionally, projecting deep into the telencephalon (arrows in M). In *robo2* +/- mice RGC axons were not seen in the preoptic region (C) or projecting deeply into the telencephalon (L) however, a small number of axons in some cases were seen projecting along the ventral surface of the telencephalon (F) or crossing the dorsal midline (I). Bar, 200μm (A-C, H-M), 250μm (E-G).

**Table 3.4- Percentage of *robo2*-deficient mice (E16.5) with aberrant RGC axons**

| **Genotype** | **Axons on surface of telencephalon** | **Axons crossing dorsal midline** |
|---|---|---|
| ***Robo2* +/-** | 40% (5) | 40% (5) |
| ***Robo2* -/-** | 100% (5) | 100% (5) |

(n) = number analysed.

## 3.3 Discussion

RGC axons display region-specific organisation and innervation patterns within the diencephalon. Additionally, although they extend adjacent to the telencephalon, they do not normally invade this tissue. By analysing mice lacking *slit1, slit2, robo1* and *robo2*, I have found that the Slit/Robo signalling pathway contributes to the guidance of RGC axons within the optic tracts. In *robo2*-deficient embryos, RGC axons project aberrantly at the optic chiasm in the same manner as seen in the *slit1/2* double mutants (Plump et al., 2002). Additionally, in the absence of Slits or Robo2, a subset of RGC axons grows into the epithalamus and telencephalon. However, many axons remain restricted to the optic tracts and reach the SC. I also observed interesting differences between the double *slit1/2*-knockout and the *robo2* knockouts supporting previous work by Dr. W. Andrews and Prof. J. Parnevelas (University College London). In *slit*- or *robo2*-deficient embryos, RGC axons project aberrantly into the telencephalon. While these are restricted to the surface in *slit*-deficient embryos, in *robo2*-deficient embryos a large number of RGC axons project deep into the telencephalon. This all suggests that multiple mechanisms act to direct RGC axon guidance within the optic tracts and that the Slit/Robo pathway is an important component of this guidance activity.

### *3.3.1 Slits and Robo2 help restrict RGC axons to the optic tracts*

The organisation and innervation pattern of RGC axons within the diencephalon correlate with the expression within the hypothalamus and epithalamus of a diffusible factor inhibitory to RGC axon outgrowth (Tuttle et al., 1998). RGCs express *robo2* and a subset of cells express *robo1* (Erskine et al., 2000; Niclou et al., 2000) (Figure 3.10). Slit1 and Slit2, potent inhibitors of RGC axon extension (Erskine et al., 2000; Niclou et al., 2000; Ringstedt et al., 2000; Plump et al., 2002) are expressed in the epithalamus and hypothalamus (Ringstedt et al., 2000) and, in the absence of these molecules or of Robo2, a subset of RGC axons extend into the epithalamus. This suggests Slits are a component of the epithalamus inhibitory

activity, acting as a barrier to Robo2-expressing RGC axon extension into this region. By contrast, guidance of RGC axons within the hypothalamus occurs normally. Whether this is because Slits are not important for RGC axons pathfinding in this region or whether they function in a redundant manner with other guidance cues is not clear.

Slit/Robo signalling also helps prevent RGC axons extending into the telencephalon. Similar to their role in the epithalamus and optic chiasm (Plump et al., 2002), this is most likely due to Slits acting as a barrier rather than to attract the axons to the optic pathway (Jin et al., 2003). *In vitro* assays and transplantation studies have demonstrated that telencephalic cells and foetal cortical explants are inhibitory to RGC axon outgrowth (Harvey et al., 1987; Ichijo and Kawabata, 2001). Furthermore, *slit1* and *slit2* are strongly expressed in the ventral region of the telencephalon and, in *foxg1* -/- embryos in which this tissue fails to develop, RGC axons cross the diencephalic/telencephalic boundary (Pratt et al., 2002), possibly due to lack of inhibitory signals from this region. Together, these demonstrate that through inhibitory signalling, expression of *slit1* and *slit2* in the ventral telencephalon helps restrict RGC axons to the optic tracts. The observed defects seen at the optic chiasm in *robo2*-deficient mice phenocopies that of *slit1/2* null mice. Confirming Slit/Robo signalling is essential for correct chiasm formation and is required to prevent inappropriate targeting at the optic nerve/ chiasm boundary.

I also found that Slit1, Slit2 and Robo2 are not key regulators of the bundling patterns of RGC axons. This is in contrast to *astray/robo2* zebrafish mutants where extensive defasciculation of the optic tracts occurs (Fricke et al., 2001). This could occur because in mammals other factors function redundantly with Robos and Slits to regulate this process. Alternatively, even though Robo1 is only expressed by a subset of RGCs, it could function to prevent defasciculation in *robo2* knockouts. In the future it would be interesting to look at *robo1/2* double knockouts.

### *3.3.2 Robo2 has non-Slit1/2 function in RGC axon guidance in the telencephalon*

Although RGC axons were able to project into the telencephalon, they were always restricted to the surface in *slit1/2*-deficient mice. However, in *robo2*-deficient mice, RGC axons are able to project away from the surface extending deep into cortical regions, which is more like the previously seen phenotype in the *astray/robo2* zebrafish mutants (Karlstrom et al., 1996; Fricke et al., 2001). This phenotypic difference could be explained by several reasons. First, the presence of Slit3, in the *slit1/2* double knockout, which is expressed in medial and dorsal regions of the telencephalon, could be preventing axons extending into these regions. Secondly, Robo-Robo interactions could be restricting RGC axons growth to the surface of the telencephalon, possibly by promoting axon extension (Hivert et al., 2002) preferentially in this region. Finally, the phenotypic differences could be due to an unknown non-Slit ligand of Robo, evidence for which has been seen by comparing axon guidance and development in the in *C. elegans* mutants; *sax3 (robo)* and *slt-1 (slit)* (Hao et al., 2001).

As *slit3* is absent from the ventral telencephalon, the restriction of RGC axons to the surface in *slit1/2*-deficient mice suggests the presence here of other factors that are inhibitory to RGC axons. For example, the class III semaphorins are known to be inhibitory to RGC axons (Campbell et al., 2001; Steinbach et al., 2002; Liu et al., 2004) and semaphorin 3A has been shown to be expressed in the *Xenopus* telencephalon (Campbell et al., 2001). Expression of semaphorin 3A would create an inhibitory environment, functioning to restrict the aberrant RGC axons to the surface of the telencephalon.

### *3.3.3 RGC axons make distinct guidance errors in slit1 -/-; slit2+/-, slit1/2 -/- and robo2-/- mice.*

A surprising finding of this study is that, in *slit1 -/-; slit2+/-* and *slit1/2 -/-* mice, RGC axons follow relatively distinct trajectories along the ventral and/or medial surfaces of the telencephalon (Figure 3.14). *In vitro*, axons tend to grow straight

(Katz, 1985) and therefore, since this is the most direct path, RGC axons may have a preference for extension along the medial surface of the telencephalon. In the absence of *slit1* and one copy of *slit2*, the remaining *slit2* in the medial telencephalon (Figure 3.14) may be sufficient to deflect the RGC axons away from this region onto the ventral surface. In 40% of *robo2* +/- and all *robo2* -/- embryos, the aberrant RGC axons extend along the ventral and medial surface of the telencephalon. Here, Robo1 might be functioning to deflect a subset of RGC axons along the ventral surface of the telencephalon, while the remainder extend straight along the medial pathway (Figure 3.14). These data highlight the extreme sensitivity of axons to the precise concentration of guidance cues and receptors and provides direct evidence that varying their levels within tissues can influence the guidance decisions made by individual axons.

### *3.3.4 Slits are not required for target innervation*

In the absence of Slits, many axons reach and innervate the SC demonstrating that Slit1 and Slit2 are not required for target innervation. Other molecules have been identified, for example, FGF2 which is required for entry into the target but not guidance within the optic tracts (McFarlane et al., 1995; McFarlane et al., 1996). Together, this demonstrates that growth of axons through the optic tracts and target innervation are separable events. *Xenopus* embryos treated with heparitinase to remove endogenous heparan sulphates, show defects in target innervation and ectopic projections into the telencephalon (Walz et al., 1997). In addition to being essential for the biological activities of FGF2 (Lin, 2004), heparan sulphates regulate Slit localisation and signalling (Hu, 2001; Inatani et al., 2003; Johnson et al., 2004; Steigemann et al., 2004). This raises the possibility that the target innervation defects induced by removal of endogenous heparan sulphates are the result of inhibiting FGF2 signalling whereas the optic tract guidance defects are a partial consequence of disrupting Slit expression and function. In support of this later possibility, zebrafish *dackel* and *boxer* double mutants that lack *ext2* and *extl3* glycosyltransferases essential for heparan sulphate biosynthesis, display RGC axon pathfinding defects similar to those in *astray* mutants (Trowe et al., 1996; Lee et al., 2004). Additionally,

chiasm defects which phenocopy *slit1/2* null mice are seen in heparan sulphate sulphotransferase mutants (*hs2st, hs6st1)* (Pratt et al., 2006) and when the heparan sulphate biosynthesis enzyme (Ext1) is disrupted in *slit2* knockouts (Inatani et al., 2003). This reveals Slit/HSPG interactions are important for accurate pathfinding at the optic chiasm and therefore may also be important for guidance along the optic tracts.

### *3.3.5 In the absence of Slits or Robo2 many RGC axons navigate normally in the optic tracts*

In the absence of Robo2 or Slit1 and Slit2, only a subset of RGC axons project aberrantly in the optic tracts. One potential explanation is that there is a subset of RGC axons that are selectively sensitive to Slits, however this seems unlikely as they all express Robo2 and are responsive to Slits *in vitro* (Erskine et al., 2000; Niclou et al., 2000; Ringstedt et al., 2000; Plump et al., 2002; Sundaresan et al., 2004). Another possibility is that the position of the axons in the optic tracts is important (Silver, 1984) such that those axons that are located closest to the diencephalic/telencephalic boundary and epithalamus are in a position to be most dependent of Slits for their guidance. I have been unable to determine whether the ectopic axons are located within a specific region of the optic tract. Backlabelling with DiI from both the telencephalon and pineal has failed to produce any consistent labelling. In addition to Slit and Robo, several other guidance cues have been identified that direct optic tract development. For example, enzymatic removal of chondroitin sulphates from chick embryos results in spreading of RGC axons into the telencephalon (Ichijo and Kawabata, 2001). Simultaneously blocking β-Integrin and N-Cadherin function also results in optic tract pathfinding errors, including extension of axons across the dorsal midline and into the pineal and telencephalon (Stone and Sakaguchi, 1996). These defects are similar to those seen in the *slit-* or *robo*-deficient mice, and there is genetic and biochemical evidence for interactions between integrins, N-Cadherin (Rhee et al., 2002; Stevens and Jacobs, 2002) and Slit/Robo signalling, suggesting that cross-talk between these pathways may be important for optic tract development. Thus the most likely explanation for the accurate

pathfinding of RGC axons in the absence of Slits and Robos is that multiple, redundant mechanisms exist for guidance in the optic tracts and, in their absence the remaining cues are sufficient to ensure the error-free navigation of many axons.

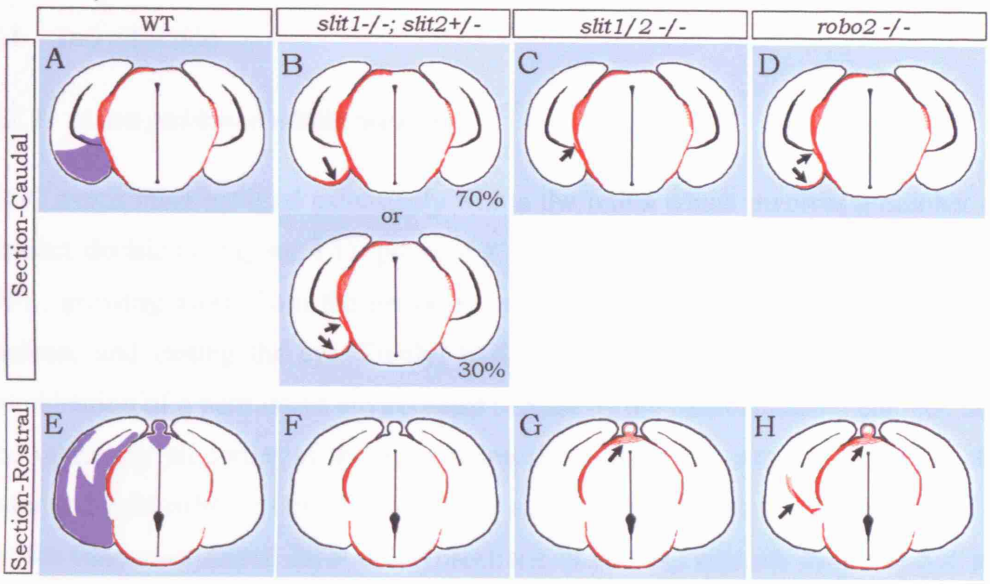


**Figure 3.14- Summary of errors seen in the optic tract in *slit*- and *robo*-deficient mice**

(A-H) Schematic diagrams illustrating the path followed by RGC axons in the contralateral (left) and ipsilateral (right) optic tracts. (A-D) rostral sections. (E-H) caudal sections. (A, E) In wildtype (WT) embryos, RGC axons are restricted to the surface of the diencephalon and avoid the epithalamus. Shaded areas indicate *Slit* expression in the ventral telencephalon and epithalamus. (B, F) In *slit1 -/-; slit2 +/-* embryos, a subset of RGC axons grow into the telencephalon and extend along either the ventral (70% of embryos) or ventral and medial (30% of embryos) surfaces. (C, G) In *slit1/2 -/-* embryos, RGC axons are restricted to the medial surface of the telencephalon and also grow into the epithalamus and across the dorsal midline and into the pineal. (D, H) In *robo2 -/-* embryos, RGC axons grow over the surface of the ventral and medial telencephalon and extend into the epithalamus and across the dorsal midline and into the pineal.

# 4 The role of Slit and Robo in the developing retina

## 4.1 Introduction

### *4.1.1 Axon guidance within the retina*

RGC axons must pathfind extensively within the retina which involves a number of distinct decisions (Figure 4.1): projecting away from the outer retina and into the OFL, growing away from the periphery and towards the optic disc in an ordered fashion, and exiting the eye. Firstly, RGC axons are restricted to the OFL by a combination of a permissive environment created by the neuroepithelial endfeet, and the inhibitory properties of the outer retina (Stier and Schlosshauer, 1995). In the Stier and Schlosshauer (1995) paper, RGC axons were shown to grow preferentially on the innermost retinal layer of cryosections in culture, whereas they avoided the outer retinal layers. This preference was lost when the neuroepithelial endfeet were selectively eliminated, and aberrant growth over the outer retinal layers could be induced by prior heat or protease treatment. These data suggest the neuroepithelial endfeet provide the permissive environment and the inhibitory properties of the outer retina are likely due to inhibitory proteins (Stier and Schlosshauer, 1995). These have not yet been found.

Directed growth towards the optic disc by the first axons appears to involve different processes to that of the later axons. The pioneering axons originate from RGCs closest to the optic disc and appear to be physically guided towards the optic nerve head. Analysis of the early developing mouse retina revealed a system of oriented intercellular spaces in the region of the optic disc which form interconnecting tunnels guiding the first RGC axons into the optic nerve (Silver and Sidman, 1980). No such channels have been found in more peripheral regions of the retina (Silver and Sidman, 1980), and it would seem later forming axons navigate towards the optic disc without such mechanical guidance (Halfter et al., 1985; Brittis et al., 1995). Prior to sending out a mature axon, immature RGCs send out minor processes

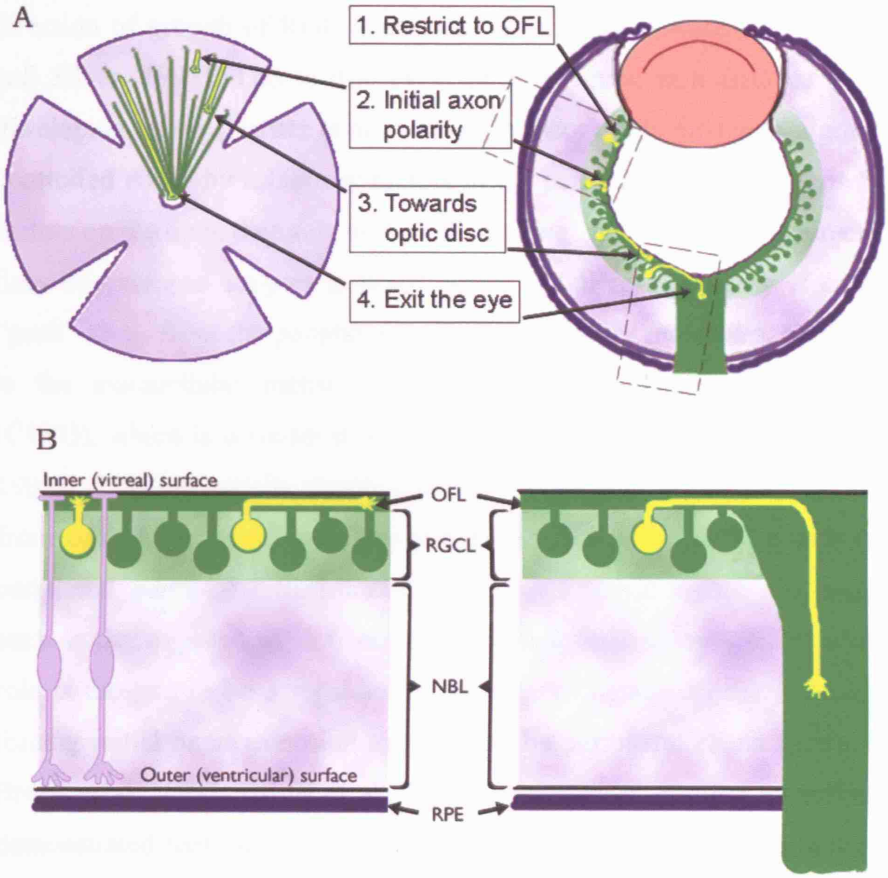


**Figure 4.1- Schematic diagram showing guidance decisions within the retina.**

(A) Left, representing a flatmount retina with RGC axons in green projecting along the surface of the retina towards the optic disc. Right, representing a sectioned retina. RGC axons must make pathfinding decisions in order to exit the eye, these are shown by yellow RGCs: 1, restriction of axons to the OFL; 2, the initial axon polarity; 3, projection towards the optic disc; and 4, exit from the eye. (B) Enlargement of boxes shown in A, RGC axons are restricted to the OFL and project away from the periphery, towards the optic disc, then exit the eye.

(Brittis and Silver, 1995), one of which would become longer forming an axon. The direction of growth of RGC axons was consistently towards the optic disc (Brittis and Silver, 1995). This is true even for cells found at a distance from any other developing axons (Halfter et al., 1985). In theory, this directed outgrowth could be controlled either by inhibitory factors in the peripheral retina, or growth promoting factors on the optic disc side of the cell "pulling" the axons in this direction. Several lines of evidence support a model where initial axon polarity is controlled by a "push" away from the peripheral retina by inhibitory molecules. One such molecule is the extracellular matrix (ECM) molecule chondroitin-sulphate proteoglycan (CSPG), which is considered to be a growth repellent for RGC axons (Snow et al., 1991). CSPG is initially distributed over the centre of the rat retina but then recedes from central regions to more peripheral locations corresponding with the central to peripheral wave of differentiation of RGCs. When retinas are treated with an enzyme that digests CSPG, axons grow in random directions (Brittis et al., 1992). Its role is thought to be a regulator of polarity of neuronal differentiation as well as forcing initial axon extension away from the peripheral retina (Snow et al., 1991; Brittis et al., 1992; Brittis et al., 1995). Importantly, grafting experiments in chick demonstrated that the optic disc does not possess significant chemotropic activity, suggesting that short-range rather then long-range cues direct intraretinal axon guidance (Halfter, 1996). With a few exceptions, the identities of these short-range signals remain largely unknown.

The short-range signals in the form of cell adhesion molecules which have been implicated in regulating distinct aspects of intraretinal axon guidance include; NCAM (neural cell adhesion molecule), NrCAM, NCAM associated PSA, L1 and Neurolin (also called DM-GRASP/BEN/SC1), (Pollerberg and Beck-Sickinger, 1993; Brittis et al., 1995; Ott et al., 1998; Monnier et al., 2001; Avci et al., 2004; Weiner et al., 2004; Zelina et al., 2005). When these molecules are individually disrupted axon guidance is disturbed in various ways:

1- axons appear defasciculated; NCAM (Figure 4.2B) (Pollerberg and Beck-Sickinger, 1993),

2- axons aberrantly project away from the main body of axons or loop around; L1 (Brittis et al., 1995), NCAM (Figure 4.2B) (Pollerberg and Beck-Sickinger, 1993), DM-GRASP/BEN (Figure 4.2C) /Neurolin (Ott et al., 1998; Weiner et al., 2004), NrCAM (Zelina et al., 2005),

3- entry into the optic disc is disturbed, NCAM (Figure 4.2B) (Pollerberg and Beck-Sickinger, 1993), NrCAM (Zelina et al., 2005), NCAM-associated PSA (Monnier et al., 2001), DM-GRASP (Avci et al., 2004).

The cell adhesion molecule BEN mediates both homophilic and heterophilic interactions and is expressed by RGC axons. In BEN-deficient mice RGC axons appear defasciculated within the retina and a small number of axons are seen looping in the wrong direction (Weiner et al., 2004). Similar but more severe guidance errors are seen in the goldfish retina following inhibition of Neurolin/BEN function (Ott et al., 1998). One explanation for the relatively small number of defects observed following loss of BEN is compensation by other cell adhesion molecules. In rat retinas, the cell adhesion molecule L1 is expressed by extending RGC axons (Brittis and Silver, 1995). Blocking L1 function in cultured rat retinas results in loss of disc-directed growth with many axons extending perpendicular to the normal direction of growth (Brittis et al., 1995). In all the cases where cell adhesion molecules are disrupted only subsets of axons within the retina appear to be affected.

Several additional factors have also been implicated in helping direct RGC axons towards the optic disc and into the optic nerve. EphB2/B3 (Figure 4.2D), Bone morphogenic protein (Bmp) receptor 1B (Figure 4.2E), Sema5A and Netrin1/DCC (Figure 4.2F) are required for targeting to and entry into the optic disc (Deiner et al., 1997; Birgbauer et al., 2000; Liu et al., 2003; Oster et al., 2003). In the absence of these proteins, subsets of RGC axons bypass the optic disc and project aberrantly within the retina. Netrin1 is expressed by the glial cells in the optic stalk and its receptor DCC is expressed by RGC axons (de la Torre et al., 1997; Deiner et al.,

1997). In mice lacking either Netrin1 or DCC, RGC axons extend normally to the optic nerve head but fail to exit the eye (Deiner et al., 1997). In zebrafish the chemokine SDF1, through its receptor chemokine receptor 4 (CXCR4), has been shown to attract RGC axons towards the optic disc When these molecules are knocked-down intraretinal axon guidance is disrupted (Li et al., 2005). However, *in vitro* SDF1 has no direct effect on chick RGCs, instead it reduces the effectiveness of the repellents Sema3a and Slit2 (Chalasani et al., 2003). This may be due to a species difference and/or an *in vitro/in vivo* difference and, the direct role of the chemokine SDF1 on axon guidance has to be fully elucidated. Recently, it has been shown in chick retinas that a wave of Sonic hedgehog (Shh) expression spreads across the retina, the front of which lies central relative to newly differentiated RGCs (Kolpak et al., 2005). Blocking or overexpressing Shh *in vivo* has a striking effect on intraretinal pathfinding, the OFL becomes extremely disorganised with axons that extend in random directions (Kolpak et al., 2005).

A number of transcription factors have also been found to influence axon guidance within the retina. For example, the POU-domain transcription factor Brn3.2 (also known as Brn3b and Pou4f2), is expressed by RGCs and when knocked-out in mice, a subset of RGC axons are unable to enter the optic disc and appear defasciculated (Erkman et al., 2000). This results in optic nerve hypoplasia and ultimately RGC death. Several downstream targets of Brn3.2 have been identified including abLIM, an actin binding protein (Erkman et al., 2000). Blocking abLIM function in developing chick retinas results in similar defects to those seen in Brn3.2-deficient mice, although it has not yet been shown to be a direct target (Erkman et al., 2000). Within the chick retina *zic3* is expressed in a high peripheral-low central gradient and *in vitro* overexpression blocks extension towards the optic disc possibly by inducing expression of inhibitory molecules (Zhang et al., 2004).

*Robo1* and *robo2* are expressed by cells in the RGC layer at the time when RGC axons are extending through the visual system (Erskine et al., 2000; Niclou et al., 2000; Ringstedt et al., 2000; Sundaresan et al., 2004). In mice, *slit1* is expressed by cells in the RGC layer in a low dorsal- high ventral gradient, whereas *slit2* is

expressed uniformly. *Slit2* is expressed by cells in the RGC layer at E14.5 however by E17.5 its expression is restricted to the INL. Therefore, using analyses of knockout mice and *in vitro* assays, I studied the role of Slit and Robo in the developing retina. I found that within dorsal retina exclusively, Slit/Robo signalling controls the initial polarity of RGC axon outgrowth and prevents a subset of RGC axons, located predominately in ventral retina, from straying away from the OFL. However, guidance within more central regions of the OFL appears to be independent of Slit/Robo signalling, and axons are able to exit the eye successfully. These data add Slit and Robo to the growing list of factors that regulate intraretinal pathfinding and demonstrate a surprising degree of regional specificity in their mode of action. I have furthermore revealed a role for the lens in signalling to guide axons within the peripheral retina, in addition to regulating growth of the eye.

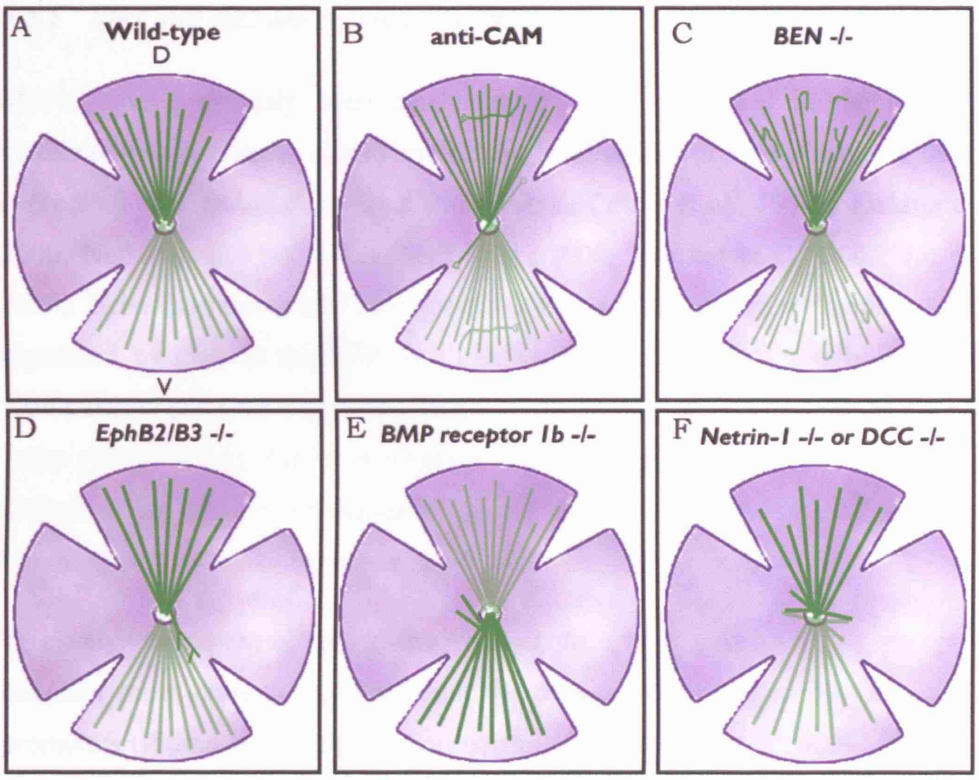


**Figure 4.2- Diagrammatic examples of intra-retinal axon guidance defects.**

(A-F) Schematics representing flatmounted retinas with RGC axons (green) projecting towards the optic disc (centre). Dorsal is top. (A) wildtype retina. (B) chick retina in culture following treatment with anti-CAM antibodies, fascicle diameter is decreased, RGC axons grow into contralateral retina and peripheral axons mis-project (Pollerberg and Beck-Sickinger, 1993). (C) in *BEN* knockout mouse RGC axons appear defasiculated and subsets of axons appear to loop around (Weiner et al., 2004). (D) *EphB2/B3* knockout mouse dorsal RGC axons bypass the optic disc (Birgbauer et al., 2000). (E) in *BMP receptor 1b* knockout mouse ventral RGC axons bypass the optic disc (Liu et al., 2003). (F) in *Netrin1-* or *DCC-*knockout mouse RGC axons do not enter the optic disc (Deiner et al., 1997).

## 4.2 Results

### *4.2.1 Slit1 and slit2 are expressed by RGCs*

*Slit1-2* have previously been demonstrated to be expressed in the developing vertebrate retina using *in situ* hybridisation, however the precise identity of the cells expressing *slit1* and *slit2* remains controversial (Yuan et al., 1999b; Erskine et al., 2000; Niclou et al., 2000; Ringstedt et al., 2000; Marillat et al., 2002; Jin et al., 2003). I repeated the *in situ* hybridisation on E16.5 mouse retinal sections. *Slit1* is expressed by cells in the RGC layer, in addition to a subset of cells in the outer retina; this expression is seen in a high ventral- low dorsal gradient across the neural retina (Figure 4.3A). *Slit2* is restricted to cells in the presumptive inner nuclear layer (Figure 4.3B). *Slit3* is not expressed by any cells in the neural retina (Figure 4.3C) however, *slit3* and *slit2* are expressed by cells of the lens (Figure 4.3B, C).

To clarify the identity of the *slit*-expressing cells, I made use of the fact that the *slit*-deficient mice express *tau*-GFP under the control of the endogenous *slit1* or *slit2* promoters (Plump et al., 2002). Consequently, any cells that normally express *slit1* or *slit2* mRNA will now express green-fluorescent protein (GFP) in their cell bodies and processes. In both *slit1* +/- and *slit2* +/- embryos, *tau*-GFP is expressed in the inner region of the retina, including the OFL and optic nerve (Figure 4.3E, F, H, I), in a pattern that correlates with the location of the RGCs and their axons (Figure 4.3D, G). In *slit2* +/- embryos *tau*-GFP also is expressed in the cornea and lens epithelium (Figure 4.3F). These data confirm the expression patterns obtained using *in situ* hybridisation (Figure 4.3A-C) (Yuan et al., 1999b; Erskine et al., 2000; Niclou et al., 2000; Ringstedt et al., 2000) and demonstrate clearly that, in the mammalian retina, both *slit1* and *slit2* mRNA are expressed by RGCs. To try and determine Slit protein expression, I and others have tested a number of commercially available anti-Slit antibodies and have been unable to get specific staining in any part of the nervous system (data not shown; Dr. W. Andrews, personal communication).

### *4.2.2 Slits help restrict RGC axons to the OFL*

To establish whether Slits are critical for axon guidance in the mammalian retina, E16.5 wildtype or *slit*-deficient retinas were stained with a neuron specific anti-β-tubulin or anti-neurofilament antibody to label all of the RGC axons. These were then viewed using confocal microscopy in flat mounts or coronal sections (Figure 4.4). In wildtype retinas, RGC axons are restricted to the OFL at the inner surface of the retina, and in only 1 of 20 retinas was a single bundle of axons seen within the outer (RGC and neuroblastic) layers (Figure 4.4C, G, K, Figure 4.5A, C). In mice lacking *slit1* alone, RGC axons remained restricted to the OFL (n=10 retinas; Figure 4.4D, H, L, Figure 4.5C). However, in *slit2*-deficient (n=9 retinas) and, more frequently, *slit1/2*-deficient retinas (n=14 retinas), a subset of RGC axons extended away from the OFL into the outer retina. These axons originated from cells located within the RGC layer and formed highly fasciculated bundles that, although less directed than axons within the OFL, extended in the overall direction of the optic disc (Figure 4.4E-F, I-J, M-N, Figure 4.5B). At all stages studied an average of five bundles of RGC axons were located within the outer layers of *slit2*-deficient retinas increasing to ~ 25 bundles in the double mutants (Figure 4.5C). A dorsoventral polarity was seen in the location of the ectopic axons. In both *slit2*- and *slit1/2*-deficient retinas, more than twice as may RGC axon bundles extended through the outer layers of ventral than dorsal retina (Figure 4.5B, D).

### *4.2.3 Slits regulate the organisation of the OFL*

Slits also are involved in regulating the directed growth of RGC axons within the OFL itself (Figure 4.6). In wildtype retinas, RGC axons originating throughout the retina extended within the OFL in a straight, directed manner toward the optic disc. Polarity in the direction of growth was evident from the outset with the axons originating from the side of each cell closest to the optic disc and extending directly toward this region (Figure 4.6A, B, F, J). Surprisingly, in *slit1*-deficient retinas, no obvious changes were found in the extent of RGC axon fasciculation or the

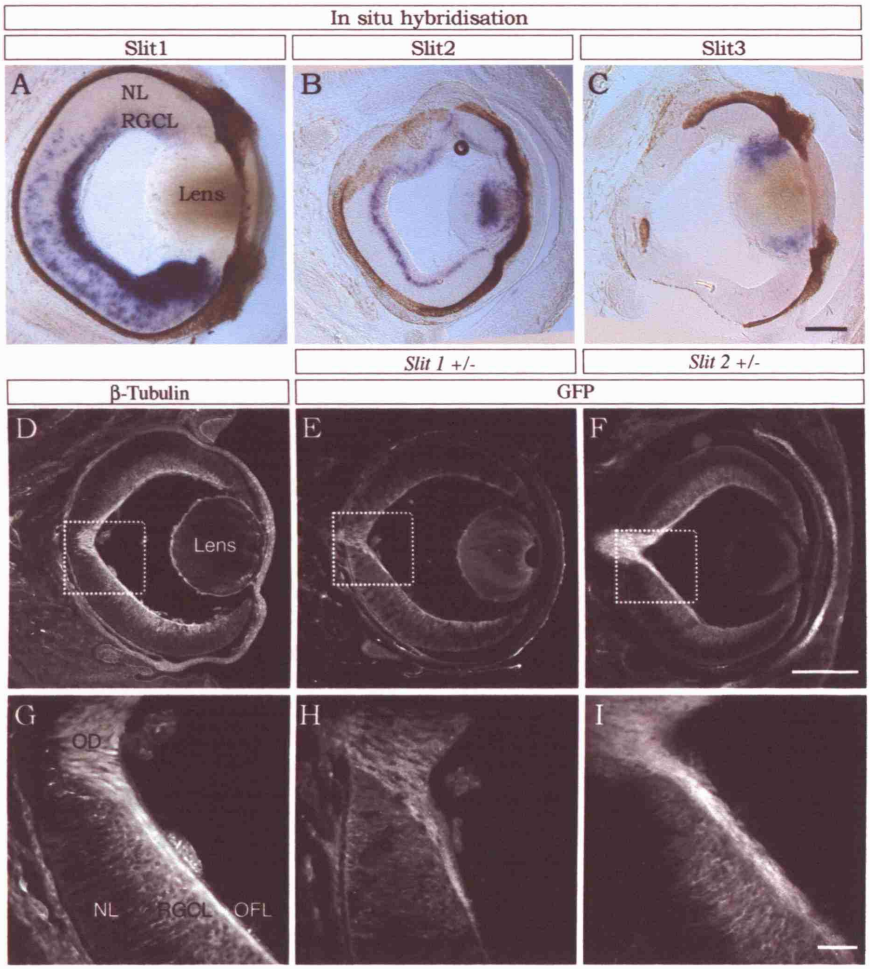


**Figure 4.3- Determination of *slit* expression in the developing visual system.**

(A-C) Coronal sections of E16.5 wildtype embryos following *in situ* hybridisation using digoxigenin-labelled riboprobes for *slit1* (A), *slit2* (B), or *slit3* (C), dorsal is up. (D-F) Horizontal sections of E15.5 retina stained with a neuron-specific anti-β-tubulin antibody to label the RFC axons (D, G) or an anti-GFP antibody (E, F, G, I). Boxed regions in D-F are shown at higher power in G-I. In both slit1 +/- (E, H) and slit2 +/- (F, I) embryos, tau-GFP is expressed by RGC axons within the OFL at the inner surface of the retina and optic nerve (E, F, H, I). NL, Neuroblastic layer; RGCL, RGC layer; OD, optic disc; OFL, optic fibre layer. Bar, 200μm (A-C), 400μm (D-F), 100μm (G-I).

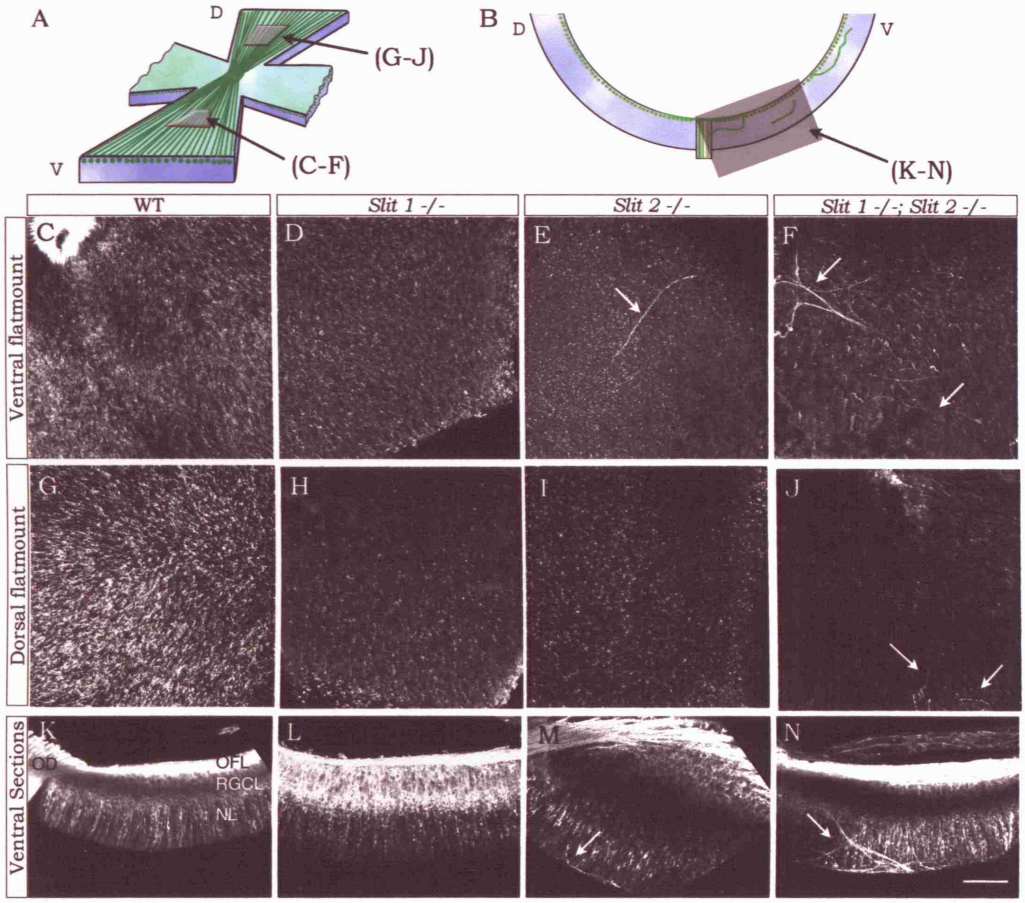


**Figure 4.4- Slits help restrict axons to the optic fibre layer.**

(A, B) Schematic diagrams illustrating the regions of the retinas imaged. (C-J) Confocal images taken at the level of the neuroblastic layer of flatmounted E16.5 retinas stained with an anti-β-tubulin antibody. The optic disc is located towards the top left of each picture. (K-N) Coronal sections of anti-β-tubulin stained E16.5 retinas. In each image the optic disc is located towards the left-hand side. In wildtype (WT; C, G, K), *slit1*-deficient retinas (D, H, L) RGC axons are restricted to the OFL and no axons are present within the outer retina. In *slit2*- (E, I, M) and *slit1/2*-deficient (F, J, N) retinas, RGC axons extend aberrantly through the outer retina. This occurs more frequently in ventral than dorsal retina (arrows in E, F, J, M, N). RGCL, retinal ganglion cell layer; NL, neuroblastic layer; OFL, optic fibre layer; OD optic disc. Bar, 100μm.

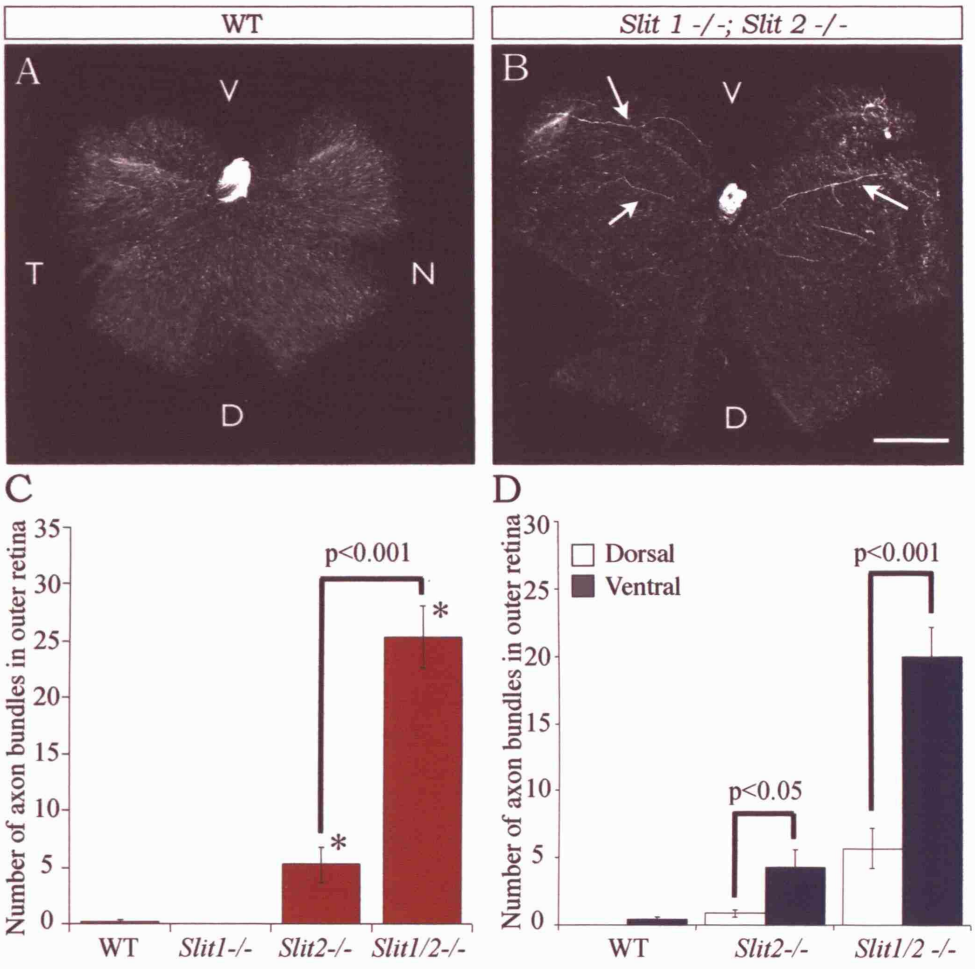


**Figure 4.5- Spatial organization and quantification of number of RGC axon bundles in the outer layers of *slit*-deficient retinas.**

(A, B) Confocal images of flat-mounted E14.5 WT (A) and *slit1/2*-deficient (B) retinas at the level of the outer retina. In *slit1/2*-deficient retinas (B) but not WT retinas (A), a subset of RGC axons originating predominately within ventral retina are present within the outer layers of the retina. D, Dorsal; N, Nasal; T, temporal; V, Ventral. Bar; 200μm. (C) Mean ± SEM number of axon bundles located within the outer retina of WT, *slit1*-, *slit2*- and *slit1/2*-deficient retinas. * p< 0.001 compared with WT. (D) Mean ± SEM number of axons bundles in the outer layers of dorsal (white bars) or ventral (blue bars) retina. In both *slit2*- and *slit1/2*-deficient retinas, significantly more bundles are found within the outer layers of ventral versus dorsal retina.

organisation of the OFL (Figure 4.6C, G, K). However, in mice lacking *slit2* or *slit1/2*, the organisation of the OFL was perturbed, with many RGC axons originating in the periphery of the retina, deviating from their normal peripheral-central orientation and forming abnormal looped and curved trajectories (Figure 4.6H, I). This was primarily attributable to the axons initially growing toward the retinal periphery before correcting their direction of growth and extending toward the optic disc (Figure 4.6H, I) (Thompson et al., 2006). Excessive crossing of axons between different fascicles also occurred (Figure 4.6H, I).

Surprisingly, these pathfinding errors were found exclusively within dorsal retina in which they were restricted to the peripheral part of the retina (Figure 4.6H, I). Because of the fact that all RGC axons were labelled, the precise number of axons with aberrant trajectories was impossible to quantify. However, in both *slit2*- and *slit1/2*-deficient mice, the guidance of most, if not all, RGC axons originating in the most peripheral 25% of dorsal retina (Figure 4.6H, I, Figure 4.8M) appeared to be affected whereas more centrally, the orderly projection of RGC axons towards the optic disc occurred normally (Figure 4.6D, E). The organisation of the OFL within the entire ventral half of the retina also was normal (Figure 4.6L, M). Within the dorsal retina, there was no difference in the severity of the OFL defects between the *slit2* and *slit1/2*-deficient retinas, demonstrating that *slit2* alone regulates this aspect of intraretinal guidance.

### *4.2.4 Development of intraretinal pathfinding defects in slit-deficient mice*

These two defects in intraretinal pathfinding, the projection of RGC axons into the outer layers of the retina and the disorganisation of the OFL, develop over different time courses. At E13.5 in the *slit1/2*-deficient mice, significant numbers of axons projected away from the OFL into the outer retina with most aberrant projections seen in the ventral retina (Figure 4.7A-D), however, the organisation of the OFL appeared as in the control retinas (Figure 4.8A-D). From E14.5 onward, both the restriction of RGC axons to the OFL (Figure 4.7H) and the organisation of the dorsal OFL were perturbed (Figure 4.8F). Furthermore, at all ages, the regional specificity

of Slits' function in the retina was maintained, with the disorganisation of the OFL occurring exclusively in dorsal retina (Figure 4.8F, J) & many more axon bundles projecting into the outer layers of ventral than dorsal retina (Figure 4.7D, H, J). This demonstrates clearly that the differential requirement for Slits within the ventral and dorsal retina is not the result of a ventrodorsal gradient in retinal maturity (Halfter et al., 1985).

As the retina develops, new cells are added at progressively more peripheral locations, resulting in a central-to-peripheral expansion of the neuroepithelium. As a result, what was peripheral retina at E14.5 is now located more centrally at later stages of development (Figure 4.8M). Despite this, at all ages, the disorganisation of the OFL in the *slit1/2*-deficient mice occurred exclusively within the peripheral 22-25% of the dorsal retina (Figure 4.8M). More centrally and within the ventral retina, axon organisation was indistinguishable from that seen in age matched wildtype retinas (Figure 4.8C, D, G, H, K, L). This suggests that, in dorsal but not ventral retina, Slits act to control the initial outgrowth of newly differentiated RGCs, and as development proceeds, the aberrant trajectory of these axons is corrected.

### *4.2.5 Retinal morphology is normal in slit-deficient mice*

One explanation for these pathfinding defects is that they occur secondarily to changes in the overall structure of the retina. Therefore the gross morphology and lamination of the *slit*-deficient retinas were examined. In *slit1*- and/or *slit2*-deficient embryos, the overall size and shape of the retinas appeared normal. To determine if the number of mitotic cells in E16.5 retinas is the same in *slit*-deficient as in wildtype retinas, counts of cells labelled with anti-phospho histone H3 (a marker of mitosis) were undertaken. The number of mitotic cells per 100μm in *slit*-deficient retinas was not found to be significantly different from that in wildtype retinas (Figure 4.9). This work was done by Umbreen Hussain, an AS-level student working in the lab for 6 weeks, with my help and under my direct supervision.

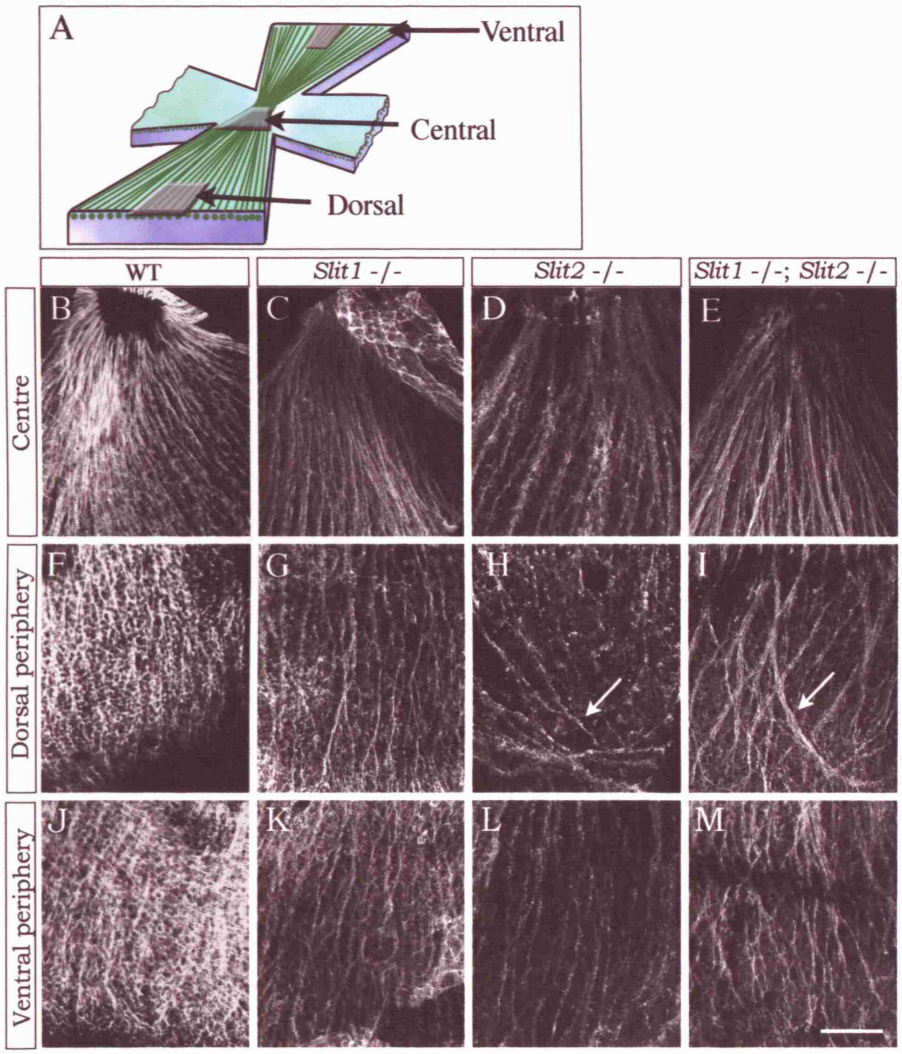


**Figure 4.6- Slits regulate the organisation of the OFL.**

(A) Schematic diagram illustrating the regions of the retina imaged. (B-M) Confocal images of E16.5 dorsal (B-I) or ventral (J-M) retinas stained with an anti-β-tubulin or an anti-neurofilament antibody taken at the level of the OFL. In each image the direction of the optic disc is towards the top of the picture. In WT (B, F, J), *slit1*-deficient (C, G, K), and ventral *slit2*- (L) and *slit1/2*-deficient (M) retinas, RGC axons extend directly towards the optic disc. In dorsal *slit2*- (D, H) and *slit1/2*-deficient (E, I) retina, the RGC axons within the peripheral (H, I) but not central (D, E) region of the OFL, have abnormal looped trajectories. Bar, 100μm.

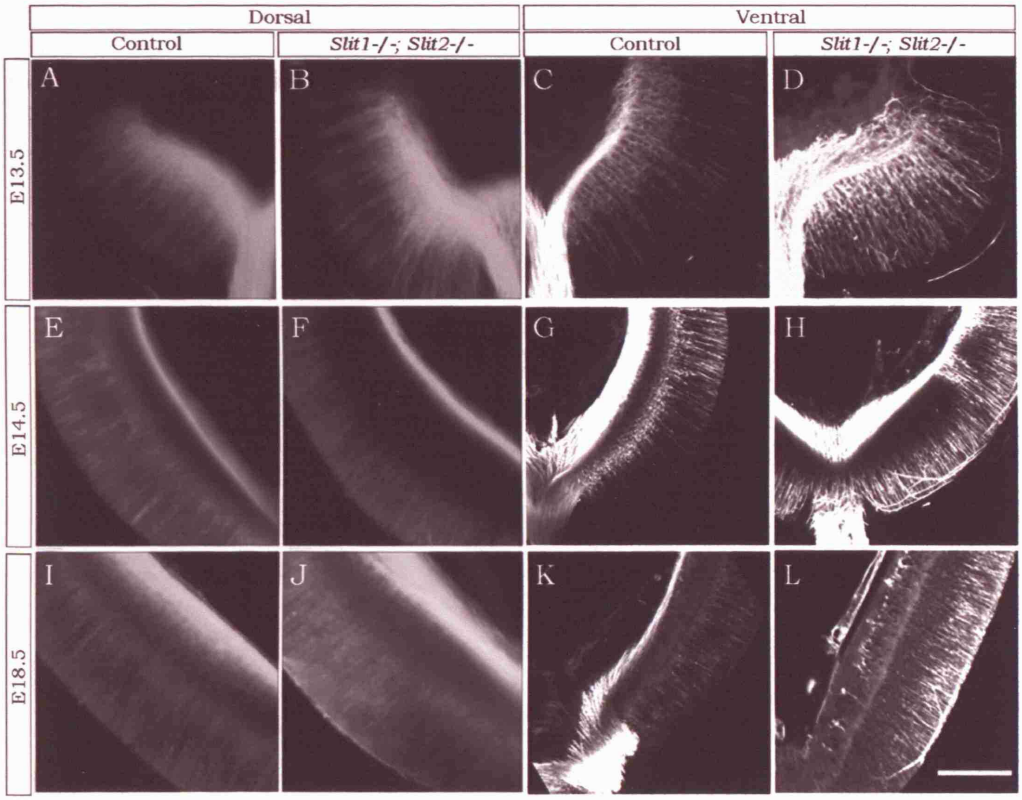


**Figure 4.7- Development of intraretinal pathfinding defects in *slit*-deficient mice.**

(A, B, E, F, I, J) Compound or (C, D, G, H, K, L) Confocal images of anti-β-tubulin stained E13.5 (A-D), E14.5 (E-H) and E18.5 (I-L) control (WT or *slit1*-deficient; A, C, E, G, I, K) or *slit1/2*-deficient (B, D, F, H, J, L) retinas viewed after sectioning coronally. In the dorsal retina of wild-type and *slit1/2*-deficient embryos RGC axons are restricted to the OFL (A, B, E, F, I, J). In E13.5- E18.5 *slit1/2*-deficient embryos, some axons extend aberrantly into the outer layers of ventral retina (D, H, L). Bar, 100μm.

**Figure 4.8- Development of optic fibre layer pathfinding defects in *slit*-deficient mice.**

(A-L) Confocal images of anti-β-tubulin stained E13.5 (A-D), E14.5 (E-H) and E18.5 (I-L) control (WT or *slit1*-deficient; A, C, E, G, I, K) or *slit1/2*-deficient (B, D, F, H, J, L) retinas viewed as flat mounts. In E13.5 *slit1/2*-deficient embryos the organisation of the OFL is normal (A-D). At older ages, the organisation of the dorsal OFL is perturbed in *slit1/2*-deficient retinas (F, J). Bar, 100μm (A-L). (M) Schematic diagram illustrating the relative size of the retina at different stages of development and the organisation of the OFL in *slit1/2*-deficient mice. Numbers indicate the percentage of the retinal radius in which aberrant organisation of the OFL occurs. D, Dorsal; V, Ventral. Bar, 500μm.

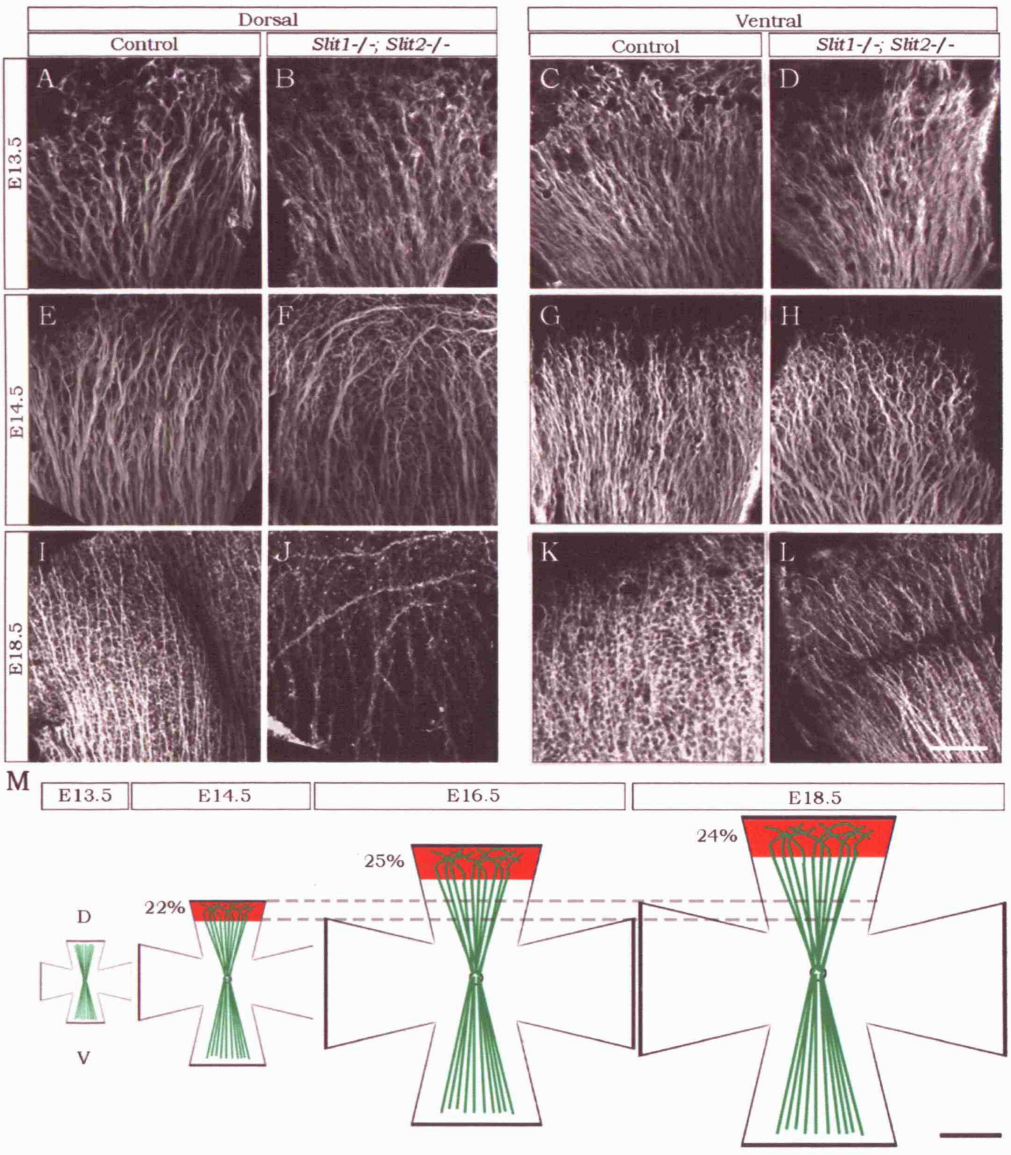
Dorsal
Ventral
Control
Slit1-/-; Slit2-/-
Control
Slit1-/-; Slit2-/-
A
B
C
D
E13.5
E
F
G
H
E14.5
I
J
K
L
E18.5
M
E13.5
E14.5
E16.5
E18.5
D
V
22%
25%
24%

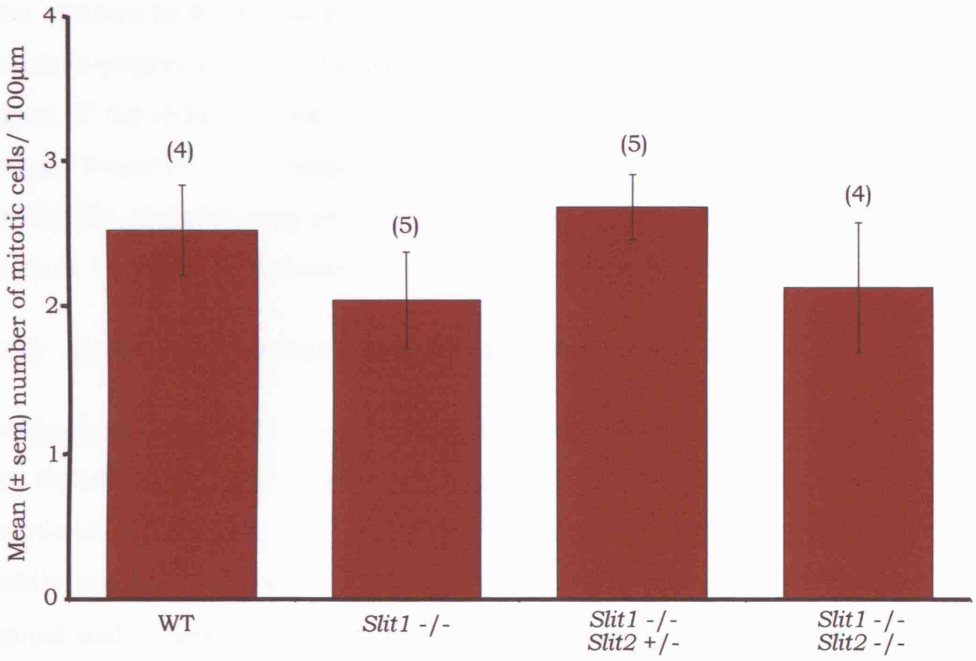


**Figure 4.9- Slits do not influence cell division in the developing retina.**

Mean ± SEM number of mitotic cells per 100µm of E16.5 WT, *slit1 -/-*, *slit1-/-*; *slit2 +/-* and *slit1/2 -/-* retinas. The numbers above each bar indicate the number of embryos analysed for each genotype.

E16.5 retinal sections were stained with cell-type-specific markers to determine whether in the *slit*-deficient mice the major classes of retinal cells are present and in their proper places. Cells labelled with an antibody against phospho-histone H3, were seen adjacent to the retinal pigment epithelium (Figure 4.10A, D), and Islet1- and calretinin-postive differentiated RGCs and amacrine cells were localised to the inner region of the retina (Figure 4.10B, C, E, F) in both wildtype and *slit1/2*-deficient retinas. Together, this strongly suggests that the intraretinal guidance defects are attributable to pathfinding errors rather than changes in the gross structure of the retina or the mis-differentiation or mis-placement of retinal components.

### *4.2.6 Robo2, but not robo1 regulates intraretinal axon guidance*

Antibody staining and *in situ* hybridisation demonstrated that Robo1 and Robo2, but not Robo3 (Rig1) and Robo4, are expressed by RGCs (see chapter 3). The functional significance of Robo1 and Robo2, in terms of murine intraretinal pathfinding was therefore examined. E16.5 *robo1*- or *robo2*- deficient retinas were stained with a neuron specific anti-β-tubulin antibody, and viewed using confocal microscopy in flatmounts or coronal sections (Figure 4.11, Figure 4.12). In *robo1*-deficient and *robo2* +/- retinas, RGC axons are restricted to the OFL (Figure 4.11), and only in 1 of 9 retinas were any axons seen within the outer retinal layers (Figure 4.11A-C, E-G, I). However, in *robo2*-/- retinas, a subset of RGC axons extended away from the OFL into the outer layers of the retina, with twice as many axon bundles seen in the ventral retina than in the dorsal retina (Figure 4.11J). In wildtype, *robo1*-deficient and *robo2* +/- retinas, axons within the OFL extended in a straight, directed manner toward the optic disc (Figure 4.6B, F, Figure 4.12A-C, E-F). However, organisation of the dorsal, but not ventral, peripheral OFL in *robo2* -/- retinas was perturbed (Figure 4.12H). These defects were essentially identical and of a similar magnitude to those seen in the *slit*-deficient mice, suggesting Slit and Robo are functioning together to guide axons through the retina.

### *4.2.7 Slit and Robo are not required for entry into the optic nerve*

A number of axon guidance molecules have been found to be important, not only in guiding axons towards the optic disc, but also for entry into the optic nerve and exit from the eye (see section 4.1.1). Both Slit and Robo have been found to be important for regulating axon pathfinding within the retina. To determine if they are also required for entry into the optic nerve head, subsets of RGC axons were visualised using focal DiI. Small crystals of DiI were placed in either the dorsal or ventral peripheral retina (Figure 4.13A) and the path of those labelled axons were examined in flatmount preparations following six hours incubation. In wildtype retinas, a subset of labelled RGC axons can be seen projecting as a fasciculated bundle through the OFL in a direct manner towards the optic disc where they exit the eye (Figure 4.13D, H). Only in two cases were any axons seen bypassing the optic disc (n=21; Figure 4.13B). This supports data seen previously by Birgbauer et al. (2000). The length of these misprojecting axons were less than 1000μm and were classified as less severe, type 2 errors (Birgbauer et al., 2000). In *slit1/2*-deficient (n=7; Figure 4.13E, I), *robo1*-deficient (n=9; Figure 4.13F, J) and *robo2*-deficient (n=11; Figure 4.13G, K) retinas, no increase in optic disc targeting errors were seen (Figure 4.13L). Again, any errors seen (1/7, *slit1/2*-deficient; 0/9, *robo1*-deficient; 1/12, *robo2*-deficient) were type 2 errors (Figure 4.13C). Additionally, the RGC axons in dorsal and ventral retina showed no difference in their targeting of the optic disc.

### *4.2.8 In vitro, Slits are secreted by the lens and inhibit outgrowth of dorsal RGC axons*

The *in situ* hybridisation data (Figure 4.3) (Erskine et al., 2000) do not show an obvious central-peripheral gradient of *slit* expression that would explain why Slit2 is required only within the most peripheral 25% of dorsal retina for normal OFL formation (Figure 4.6, Figure 4.8). My working model is that this reflects release of Slit2 from non-retinal ocular tissues. An excellent candidate for this source of Slit is the developing lens. The lens is ideally situated within the developing eye to preferentially influence the outgrowth of axons located within the retinal periphery.

Furthermore, the lens expresses *slit2* (Figure 4.3) (Yuan et al., 1999b; Erskine et al., 2000; Niclou et al., 2000), and *in vitro*, diffusible factors secreted by the lens inhibit outgrowth of chick RGC axons (Ohta et al., 1999).

To test whether loss of *slit2* from the lens potentially underlies the defects in OFL organisation, E15.5 wildtype retinal explants from peripheral dorso-temporal or ventro-temporal retina were cultured either alone or with lenses from age-matched wildtype or *slit*-deficient embryos (Figure 4.14). Lenses from wildtype, *slit1*-/-, and *slit1*-/-; *slit2*+/- embryos had a potent inhibitory effect on outgrowth from dorsal retinal explants, inducing an approximate 40% decrease compared to explants cultured alone (Figure 4.14B, C, E). However, in cultures containing *slit1/2*-deficient lenses, significantly more outgrowth occurred than in cultures containing lenses of the other genotypes (Figure 4.14B-E). Some inhibition of outgrowth still occurred with the *slit1/2* deficient lenses inducing an approximate 20% decrease in the extent of outgrowth seen in the absence of the lens (Figure 4.14E). This strongly suggests that Slit2 is a component of the inhibitory activity secreted by the developing lens. In contrast, both wildtype and *slit*-deficient lenses had only a weak inhibitory effect on outgrowth from ventral retinal explants, inducing only approximately 20% decrease in the extent of axon outgrowth. Furthermore, no difference was seen in the potency of the tissues tested (Figure 4.14F).

### *4.2.9 The lens influences growth of the eye*

To test directly the role of the lens in intraretinal pathfinding, the lens was removed *in ovo* from the right eye of embryonic day four (E4) chicken embryos. This would allow the effect of lens removal on axon guidance to be studied in more detail. Interestingly, following collection two days later at E6, the eye in which the lens was removed, appeared a good deal smaller than the unoperated left eye. Following this exciting discovery, the rest of my PhD project will look in further detail at the possible role of the lens in coordinating growth of the eye.

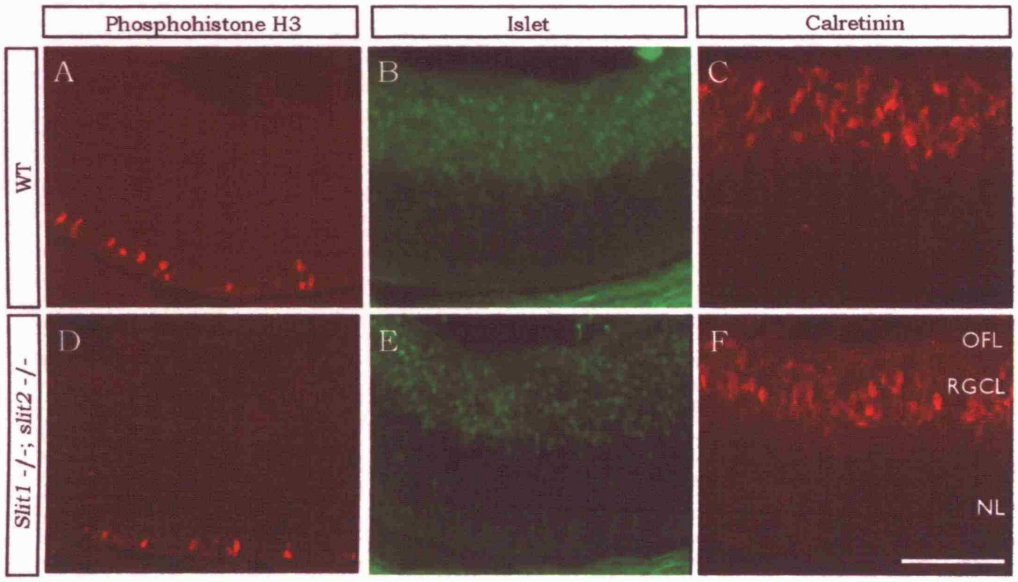


**Figure 4.10- Morphology of *slit*-deficient retinas is normal.**

(A-F) Coronal sections of E16.5 WT (A-C) and *slit1/2 -/-* (D-F) retinas stained with antibodies against phosphohistone-H3 (A, D), Islet1 (B, E) or Calretinin (C, F). In *slit1/2 -/-* retinas, both mitotic (D) and differentiated (E, F) cells are arrayed similar to WT (A-C). RGCL, RGC layer; NL, Neuroblastic layer. Bar, 150μm.

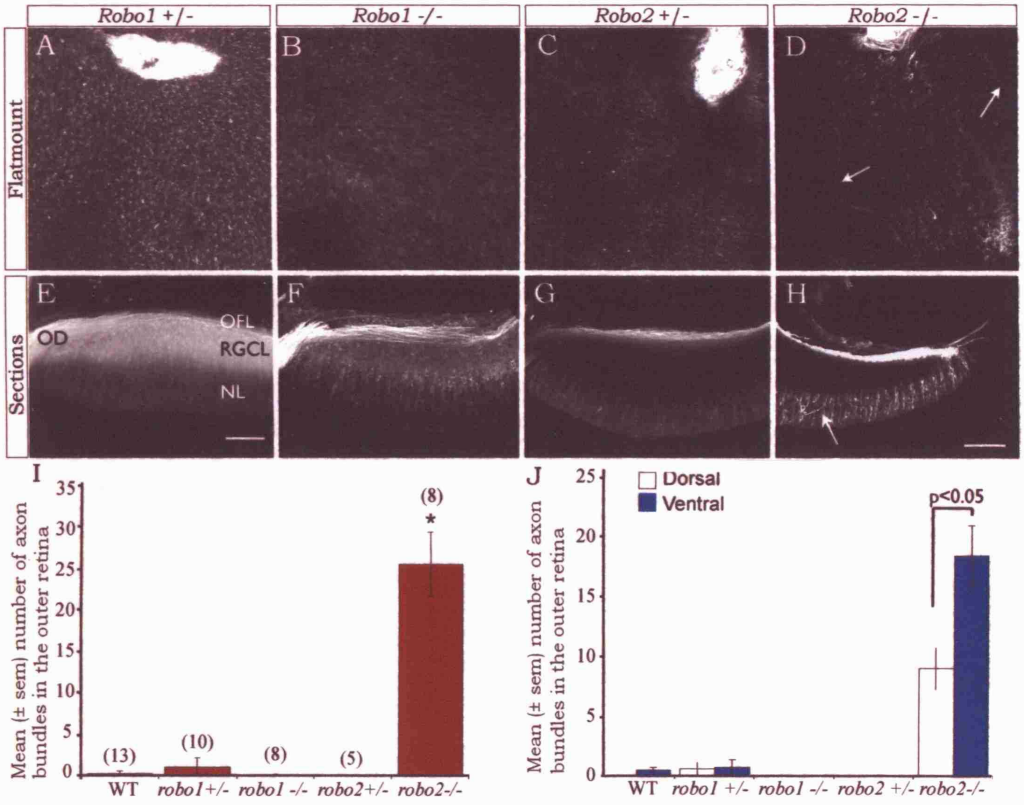


**Figure 4.11- Robo2, but not Robo1, helps restrict axons to the optic fibre layer.**

(A-D) Confocal images taken at the level of the neuroblastic layer of flatmounted E16.5 retinas stained with an anti-β-tubulin antibody. The optic disc is located towards the top of each picture. (E-H) Coronal sections of anti-β-tubulin stained E16.5 retinas. In each image the optic disc is located towards the left-hand side. In *robo1* +/- (A, E), *robo1*-/- (B, F) and *robo2* +/- (D, G) retinas RGC axons are restricted to the OFL and no axons are present within the outer retina. In *robo2*- deficient (D, H) retinas, large bundles of axons are located within the outer retina (arrows). RCGL, RGC layer; NL, neuroblastic layer; OFL, optic fibre layer; OD optic disc. Bar, 100μm. (I) Mean ± SEM number of axon bundles located within the outer retina of *robo1* +/-, *robo1* -/-, *robo2* +/- and *robo2*-/- retinas. * p< 0.001 compared with *robo1* +/- . (J) Mean ± SEM number of axons bundles in the outer layers of dorsal (white bars) or ventral (blue bars) retina. In *robo2* -/- retinas, significantly more bundles are found within the outer layers of ventral versus dorsal retina.

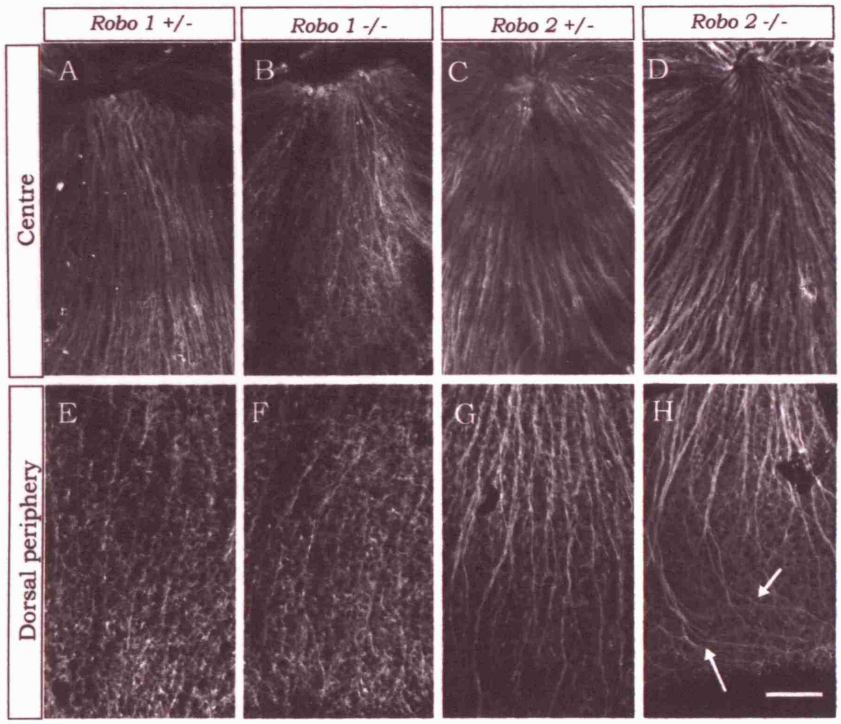


**Figure 4.12- Robo2 helps regulate the organisation of the OFL.**

(A-H) Confocal images of E16.5 dorsal retinas stained with an anti-β-tubulin taken at the level of the OFL. In each image the direction of the optic disc is towards the top of the picture. In *robo1*-deficient (A, B, E, F) and *robo2* +/- (C, G) retinas, RGC axons extend directly towards the optic disc. In *robo2* -/- (D, H) dorsal retina, RGC axons within the peripheral (H) but not central (D) region of the OFL, adopt abnormal looped trajectories (arrows). Bar, 100μm.

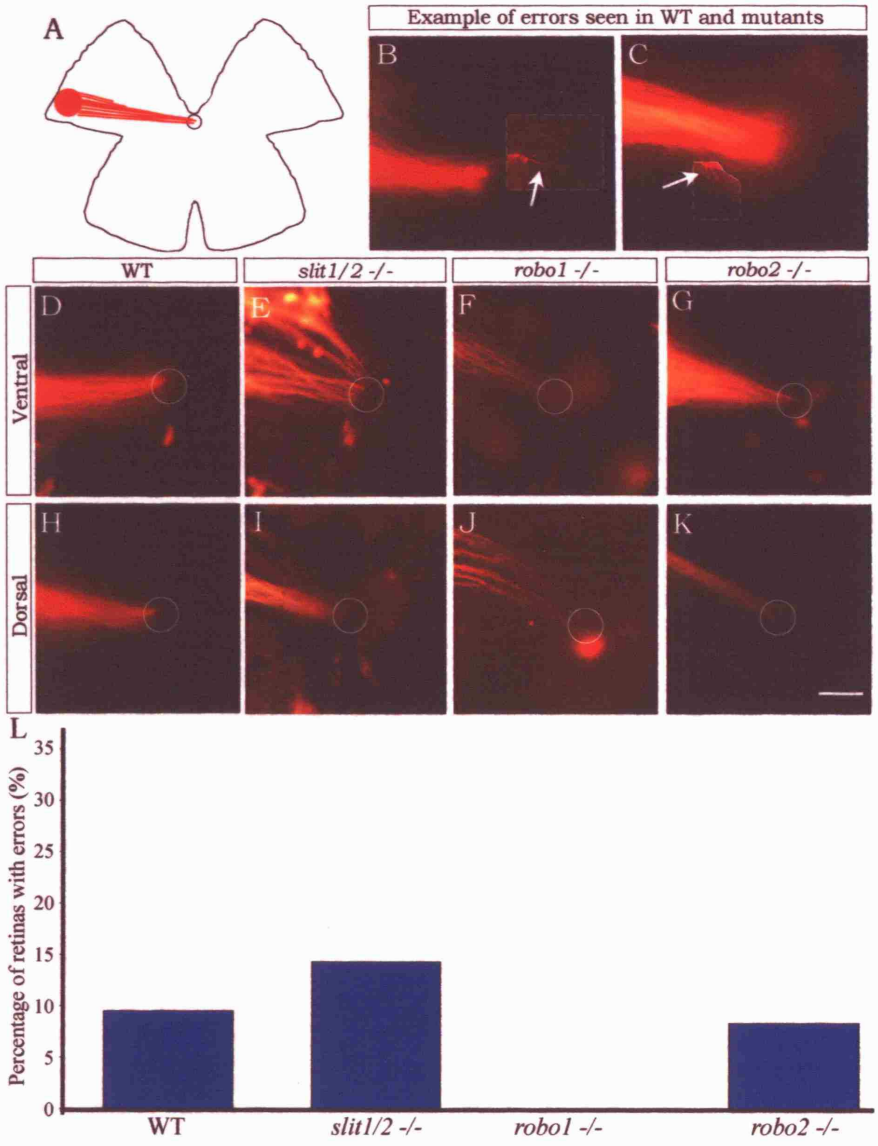


**Figure 4.13- Slit and Robo are not required for RGC axons to exit the eye.**

(A) Schematic diagram illustrating the DiI position within the flatmount retina, either dorsal or ventral. (B-K) Focal DiI-labelled E15.5-E18.5 flatmount retinas, focusing on the optic disc (circle). (B, C) Examples of the small errors seen in targeting the optic disc. (D-G) Ventral focal DiI-labelling of wildtype (D), *slit1/2 -/-* (E), *robo1 -/-* (F) and *robo2 -/-* (G) RGC axons. (H-K) Dorsal focal DiI-labelling of wildtype (H), *slit1/2 -/-* (I), *robo1 -/-* (J) and *robo2 -/-* (K). The large percentage of retinas did not have any optic disc targeting errors. Bar, 50μm (B-C) 100μm (D-K). (L) Percentage of retinas where small optic disc targeting errors were seen.

**Figure 4.14- Slit proteins from the lens inhibit RGC axons outgrowth from dorsal retinal explants.**

(A) Schematic diagram illustrating the potential role of signals from the lens (red) in regulating the initial direction of RGC (green) axon outgrowth. (B-D) Representative examples of E15.5 dorsal retinal explants cultured alone (B) or with an E15.5 WT (C) or *slit1/2*-deficient (D) lens. Significantly more outgrowth occurs in the presence of the *slit*-deficient lens than the WT lens. Bar, 250μm. (E, F) Quantification of the extent of axon outgrowth in co-cultured of dorsal (E) or ventral (F) retinal explants with an age-matched WT or *slit*-deficient lenses. Numbers above bars indicate numbers of explants analyzed in four independent experiments. *$p<0.05$ compared with WT lens.

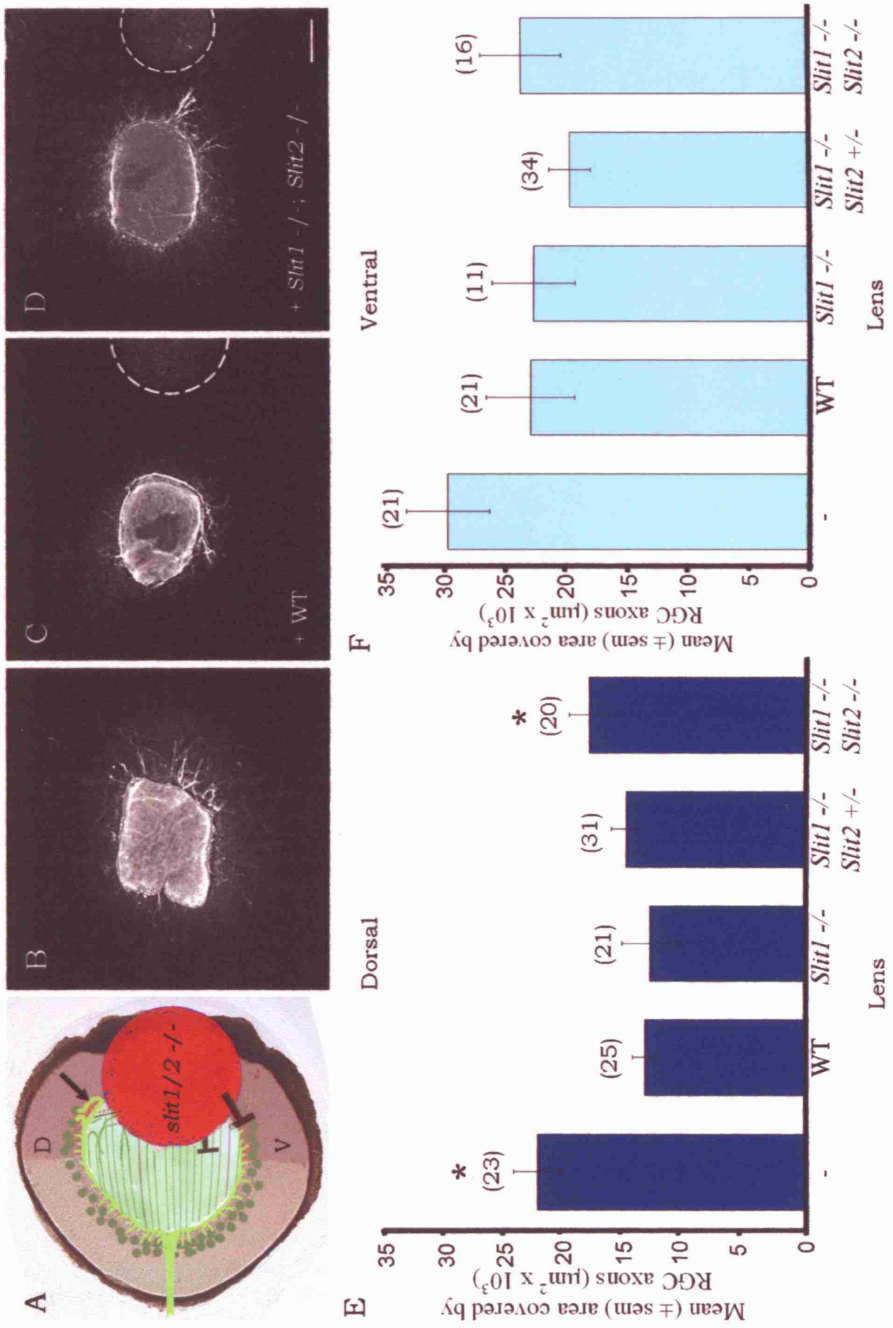
A
slit1/2 -/-
D
V
B
C
+ WT
D
+ Slit1 -/-; Slit2 -/-
E
Dorsal
Mean (± sem) area covered by RGC axons (μm² x 10³)
35
30
25
20
15
10
5
0
*
(23)
(25)
(21)
(31)
*
(20)
-
WT
Slit1 -/-
Slit1 -/- Slit2 +/-
Slit1 -/- Slit2 -/-
Lens
F
Ventral
Mean (± sem) area covered by RGC axons (μm² x 10³)
(21)
(21)
(11)
(34)
(16)
-
WT
Slit1 -/-
Slit1 -/- Slit2 +/-
Slit1 -/- Slit2 -/-
Lens

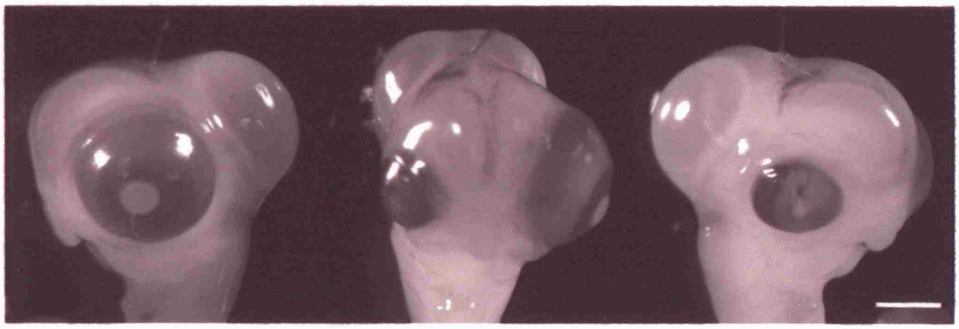

**Figure 4.15- The lens influences growth of the eye.**

Comparison of operated and unoperated eyes at E6 in chick (centre). The lens was removed from E4 chick embryos in ovo, then reincubated for a further two days in order to look at the role of the lens on intraretinal axon guidance. Interestingly, at E6 the unoperated eye (left) is now larger than the operated eye (right). Bar, 250μm.

## 4.3 Discussion

Surprisingly, I found Slit/Robo signalling regulates distinct aspects of RGC axon guidance within different regions of the retina. In ventral retina, they act specifically to help restrict RGC axons to the OFL, whereas in dorsal retina, the function is predominately to regulate the ordered growth of RGC axons within the OFL itself (Figure 4.16). Furthermore, Slits and Robos are also not required for targeting to the optic disc in the central retina. This is despite the expression of *slit* and *robo* throughout the retina, and the ability of dorsal and ventral RGCs to mediate Slit-signalling (Erskine et al., 2000). I also identified the lens as a potential source of Slit, regulating the initial polarity of outgrowth within the dorsal OFL. Robo1 is only expressed by a subset of RGCs and *robo1*-deficient retinas displayed no RGC axon defects in intraretinal pathfinding, indicating that Robo2 is the predominant Robo receptor in axon guidance within the retina. These data clearly demonstrate that multiple mechanisms exist in the retina for axon guidance, of which the Slit/Robo signalling pathway is an important component.

### *4.3.1 Slits regulate distinct aspects of intraretinal guidance in the mammalian and chick retina.*

Although *slit1* is expressed in the murine and chick retina, its localisation and function are not conserved. In chicks, *slit1* is expressed by amacrine cells and plays an important role in controlling the fasciculation of RGC axons as they extend toward the optic disc (Jin et al., 2003). In contrast, I found that in mouse, both *slit1* and *slit2* are expressed predominately, if not exclusively by RGCs and that loss of *slit1* alone has no effect on intraretinal pathfinding. Other guidance cues, for example CSPGs, also have different patterns of expression in rodent and chick retinas. In rats, CSPGs are dynamically expressed with a wave of expression spreading peripherally in front of the central-to-peripheral pattern of RGC differentiation (Brittis et al., 1992). In contrast, in chicks CSPGs are located in regions where RGC axons extend actively (McAdams and McLoon, 1995; Ring et

al., 1995). Together, this suggests that fundamentally distinct mechanisms may regulate intraretinal axon guidance in the mammalian and chick retina.

### *4.3.2 Slit and Robo help prevent RGC axons from extending into the outer layers of the retina*

In the absence of Slits or Robo2, a subset of RGC axons project aberrantly through the outer layers of the retina. Although I cannot exclude that the normal function of Slits is to attract RGC axons toward the OFL (Jin et al., 2003), the preferred model is one in which they function in an inhibitory manner to prevent Robo2-expressing RGC axons extension away from this region. *In vitro*, both Slit1 and Slit2 are potent inhibitors of RGC axon outgrowth, and their expression within the RGC and presumptive inner nuclear layers of the retina place them in an ideal location to act as a barrier to RGC axon extension (Erskine et al., 2000; Niclou et al., 2000; Ringstedt et al., 2000; Plump et al., 2002). Furthermore, removal of pre-existing axons from the OFL is not sufficient to induce ectopic projection of RGC axons into the outer layers of the retina (Stier and Schlosshauer, 1995) and therefore, loss of Slit from the OFL alone is unlikely to be responsible for the observed guidance defects.

Although displaced from the OFL, the mis-localised axons project through the outer retina in a highly directed manner toward the optic disc. This demonstrates that the cues that direct axons toward the optic disc are not localised exclusively within the OFL, and signalling molecules other than Slits, are key regulators of this aspect of intraretinal guidance. For example, Shh which, when disrupted with cyclopamine, results in a complete loss of centrally projecting RGC axons (Kolpak et al., 2005), and downstream targets of zic3 which could be inhibiting RGC axons (Zhang et al., 2004). Furthermore, as the displaced axons extend through the outer retina, they form tightly fasciculated bundles, demonstrating that the outer retina is still partially inhibitory to RGC axon outgrowth. This suggests that other guidance cues function cooperatively with Slits to prevent extension into the outer retina, and redundancy

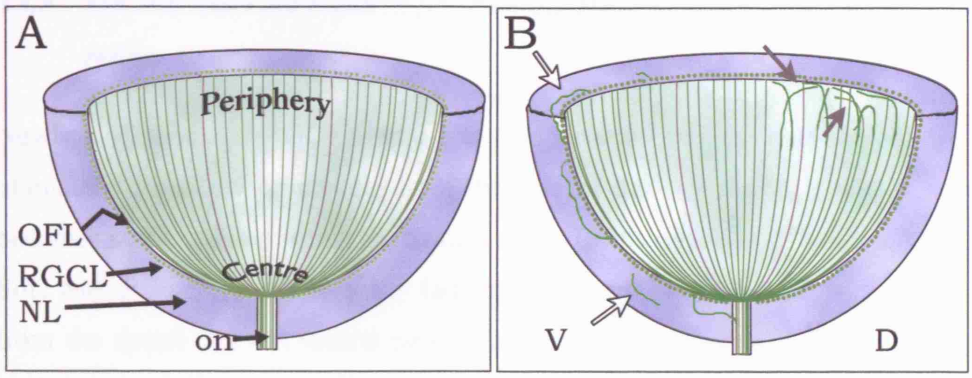


**Figure 4.16- Summary diagram illustrating the intraretinal pathfinding defects that occur in *slit*- or *robo2*- deficient mice.**

(A) In WT retinas RGC extend their axons into the OFL at the inner surface of the retina where they extend in a highly directed manner towards the optic disc. (B) Robo2/Slit signalling helps prevent axons originating predominately in ventral retina from straying away from the OFL into the outer layers of the retina (white arrows) and control the initial direction of growth from recently differentiated RGCs located in the dorsal retina (grey arrows).

between the cues is the simplest explanation for why in the absence of Slits or Robo2 the majority of axons remain restricted to the OFL.

### *4.3.3 Slit and Robo are required for axon guidance in peripheral, but not central retina.*

Newly differentiated RGCs extend transient processes in random directions until ultimately a process originating from the side of the cell closest to the optic disc becomes stabilised and forms the mature axon (Brittis and Silver, 1995). I identified Slit2 and its receptor Robo2 as key factors regulating the initial polarity of outgrowth from the dorsal but not ventral retina. Furthermore, I found that the lens, a tissue known to be inhibitory to RGC axon outgrowth (Ohta et al., 1999), secretes Slit2. Because of its position in the eye, signals from the lens will influence preferentially RGCs located in the retinal periphery (Figure 4.14D). Thus, I propose a model where it is an extrinsic source of Slit that regulates the initial polarity of RGC axon outgrowth within the dorsal retina. Slit2 alone, however, is not a critical factor in determining the overall growth of RGC axons towards the optic disc, and other factors ultimately compensate for its loss, as axons appear to loop back towards the optic disc and are seen to exit the eye (Figure 4.6) (Thompson et al., 2006). Signals from the lens in combination with inhibitory guidance molecules, such as CSPGs within the extreme periphery of the retina (Brittis et al., 1992; Brittis et al., 1995), and attractive cues emanating from more central regions (Kolpak et al., 2005) may underlie this corrected growth.

Entry into the optic disc and exit from the eye is dependent on a number of signals including Netrin/DCC (Deiner et al., 1997), EphB2/B3 (Birgbauer et al., 2000) and BmpR1b (Liu et al., 2003). These molecules appear only to regulate axon guidance within the central region of the retina, and are not required in medial or peripheral regions. In contrast, I have found that the Slit/Robo signalling pathway is essential for regulating intraretinal pathfinding within more peripheral regions, but is not required for RGC axon targeting in the central retina. Thus the retina may consist of several guidance regions, one near the optic disc in which Netrin/DCC, EphB2/B3

and BmpR1b are needed, and others in more peripheral locations of the retina requiring CSPGs and Slit/Robo signalling.

### *4.3.4 Slit and Robo regulate distinct aspects of axon pathfinding within different regions of the retina.*

There are many known developmental differences between dorsal and ventral retina. These regions are defined by differential expression of transcription factors, including Tbx and Vax2 (Barbieri et al., 1999; Sowden et al., 2001). Retinoid-metabolising enzymes are also expressed differentially between dorsal and ventral retina (Li et al., 2000; Wagner et al., 2000). Many guidance cues are also expressed differentially within dorsal and ventral retina, and this is related to both the topographic mapping of the axons within the targets, and regulation of intraretinal pathfinding within specific regions of the retina (Liu et al., 2003; McLaughlin and O'Leary, 2005). Furthermore, several cues that are uniformly expressed throughout the retina are required specifically for guidance within either dorsal or ventral regions (Ott et al., 1998; Birgbauer et al., 2000). For example, *EphB* receptors are expressed uniformly across the retina but in *EphB2/B3* double mutants more errors are seen in ventral, than dorsal retina (Birgbauer et al., 2000).

Unexpectedly, I found that Slits and Robo2 are required within both dorsal and ventral retina but mediate distinct aspects of intraretinal guidance. The reason for this regional specificity is not known. Whereas *slit1* is expressed in a high ventral-low dorsal gradient, *slit2 and robo2* are distributed uniformly (Erskine et al., 2000) (Figure 4.3). Furthermore, both dorsal and ventral RGCs mediate Slit signalling (Thompson et al., 2006). The function of individual guidance cues is dependent critically on the context in which they are encountered. The composition of the extracellular environment, as well as intrinsic factors such as the combination of receptors expressed can modulate guidance responses. HSPGs with distinct heparan sulphate structures are important modulators of Slit localisation and function (Hu, 2001; Inatani et al., 2003; Johnson et al., 2004; Steigemann et al., 2004), and specific heparin-sulphate modifying enzymes are expressed in distinct regions of the optic

pathway (Irie et al., 2002; Pratt et al., 2006). Thus, one possibility is that the localisation of individual heparan sulphate structures may modulate the response of dorsal and ventral RGCs to Slits. Other guidance cues that function redundantly with Slits may also compensate differentially for loss of Slits within dorsal and ventral retina. This suggests that the regional specificity of Slits is likely to be determined by other factors present in the local environment and highlights the complexity of the mechanisms regulating axon guidance.

### *4.3.5 Robo is expressed and functional before crossing the midline.*

It has been shown that the midline of the nerve cord in *Drosophila* and the spinal cord in vertebrates secretes Slits and is inhibitory to CNS axons which express Robos (Battye et al., 1999; Kidd et al., 1999; Zou et al., 2000; Long et al., 2004). Expression of Robo on commissural axons is dynamically regulated, with surface expression on growth cones initially at very low levels, but upon crossing this expression at the growth cone is dramatically upregulated (Kidd et al., 1998b). During crossing the low level of Robo on the growth cone would mean the Slit/Robo inhibitory pathway is not functioning, and only becomes functional in post-crossing commissural axons. In the visual system, those RGC axons which will cross the CNS midline are largely concentrated in the dorsal retina. These axons, in addition to those in ventral retina, show pathfinding defects in *slit/robo*-deficient embryos. This clearly shows that Robo proteins are expressed, and are functioning as a regulator of RGC axon guidance, before the axons reach the CNS midline. Furthermore, RGC axons do not express *rig1*, suggesting that regulation of Robo function does not occur in the developing visual system. Robo expression and function, therefore, is not activated following midline crossing in all commissural axon cell types within the CNS, at least in vertebrates. This highlights the difference in the role of Slit/Robo signalling in the brain compared to other regions of the nervous system.

### *4.3.6 The lens is required for growth of the eye*

Removal of the lens from E4 chicken embryos, followed by examination after two days incubation, resulted in microphthalmia of the aphakic eye. This suggests the

lens may have a role in coordinating eye growth, after lens induction, during development. This fact was first noted in the 1960s (Coulombre and Coulombre, 1964), but the factor in the lens regulating this growth was not elucidated. I will now examine this interesting finding further, and try to discover what factors the lens expresses that could influence growth of the eye.

# 5 The role of the lens in coordinating growth of the eye

## 5.1 Introduction

The first stage in lens development is lens induction, which was originally thought to simply consist of an interaction of the optic vesicles with the overlying surface ectoderm. However, current induction models are more complex, involving a number of steps, and differences are seen between species in the tissues needed for lens induction. Induction then leads to lens specification and development, which requires signals from the mesoderm and foregut during early development and signalling from the optic vesicles when in close contact. These signals and timings are variable between species, but a role for Bmp4 in the optic vesicles has shown this molecule is necessary although not sufficient for lens specification (Furuta and Hogan, 1998; reviewed by Donner et al., 2006). Nevertheless, however the lens ectoderm is specified, this region will express the transcription factors *pax6* and *sox2*, it thickens to become the lens placode then starts to differentiate rounding up and pinching off from the surface to form the lens vesicle. Lens placode formation is coincident with the onset of crystallin expression and the start of lens fiber cell differentiation (reviewed by Chow and Lang, 2001). Lens differentiation occurs following close contact of the surface ectoderm with the underlying optic vesicles, and involves a number of genes. For example *pax6* in vertebrates, is expressed in the surface ectoderm overlying the optic vesicles in addition to the optic vesicles themselves, and expression in the lens placode increases following close contact with the optic vesicle (Grindley et al., 1995). As the lens begins to differentiate, *pax6* expression becomes restricted to the proliferating lens epithelial cells, which is consistent with its role in the activation of crystallins (Grindley et al., 1995). Its important role in eye development, which is evolutionarily conserved, is shown by its ability to induce ectopic eyes in *Drosophila* and in vertebrates (Halder et al., 1995; Chow et al., 1999). Furthermore, *pax6* null mice are anophthalmic (Hill et al., 1991). In the absence of Pax6, contact between the surface ectoderm and optic vesicle is initiated,

but not maintained and the neural retina and RPE do not differentiate and finally the optic vesicle degenerates (Grindley et al., 1995).

A number of transcription factors functioning downstream of *pax6* (Figure 5.1) are also important for lens development, these include; *pitx3* and *foxe3*, expression of which is reduced or is lost, respectively, in *pax6*-deficient mutant mice (Brownell et al., 2000; Chauhan et al., 2002). *pitx3* and *foxe3* are required for lens vesicle closure and proliferation (Semina et al., 1997; Blixt et al., 2000; Brownell et al., 2000). Furthermore, morpholino knockdowns of *pitx3* in zebrafish have reduced *foxe3* expression, indicating a hierarchy of control (Shi et al., 2005; Shi et al., 2006). Other transcription factors include *six3* and *prox1*. Expression of these genes is also absent with the loss of *pax6*, in surface ectoderm-conditional knockouts (Ashery-Padan et al., 2000), and additionally, Sox2, which works in complex with Pax6 to regulate crystallin expression and thus lens development (Kamachi et al., 2001).

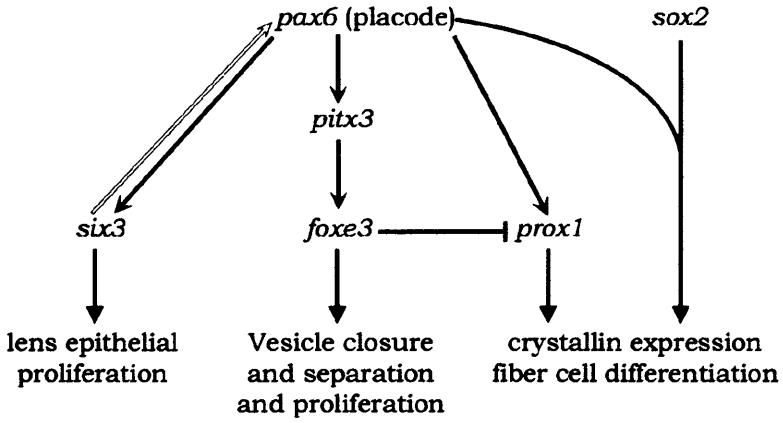


**Figure 5.1- A model for the genetic pathway regulating lens differentiation.**

The homeodomain transcription factors *six3* and *prox1* lie genetically downstream of *pax6* expression in the placode. The transcription factor *foxe3* lies downstream of *pitx3* and *pax6*. *sox2* and *pax6* are the first markers of lens specification and are needed together for crystallin expression. Adapted from Lang et al. (2004).

### *5.1.1 Signalling from the lens*

During specification and development, the lens is known to receive signals from a number of tissues and, conversely, signal to surrounding tissues (Figure 5.2). For example, interaction of the presumptive lens ectoderm is required for neural retina development and patterning. In its absence the optic vesicle fails to pattern correctly, the bilayered optic cup fails to differentiate into neural retina and RPE, and finally the optic cup degenerates. In chick this can be partially rescued by FGFs 1 or 2 (Hyer et al., 1998; Nguyen and Arnheiter, 2000), suggesting FGF signalling is required, possibly directly from the surface ectoderm. Additionally, explant studies have shown that *chx10* expression occurs in response to inductive signals from the presumptive lens ectoderm (Nguyen and Arnheiter, 2000). *chx10 is* the earliest transcription factor expressed in the presumptive neural retina. Later in development, the lens has been shown to be essential for the formation of anterior segment structures of the eye such as the cornea, iris, ciliary body and the anterior chamber (Genis-Galvez, 1966; Zinn, 1970; Kaur et al., 1989; Beebe and Coats, 2000; Thut et al., 2001). The lens was first found to be needed for accurate cornea formation over 40 years ago, and now it has been directly shown that a secreted molecule from the lens epithelium is needed for corneal development, however this secreted molecule remains unknown (Zinn, 1970; Beebe and Coats, 2000). It has also been shown that ectopic lenses can stimulate expression of optic cup margin markers in the neural retina (Thut et al., 2001), and lens-specific expression of the Bmp antagonist, Noggin, can prevent the formation of the ciliary body (Zhao et al., 2002). These data show a functional action of the lens on surrounding tissues. Secreted factors from the lens have been shown to have an affect over some distance (<400μm), in culture assays the lens inhibits RGC axon extension (see chapter 4) (Ohta et al., 1999).

Having established the lens is required for optic cup development and patterning, and anterior eye structure development, the other less known roles of the lens will now be looked at.

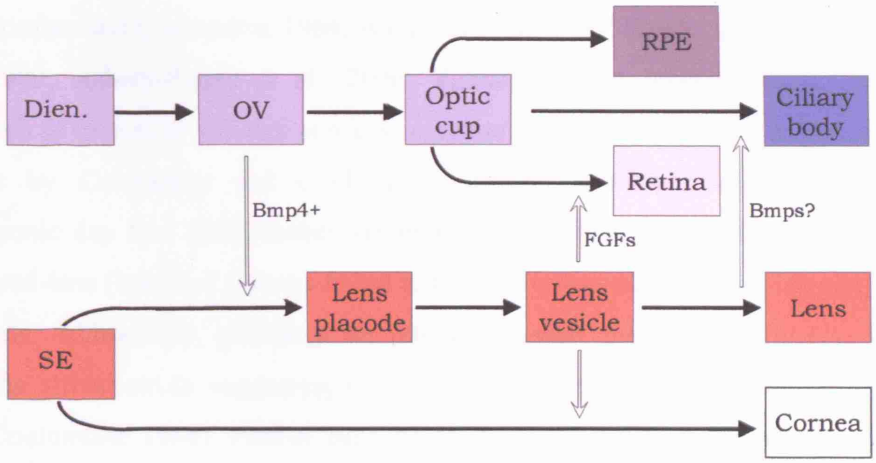


**Figure 5.2- Overview of development of and signalling between eye structures.**

The optic cup develops from the optic vesicle (OV), an outgrowth from the diencephalon (Dien.). The bilayered optic cup will become the retinal pigment epithelium (RPE) and the neural retina and the ciliary body will develop at the edges of these structures. The surface ectoderm will become the lens and cornea. Bmp4 in the optic vesicle signals to the overlying ectoderm and is necessary for placode formation. FGFs are required for optic cup patterning. The lens epithelium is required for cornea development, and Bmp signalling in the lens is required for ciliary body development. SE, surface ectoderm.

### *5.1.2 The lens is needed for growth of the eye*

A number of surgical, mutational and genetic-ablation studies have shown the lens is also required for growth of the eye and for normal organisation of the retina (Coulombre and Coulombre, 1964; Breitman et al., 1987; Landel et al., 1988; Kaur et al., 1989; Ashery-Padan et al., 2000; Yamamoto and Jeffery, 2000). The first research to recognise the lens as a key regulator of eye growth was performed in the 1960s by Coulombre and Coulombre (1964). Following lens removal from embryonic day four (E4) chicken embryos and two further days of incubation, the removed-lens (aphakic) eye was found to be microphthalmic compared to unoperated controls. Additionally, growth of the retina continued resulting in extensive folding into the vitreal cavity suggesting its growth is independent of the lens (Coulombre and Coulombre, 1964). Further experiments where solid-glass or hollow rods were inserted into the eye, which either prevented or allowed vitreous escape, demonstrated the vitreous is needed for ocular growth (Coulombre, 1956). The hypothesis was developed that the lens is necessary for the accumulation of vitreous, which exerts mechanical force needed for growth of the eye, and shaping the retina (Coulombre, 1956; Coulombre and Coulombre, 1964). Whether the lens is acting as a physical barrier to prevent vitreous leakage was then tested. The lens was removed, boiled to denature proteins then replaced, but the resulting eyes were also microphthalmic with the same retinal abnormalities. This demonstrated the need for a living lens which can secrete factors needed for ocular growth (Coulombre and Coulombre, 1964).

The origin of the vitreous is largely unknown, however by looking at mRNA expression of vitreal components, in the cells surrounding the vitreal cavity, it has been hypothesised that the ciliary body is a major contributor (Bishop et al., 2002). Collagen is the major component of the vitreous and in chick *collagen type IX* expression is seen in the presumptive ciliary body from E3.5-E15 (Linsenmayer et al., 1990). However, *collagen type II* expression is seen in the inner layers of the optic cup from E3.5 until E7, when it then becomes restricted to the presumptive

ciliary body. Both these collagens are also expressed at low levels by the lens at E5 and at higher levels at E7 (Linsenmayer et al., 1990).

### *5.1.3 Further evidence the lens is required for eye development*

Further evidence that the lens is required for ocular growth and normal retinal development is seen with selective ablation of the lens in mice *in vivo* (Breitman et al., 1987; Landel et al., 1988; Kaur et al., 1989). A number of transgenic mice were created using toxins under control of crystallin promoters, all of which initiated lens and optic cup development. These toxins killed the lens during differentiation which resulted in microphthalmia or anophthalmia with extensive folding of the neural retina, which in some cases entirely filled the vitreal cavity (Landel et al., 1988; Breitman et al., 1989; Kaur et al., 1989). Interestingly, in mice heterozygous for the toxin, where a small lens remains present, the sizes of the eyes are mid-way between controls and aphakic eyes and the retinal morphology is normal (Kaur et al., 1989). This suggests, that growth of the eye appears to be coordinated with continued growth of the lens, and absence of the lens prevents growth of the eye, which supports the findings seen in chick (Coulombre and Coulombre, 1964). However, in heterozygous mice a small lens being present is enough for the retina to grow and form correctly, even in a small eye, suggesting growth of the retina is not independent of the lens, or a partially folded retina would have been seen.

Pax6 plays an important role in early ocular development, its importance is shown in *pax6* null mice where eye development is initiated but then halts and degenerates resulting in anophthalmia (Hill et al., 1991). This degeneration prevented analysis of the role of Pax6 at later stages of eye development, until a conditional *pax6* knockout was generated (Ashery-Padan et al., 2000). In this knockout, *pax6* expression is lost in the surface ectoderm only, concurrently with lens induction, preventing development past the placode stage, at which point the retina is already patterned. However, the neural retina appeared to fold extensively and was hypothesised to be forming multiple retinas (Ashery-Padan et al., 2000). Interestingly, a similar extensive folding of the retina was seen when the lens was removed by selective

ablation in mice (Landel et al., 1988; Breitman et al., 1989) or surgical removal in chick (Coulombre and Coulombre, 1964). Pax6 is upstream of a number of transcription factors needed for normal lens development (Figure 5.1), it is therefore a reasonable hypothesis that the fully developed lens is needed to signal to the retina and influence its development.

Further support of this is seen in *foxe3* null mice which have microphthalmia, anterior segment abnormalities, an extensively folded retina, a persistent lens stalk and the surviving lens is vacuolated, small and irregular, which is similar to dysgenetic lens mice (Sanyal and Hawkins, 1979; Brownell et al., 2000; Medina-Martinez et al., 2005). Dysgenetic lens mice have mutations in *foxe3* and are used as a model for the human syndrome Peter's anomaly. *Foxe3* is a transcription factor downstream of Pax6 which is expressed in the lens epithelium and is essential for its proliferation and for closure of the lens vesicle (Blixt et al., 2000; Brownell et al., 2000; Medina-Martinez et al., 2005). Another transcription factor found downstream of Pax6 which has also been linked to lens development defects and severe microphthalmia, is *pitx3* (Semina et al., 1997; Semina et al., 2000; Rieger et al., 2001). Defects in this gene are seen in the aphakia mouse (Varnum and Stevens, 1968) which is characterised by the absence of the lens and is comparable to the human disorder primary congenital aphakia. Lens development halts following vesicle formation, leaving a persistent lens stalk, and the disorganised lens material is pushed aside as the retina folds into the vitreal space (Varnum and Stevens, 1968; Grimm et al., 1998). Disruption in either of these genes leads to incomplete lens development, microphthalmia and extensive retinal folding.

There are a number of human conditions and syndromes where microphthalmia or anophthalmia is seen. Many of these appear to be associated with disruption of the lens, for example Peter's anomaly which is characterised by the addition of a persistent lens stalk; human microphthalmia, often associated with cataracts and iris abnormalities; and primary congenital aphakia, where the lens is lost early in development. The dygenetic lens (*foxe3* null) mice are a model for the human syndrome Peter's anomaly which is a congenital disease sharing a number of the

mutant phenotypes. Analysis of DNA from patients with Peter's anomaly have identified a mutation in the *foxe3* gene (Semina et al., 2001; Ormestad et al., 2002). It must be noted that Peter's anomaly, like many congenital ocular diseases, is due to various genetic mutations some in the same genetic pathway as *foxe3*, such as *pax6* or *pitx3*, but in most cases the genetic basis has yet to be discovered (Medina-Martinez and Jamrich, 2007).

More evidence showing the importance of the lens for continued growth of the eye is seen in the blind cavefish *Astyanax mexicanus*. The eye starts to develop, but then degenerates following naturally occurring apoptosis of lens cells, as the lens matures. Lens transplantation studies from a related eyed surface-dwelling fish rescues this degeneration (Yamamoto and Jeffery, 2000). This demonstrates a factor is present in the lens which is important for continued eye growth and this factor has been lost to the blind cavefish through evolution. Intriguingly, none of the studies seen above have focused on finding the signal from the lens which regulates growth of the eye and coordinates retinal development.

### *5.1.4 FGFs in eye development*

There are 22 FGFs and 4 FGFRs in humans, and orthologs of most have now been found in chick. FGFs have numerous roles in development, for example FGF2, 4 and 8 have been shown to act as chemoattractants to mesencephalic neural crest and mesenchymal cells in the limb. They also have roles in patterning, limb induction and morphogenesis, bone formation, and neural induction (Thisse and Thisse, 2005). Furthermore, several members of the FGF family are expressed in the developing vertebrate eye and function in lens fibre differentiation (Schulz et al., 1993), neuronal differentiation (Guillemot and Cepko, 1992; Martinez-Morales et al., 2005) and patterning the optic cup (Guillemot and Cepko, 1992; Hyer et al., 1998; Nguyen and Arnheiter, 2000). Interestingly, the lens fibre-differentiating ability of FGF1 and 2 was found to be concentrated in the vitreous (Schulz et al., 1993), indicating a role for the vitreous in signalling.

Although it is clear that the lens is needed during development for correct ocular formation, most studies have focused on elucidating why the lens degenerates (Yamamoto et al., 2004), or finding the molecules needed for correct lens development (Ashery-Padan et al., 2000; Medina-Martinez and Jamrich, 2007). Where the influence of the lens on surrounding tissues has been studied, the focus has been on development of anterior eye structures. I have therefore, using chick as a model, characterised the affect of aphakia on eye growth at a range of ages following lens removal *in ovo*. In addition I have tried to determine if the growth of the retina is independent of the lens. My findings confirmed the lens is needed for continued growth of the eye, but, by measuring total retinal cell numbers I found that growth of the retina is reduced following lens removal. Finally, as no one has tried to find the factor in the lens which influences eye growth, I have looked at lens expression of potential signalling molecules and tested the ability of FGF8 and FGF2 to rescue aphakic-induced microphthalmia.

## 5.2 Results

### *5.2.1 The lens regulates growth of the eye*

Removal of the chick lens at E4 *in ovo* produced microphthalmia when viewed after two days incubation (Figure 5.3A, B). The left eye of each chick embryo, acting as a control was always much larger than the operated right eye. The hole formed by lens removal had almost completely vanished. To determine if this phenotype was due to damage caused by the lentectomy, two controls were performed: firstly, the eye was opened as if to remove the lens, in a sham operation, and secondly the lens was removed and then immediately replaced. The size of these control eyes was largely the same as the unoperated eyes (Figure 5.3C, D). Further experiments eyes where the lens was removed then replaced are used as the only, and referred to as controls.

To compare growth in unoperated eyes, aphakic eyes and control eyes, the diameter of each eye was measured at different time points following the lentectomy (E4-E10; Figure 5.4A-E, Figure 5.4F; $4<n<28$). The unoperated eyes grow quickly and at E5 were already twice the size of E4 eyes. This growth continued at a similar rate up to the last point measured; E10. Growth of control eyes is close to, but at all time points measured, is slightly smaller than the unoperated eyes; this is likely to be due to a post-operative delay in growth as the eyes heal. Growth of the aphakic eyes is less than the control eyes, and appears to have halted around E7 (Figure 5.4F).

### *5.2.2 Lens removal affects retina structure*

To examine in greater detail the structure of the eye following lens removal, E6 eyes were sectioned coronally and viewed on a bright-field microscope or after staining with cell-type-specific markers. The retinas of unoperated and control eyes are closely associated with the RPE along their whole length (Figure 5.5A, C). However, the retinas of aphakic eyes appear highly convoluted, folding away from the RPE and into the centre of the eye (Figure 5.5B).

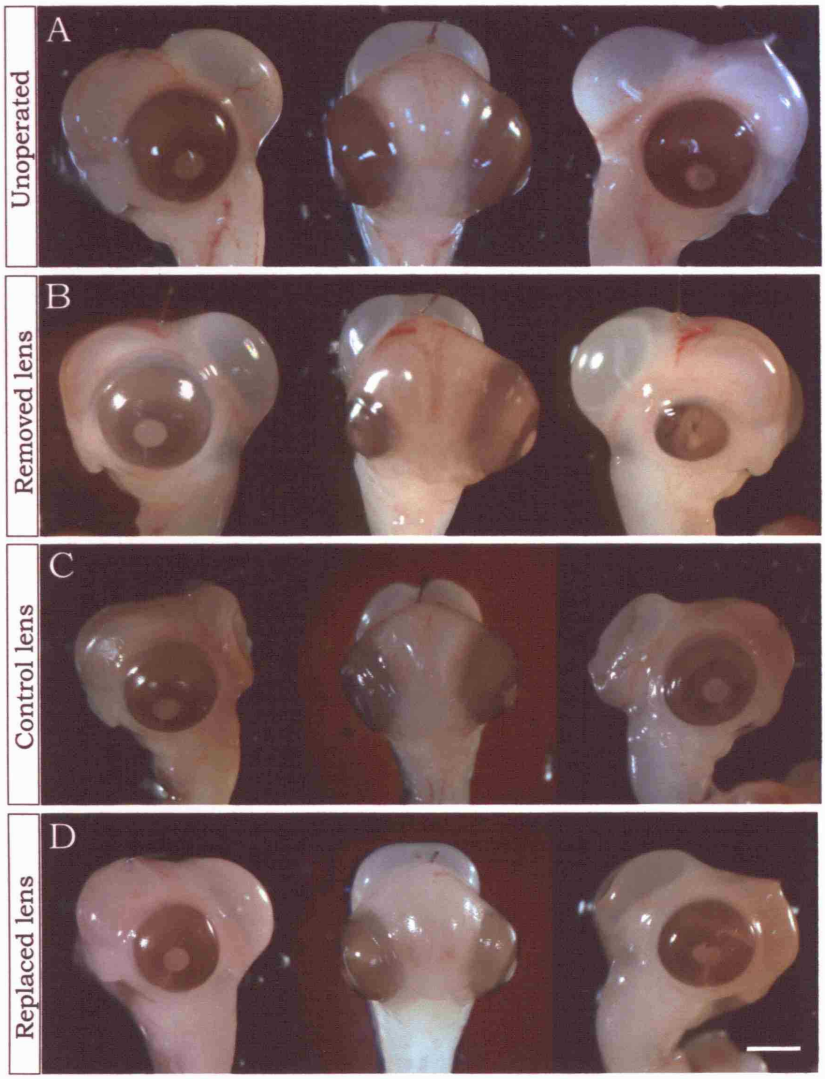


**Figure 5.3- Removal of the lens induces microphthalmia, not seen in controls**

(A-D) Comparison of left, both and right eyes in unoperated (A), removed lens (B), control lens (Sham operated) (C) and replaced lens (D) embryos at E6 following operations at E4. Operations were performed on the right eyes and the left eye was used as a control. Bar, 250μm.

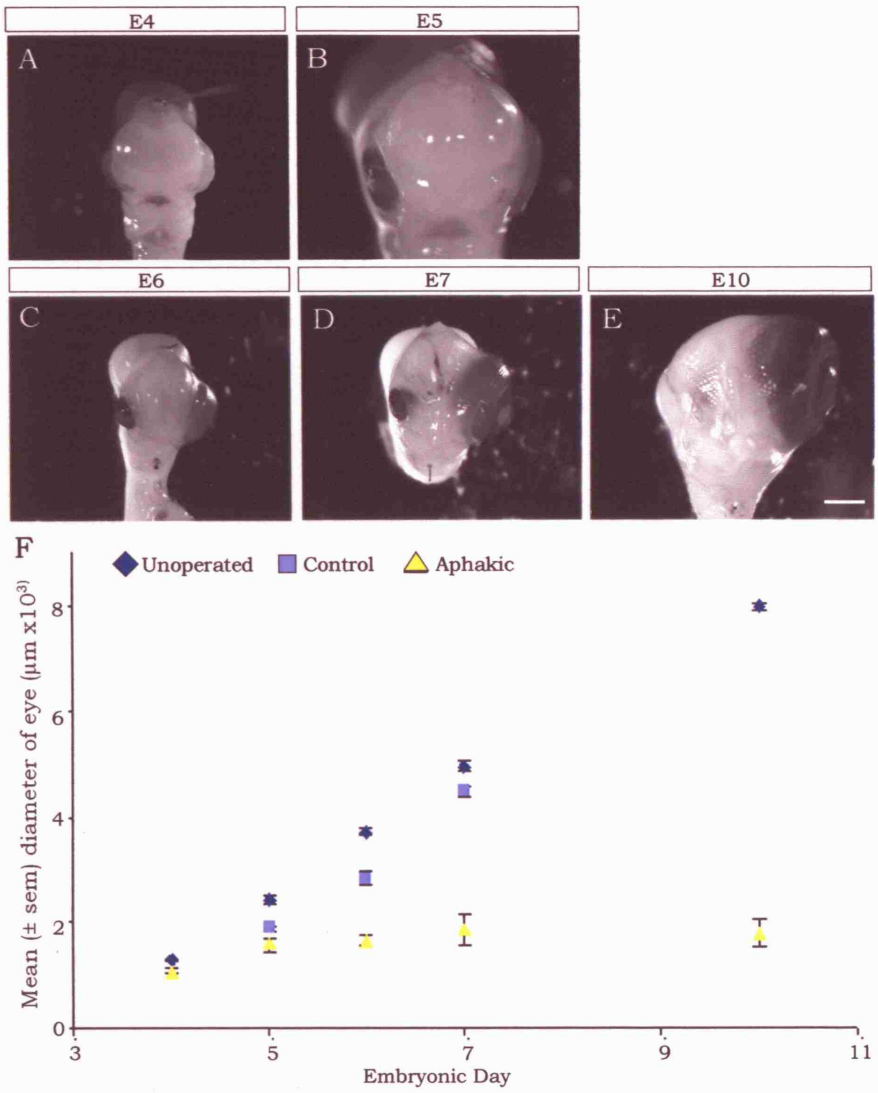


**Figure 5.4- Following lens removal, the eye grows at a much slower rate than controls**

(A-E) Whole head images showing both the aphakic (left) and unoperated (right) eyes at E4 (A), E5 (B), E6 (C), E7 (D) and E10 (E), following operations at E4. The aphakic eye is much smaller than the unoperated eye from E5 onwards (B-E). Bar, 100µm (A, B); 250µm (C-E). (F) Mean ± SEM diameter of unoperated (dark blue), control (light blue) or aphakic (yellow) eyes (µm x $10^3$) from E4 to E10. All eyes grow over time. The control eyes are slightly smaller than the unoperated eyes. The aphakic eyes are significantly smaller than unoperated eyes from E5 onwards (students t-test, $p<0.05$).

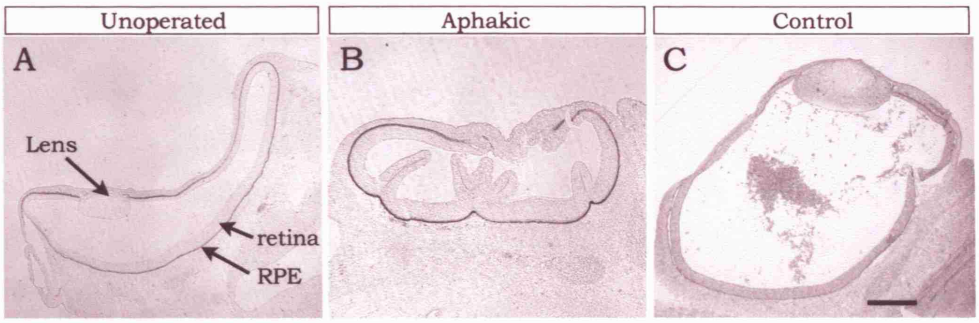


**Figure 5.5- The removal of the lens causes retinal folding.**

(A-C) Coronal sections of E6 unoperated (A), aphakic (B) or control (C) eyes, seen with bright-field microscopy. The retinas of unoperated and control eyes are closely associated with the RPE along the whole length. The retinas of aphakic eyes fold away from the RPE into the centre of the eye. Bar, 300μm (A, C), 500μm (B).

In order to determine if retinal morphology and lamination is affected by lens removal and retinal folding, E6 retinas stained with antibodies against Islet1 (labels differentiated cells in the retina; Figure 5.6A-F) or phospho-histone H3 (labels mitotic cells; Figure 5.6G-L) were examined. In the chick at E6, retinas are composed of three layers: the optic fibre layer at the inner surface of the retina, an inner differentiated region, and an outer neuroblastic layer. Islet1-positive differentiated RGCs and amacrine cells are located in the inner differentiated layer of the retina, with differentiation occurring in a central to peripheral gradient. An outer limit to differentiation is seen, with no Islet1-positive cells in the far peripheral retina. In all retinas examined, Islet1-postive cells were localised to the inner region of the retina and differentiated cells were only seen in more central regions of the retina. In the aphakic eyes, the folds in the retina have outer limits in differentiation as seen in the normal retinas. Mitotic cells, labelled with anti-phospho-histone H3, were located on the outer surface of the retina in the outer neuroblastic layer, normally adjacent to the RPE (Figure 5.6G-L). In the aphakic retinas, mitotic cells are located along the length of the outer retina, and therefore, where the retina folds into the eye these mitotic cells are back to back and not adjacent to the RPE.

The retina forms a highly organised layered structure as it matures. To visualise this and compare with aphakic eyes, E10 retinas were stained with Islet1 or phospho-histone H3 or treated with DAPI (Figure 5.7). At this stage, three of the mature retinal layers have formed; the RGC layer, the inner plexiform layer (IPL) and the inner nuclear layer (INL). Islet1 labels differentiated cells in the RGC layer and INL and also newly differentiated cells following their terminal differentiation in the neuroblastic layer. DAPI labels all cell nuclei. In aphakic eyes the retinal layers appear to be positioned approximately correctly in the retina, however the layers appear thicker and slightly disorganised in regions where folding occurs (Figure 5.7B, D). At E10, mitotic cells are still found along the surface of the outer retina in both control and aphakic eyes (Figure 5.7E-F). This disorganisation in the retinal layers in folded regions is not surprising considering the role of the RPE in maintaining retinal laminar structure (Raymond and Jackson, 1995).

### *5.2.3 The folded retina contains fewer cells than controls*

When these experiments where first performed in the 1960s (Coulombre and Coulombre, 1964) it was thought the lens affected growth of tissues in the eye but retinal growth was independent of the lens and, due to lack of space, this resulted in the extensive folding. However, mice heterozygous for lens-specific expression of α-crystallin-diptheria, were slightly microphthalmic but growth of the neural retina appeared coordinated with growth of the eye. To determine if retinal growth is independent of the lens, total retinal cell counts were performed. Cells of the neural retinas in E4 (n= 7) and E6 (n=9) unoperated retinas, or E6 aphakic (n=6) and control (n=6) retinas, were dissociated and counted using a haemocytometer. All retinas showed an increase in cell number between E4 and E6. At E6, the retinas of aphakic eyes were found to be significantly smaller than controls (using student's t-test $p<0.05$)(Figure 5.8), therefore, even though the retina is highly convoluted the number of cells is less than the unoperated eye.

### *5.2.4 Dorsal/ventral patterning of the retina is unaffected by lens removal*

Recent evidence has shown that specific loss of *pax6* from the surface ectoderm at the time of lens induction prevents the lens maturing correctly and results in the apparent formation of multiple neural retinas (Ashery-Padan et al., 2000). In order to determine if the folded retina seen in aphakic eyes is the first step in the formation of multiple retinas, dorsal/ventral patterning markers were analysed. *Tbx5* is a gene known as a marker for dorsal retina, and therefore riboprobes against it were used on E6 embryos sectioned coronally. *In situ* hybridisation was performed on unoperated (Figure 5.9A, C) and aphakic (Figure 5.9B, D) eyes. *Tbx5* is expressed strongly by a subset of cells localised to the inner region of dorsal retina, in addition to weak expression by cells throughout the dorsal retina. *Tbx5* in the ventral half of the retina is only expressed by a subset of cells on the inner surface of the retina. This was seen in both unoperated (Figure 5.9A) and aphakic (Figure 5.9B) eyes. This shows that two days following lens removal, even though the retina is greatly

convoluted, this dorsal retina marker is unchanged, suggesting patterning is unaltered.

### *5.2.5 FGFs from the lens may be involved*

Previous lens removal studies suggest a factor in the lens is important for growth of the eye and coordinated growth of the retina (Coulombre and Coulombre, 1964; Breitman et al., 1987; Kaur et al., 1989). This may be the factor secreted by the lens in surface-dwelling fish which rescues eye degeneration in the cave-dwelling blind cavefish (Yamamoto and Jeffery, 2000). The nature of this factor has not been elucidated; however it is likely to be a secreted molecule which can signal to surrounding tissues. A growth factor is an obvious option, and one that has been shown to induce growth in other tissues may also induce growth in the eye, for example FGFs from the apical ectodermal ridge maintain proliferation in the developing limb bud (Martin, 1998). Those FGFs expressed by the apical ectodermal ridge were chosen as potential lens factors, and the expression patterns of these; *fgf2, fgf4* and *fgf8* were found using *in situ* hybridisation and/or RT-PCR. Expression of *fgf4* (Figure 5.10B, C) and *fgf8* (Figure 5.10D, E) were found using *in situ* hybridisation on coronal sections of E6 embryos, and of *fgf2, fgf4* and *fgf8* using RT-PCR (Figure 5.10F-G) on cDNA made from RNA extracted from the lens and limb at E4 and E6. *fgf2* expression is detected in the lens at E4 and E6 using RT-PCR. *fgf4 is* expressed within the lens epithelium and in the outer-most lens fibre cells at E6 and expression in the lens is confirmed by RT-PCR. Using *in situ* hybridisation, *fgf8* expression was seen in the lens epithelium at E4, but at E6 expression was seen throughout the lens expression in the lens was confirmed using RT-PCR. The RT-PCR primers were all designed to span exon/intron boundarys so any contamination with genomic DNA would be detected. No genomic DNA contamination was seen in any of the results. Each *in situ* hybridisation was repeated several times to be sure of the results and the RT-PCR results were repeated by a final year BSc student Camilla Gabriel, under my supervision. These molecules could all potentially be secreted by the lens and influence surrounding tissues.

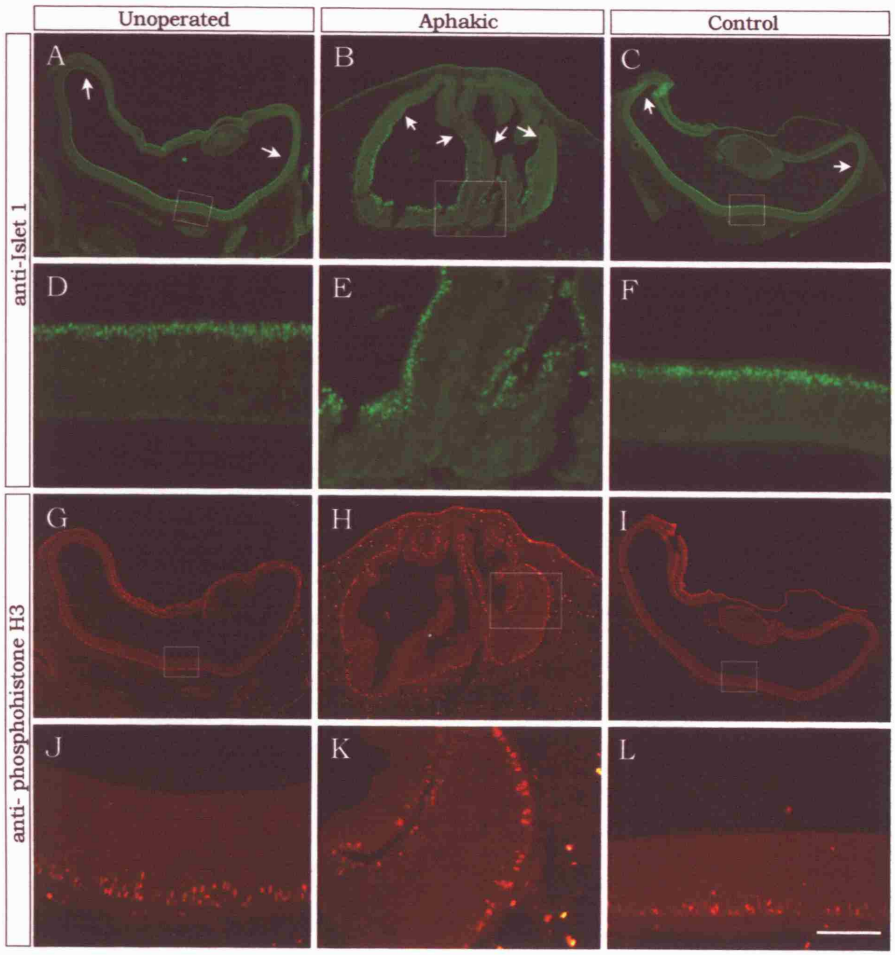


**Figure 5.6- Location of proliferating and differentiated cells is largely normal in aphakic eyes**

(A-L) Coronal sections of E6 unoperated (A, D, G, J), aphakic (B, E, H, K) or control (C, F, I, L) retinas stained with antibodies against Islet1 (A-F) or phosphohistone (H3; G-L). Arrows in A-C show the furthest edge where differentiated cells have thus far formed. Differentiation occurs in a central to peripheral gradient. Boxed regions in A-C and G-I are shown at higher power in D-F and J-L respectively. In the retinas of aphakic eyes, both differentiated (B, E) and mitotic (H, K) cells are arrayed similar to unoperated (A, D, G, J) and control (C, F, I, L) retinas. Bar, 100μm (D-F, J-K), 400μm (B, H), 800μm (A, C, G, I).

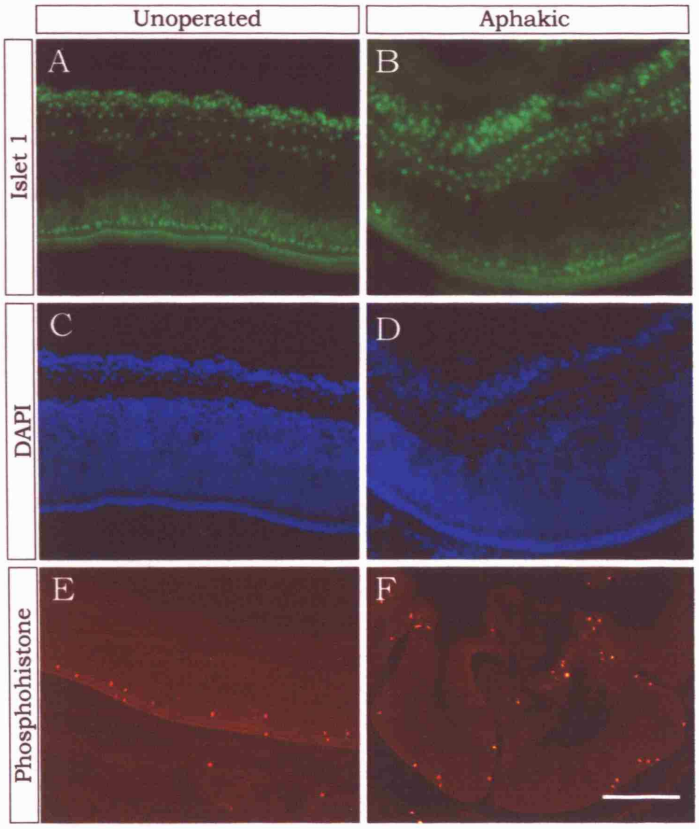


**Figure 5.7- Retinal layers are disrupted within the retinal folds in aphakic eyes.**

(A-F) Coronal sections of E10 unoperated (A, C, E) or aphakic (B, D, F) retinas stained with antibodies against Islet1 (A-B) or phosphohistone-H3 (E-F) or treated with DAPI (C-D). Layers have formed but are slightly disrupted in the retinas of aphakic eyes (B, D) compared to the retinas of unoperated-eyes (A, C). In retinas of aphakic eyes (F) mitotic cells are arrayed as in unoperated (E) retinas, with a sparse distribution of cells seen on the outer surface of the retina. Bar, 100μm (A-D); 200μm (E-F).

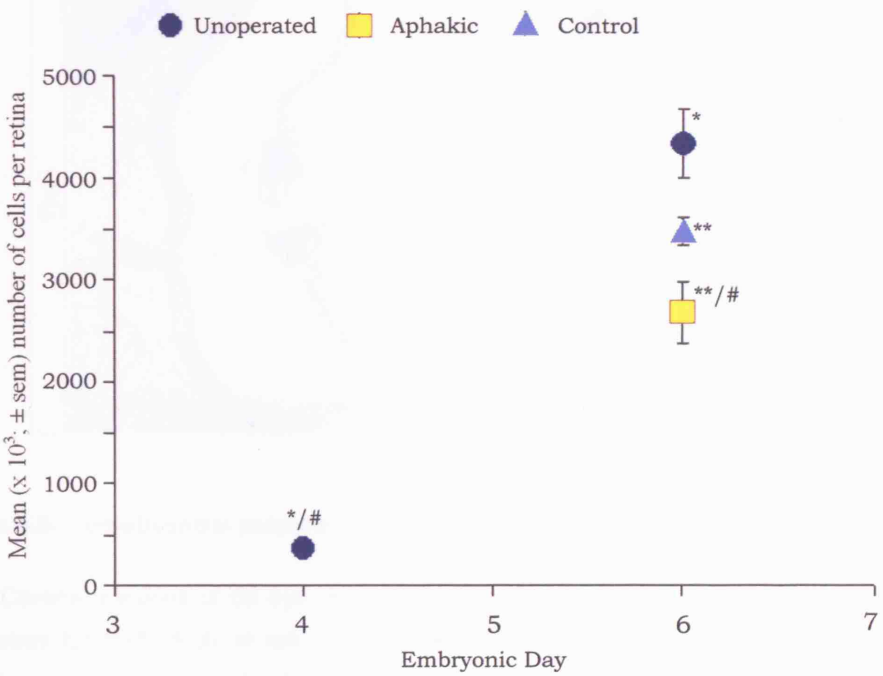


**Figure 5.8- The folded retina is significantly smaller than controls**

Mean ± SEM number of cells in the retinas of unoperated, aphakic and control eyes. The number of cells in aphakic retinas (yellow) is significantly fewer cells than control (blues) retinas. An increase in retinal numbers is seen in all retinas between E4 and E6. All the data are significantly different to each other (*-*, **-**, #-#).

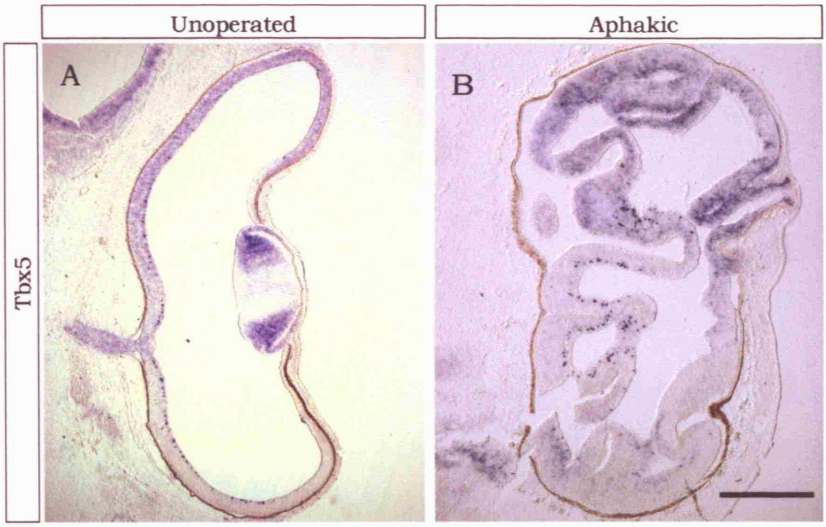


**Figure 5.9- Dorsal/ventral patterning of the retina is unaffected by lens removal**

(A-B) Coronal sections of E6 eyes following *in situ* hybridisation using digoxigenin-labelled riboprobes for *tbx5* (A-B), in retinas of unoperated (A) or aphakic (B) eyes. Dorsal is up. *Tbx5* is expressed strongly in all layers of the dorsal retina, but only expressed by a subset of cells in the ventral RGC layer. Bar, 500μm (A); 400μm (B).

One approach tested, to determine if FGF signalling from the lens could be influencing growth of the eye and retina, was to use electroporation to target DNA into the neural retina. This would allow transfection of retinal cells with a dominant negative (dn) FGFR construct, therefore blocking FGF signalling within the retina. However, in pilot experiments using a GFP marker, only low expression of GFP was seen. This would mean a large proportion of cells still expressing a functional FGFR would be present, possibly rescuing any effect of the dnFGFR. Therefore another approach was used which would affect a larger number of cells.

Beads soaked in SU5402 were implanted into the eye at E4 and the effect studied at E5 and E6 (Figure 5.11) to determine if FGF signalling from the lens could be influencing growth of the eye and retina. SU5402 inhibits FGF signalling by preventing activation of FGFRs (Mohammadi et al., 1997). This would therefore reveal if FGF signalling is needed for growth of the eye, however it would not specify if this signalling is from the lens. DMSO beads, which were used to dilute SU5402, were used as controls; these eyes were ~10% smaller than the unoperated eyes, possibly due to post-operative delay in growth (n=8 at E5, n=7 at E6; Figure 5.11A, B, K). The DMSO beads do not appear to affect the gross morphology of the retina, as seen when sectioned (Figure 5.11G, H). However, following implantation of SU5402 beads, these eyes are significantly smaller than controls in both E5 and E6 embryos (Figure 5.11C, D), the eye diameter is 69% of the unoperated eye at E5 ($n=9$; $p<0.05$) and 78% at E6 ($n=11$; $p<0.05$). The difference seen between E5 and E6 could be due to the limited supply of drug on the bead. Interestingly, in 90% of coronal sections where SU5402 beads have been implanted into the eye, folding of the retina in the region adjacent to the bead was seen (Figure 5.11; n= 10). This was only seen in 40% of cases in the presence of control beads (Figure 5.11H; n=10). These data suggest a role for FGF signalling in growth of the eye.

To test if FGF signals from the lens could be the factor influencing growth of the eye, the lens was removed and replaced with a source of FGF bound to heparin beads. Following lens removal, FGF8 protein bound to heparin beads was implanted

into the eye at E4 and the effect observed a day later. E5 aphakic eyes are microphthalmic compared to unoperated eyes (Figure 5.4, Figure 5.12F; 60% of unoperated, n= 4). The eyes containing implanted heparin beads or FGF beads are also microphthalmic (Figure 5.12A, B, F; 57% n= 6, 53% n= 9). FGF8 beads do not appear to rescue the microphthalmic phenotype produced by lens removal. To confirm FGF8 protein is being released from the bead and having an affect on surrounding tissue, control experiments were performed by inserting a FGF8 bead into the flank of E3 chicken embryos. Expression of downstream targets of FGF8 were analysed using *in situ* hybridisation, and *pyst1* was found to be induced in the area surrounding the FGF8 beads (Figure 5.12G) but not the control heparin beads (Figure 5.12H). Comparable results were seen when FGF2 beads were inserted into aphakic eyes in experiments performed by Camilla Gabriel, a BSc student under my supervision, and in experiments repeated by me. Implantation of FGF2 beads did not rescue the aphakia-induced microphthalmia, and sectioning revealed the retina was also highly convoluted. These data suggest neither FGF8 nor FGF2 alone can rescue the microphthalmic phenotype produced by lens removal, and therefore are unlikely to be the essential FGFs secreted by the lens needed for growth of the eye.

### *5.2.6 Other potential signalling cues from the lens*

Clearly, FGFs are not likely to be the only factors expressed by the lens, therefore the expression of a selection of other potential molecules, which could influence ocular growth were examined. The expression patterns of *shh* (Figure 5.13B), *bmp2* (Figure 5.13C), *bmp4* (Figure 5.13D), *ephrinB2* (Figure 5.13G) and *ephrinB3* (Figure 5.13H) were found using *in situ* hybridisation on coronal sections of E6 embryos. *Shh, bmp2, bmp4* and *ephrinB2* are expressed within the lens epithelium and in the outer-most lens fibre cells. Shh and Bmps could potentially be secreted by the lens, and Ephrins could have a local affect on surrounding tissues.

**Figure 5.10- Expression of FGFs in the lens**

(A) Schematic diagram illustrating the structure of the lens in relation to the eye. Nr, neural retina; LFCs, lens fibre cells; lens ep, lens epithelium. (B-E) Coronal sections of E4 (B, D) or E6 (C, E) eyes following *in situ* hybridisation using digoxigenin-labelled riboprobes; *fgf4* (B, C), or *fgf8* (D, E). *fgf4* is expressed by the lens epithelium and the outer lens fibre cells, most strongly at the lateral edges at E6 (C). *Fgf8* (E) does not appear to be expressed in the lens. Bar, 200μm. (F, G) RT-PCR results from RNA extracted from E4 (F) or E6 (G) lens and limb tissue with primers against the positive control GAPDH, and FGFs 2, 4 and 8. All primers detect expression in lens and limb tissue but not in no-DNA PCR controls, and are all the size expected: GAPDH= 401bp, FGF2= 318bp, FGF4= 380bp, FGF8= 291bp.

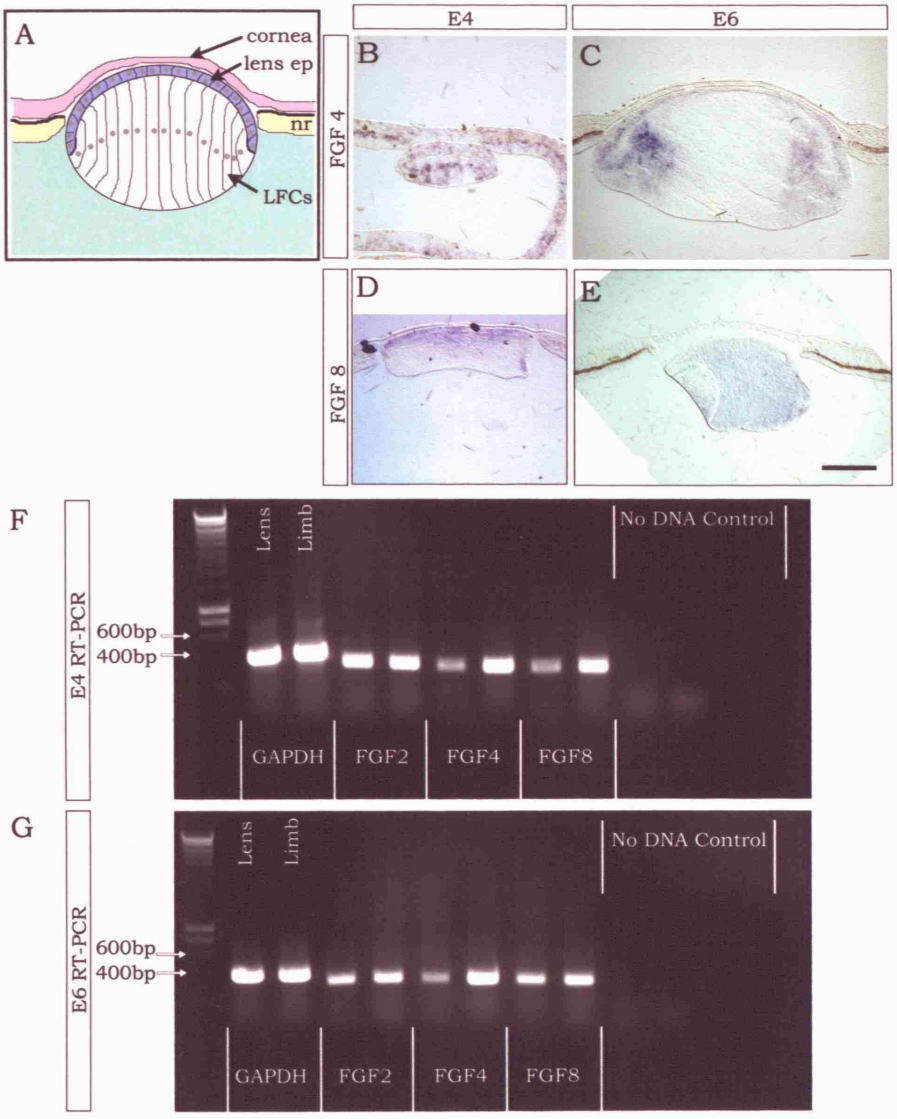
A
cornea
lens ep
nr
LFCs
E4
E6
FGF 4
B
C
FGF 8
D
E
F
E4 RT-PCR
600bp
400bp
Lens
Limb
No DNA Control
GAPDH
FGF2
FGF4
FGF8
G
E6 RT-PCR
600bp
400bp
Lens
Limb
No DNA Control
GAPDH
FGF2
FGF4
FGF8

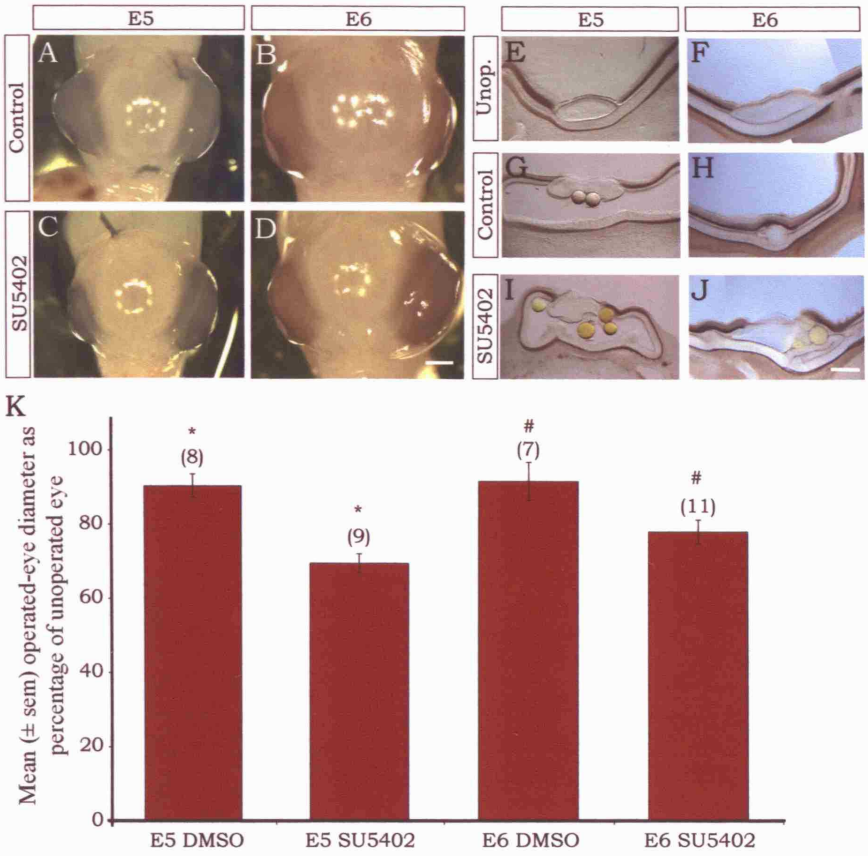


**Figure 5.11- FGF signalling is required for growth of the eye and correct formation of the retina**

(A-D) Whole head images showing both the operated-eye (with beads inserted; left) and unoperated control (right) at E5 (A, C) and E6 (B, D), with DMSO control (A, B) or SU5402/ DMSO (C, D) beads. (E-J) Coronal sections of E5 (E, G, I) or E6 (F, H, J) eyes of unoperated (no beads; E, F), control beads (G, H) or SU5402 beads (I, J). (K) Mean ± SEM operated-eye diameter as a percentage of unoperated-eye control. The DMSO control beads result in the operated eye being ~90% of the unoperated-eye at E5 and E6; however the SU5402-bead treated eye is 69% at E5 increasing to 78% at E6. The number above the bars indicates the number of embryos analysed in each case. The SU5402-bead data is significantly different to the DMSO-bead data at both ages ($p<0.05$ *-*, #-#). The SU5402-bead data at E5 is significantly different to the SU5402-bead data at E6 ($p<0.1$). Bar, 1mm (A-D), 250μm (E-J).

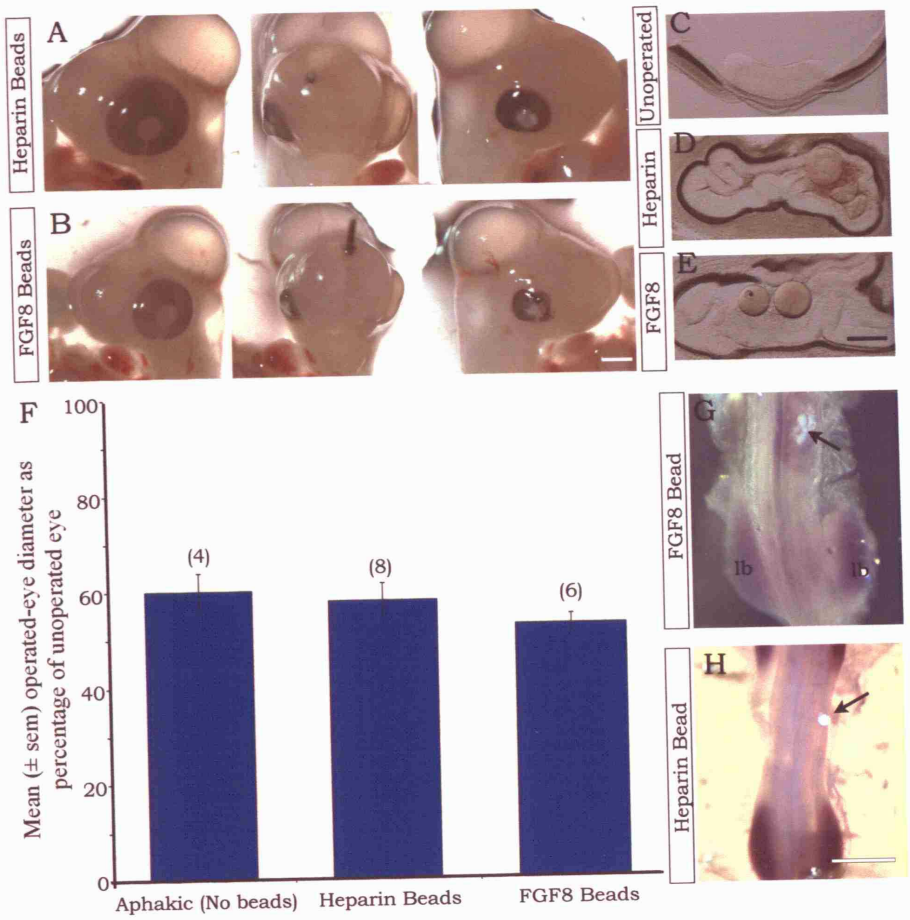


**Figure 5.12- FGF8 beads do not rescue the removed lens phenotype**

(A, B) Whole head images showing both the operated-eye (with the lens removed and beads inserted; right) and unoperated control (left) and both together (centre) at E6, with heparin control (A) or FGF8/ heparin (B) beads. (C-E) Coronal sections of E6 eyes of unoperated (no beads; C), control beads (D) or FGF8 beads (E). (F) Mean ± SEM operated-eye diameter as a percentage of unoperated-eye control, comparing removed-lens, heparin-beads and FGF8-beads. The number above the bars indicates the number of embryos analysed in each case. There is no significant difference between each of the data. (G, H) Stage 20 chicks with a FGF8 (G) or heparin (H) bead inserted into the flank for ~ 6hrs followed by *in situ* hybridisation using digoxigenin-labelled riboprobe against *pyst1*. The FGF8 bead induces *pyst1* expression in the flank (arrow in panel G), but the control heparin bead doesn't (H). lb- limb bud. Bar, 1mm (A, B), 200μm (C-E), 500μm (G, H).

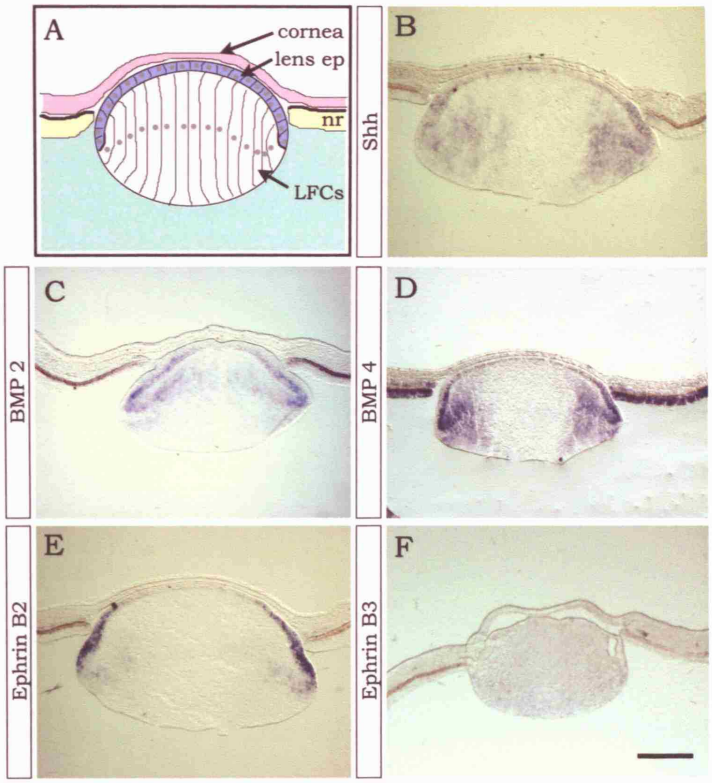


**Figure 5.13- Expression patterns of potential signalling cues in the lens**

(A) Schematic diagram illustrating the structure of the lens in relation to the eye. Nr, neural retina; LFCs, lens fibre cells; lens ep, lens epithelium. (B-F) expression of Shh (B), Bmp2 (C), Bmp4 (D), EphrinB2 (E) and EphrinB3 (F) in the lens at E6. Shh, Bmp2, Bmp4 and EphrinB2 are all expressed by the lens epithelium and marginal lens fibre cells. EphrinB3 is not expressed by the lens.

## 5.3 Discussion

Using chick as a model system I have characterised the affect of aphakia on eye growth following lens removal *in ovo*, in addition to determining if the growth of the retina is independent of the lens. Following lens removal at E4, eye growth is reduced and finally stops around E7. Surprisingly, the number of cells in the neural retina is reduced following lens removal, suggesting the extensive folding is not, as previously described, because growth of the retina is unaffected by lens removal. To try and determine the factor expressed by the lens which influences coordinated growth of the eye, I have examined FGF expression in the lens and using the FGFR inhibitor SU5402, I found blocking FGF signalling in the eye results in microphthalmia. Finally, I tested the ability of FGF8 and FGF2 to rescue aphakic-induced microphthalmia.

### *5.3.1 The lens regulates growth of the eye*

Confirming and extending previous research, which used a number of surgical, mutational and genetic-ablation studies to show the lens is required for growth of the eye (Coulombre and Coulombre, 1964; Breitman et al., 1987; Landel et al., 1988; Kaur et al., 1989; Ashery-Padan et al., 2000; Yamamoto and Jeffery, 2000), I have shown removal of the chick lens at E4 causes microphthalmia. Interestingly, the result of lens removal depends on what point it is removed. If the lens ectoderm is removed early (~St10, chick), before it makes contact with optic vesicles, the optic cups degenerate and no eyes develop (Hyer et al., 1998). However, if the lens is removed (~St22, chick), ablated, or development arrests (section 5.2.1) (Coulombre and Coulombre, 1964; Landel et al., 1988; Kaur et al., 1989; Semina et al., 2000; Yamamoto and Jeffery, 2000; Medina-Martinez et al., 2005) later in development, when the optic cup has been specified, the eye is microphthalmic and the retina shows extensive folding. This indicates the lens is continually signalling to the surrounding tissues to coordinate development of the eye (Figure 5.14).

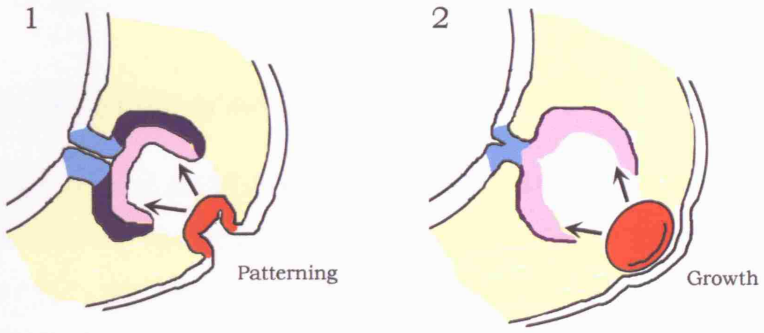


**Figure 5.14- Schematic diagram representing signalling from the lens**

1- early in lens development, the lens ectoderm is needed for patterning the optic cup layers.
2- later in lens development, the lens is needed for growth of the eye and coordinated growth of the retina.

I have shown that lens removal does affect growth of the retina. Total retinal cell counts revealed the aphakic-eye retina has grown since lens removal, but is significantly smaller than controls. This therefore contradicts what has previously been suggested: retinal growth is independent of the lens. Whether the retina grows normally until mitosis is inhibited by lack of free space is however possible, but seems unlikely, as sectioning reveals neural retina-free areas in the vitreal cavity (see Figure 5.5).

### *5.3.2 FGFs affect growth of the eye*

Following application of the FGF-signalling inhibitor SU5402 into the eye, growth of the eye is reduced, implicating FGFs as regulators of eye growth. This is not surprising as FGFs are expressed in the eye, are known mitogens and have been shown directly to increase proliferation in retinal cultures (Lillien and Cepko, 1992). Outside the visual system, FGF2, 4 and 8 are expressed by the apical ectodermal ridge and are needed to pattern the limb and maintain proliferation in the underlying progress zone, needed for continued growth of the limbs (Reviewed by Powers et al., 2000). These data do not reveal whether SU5402-induced microphthalmia is a result of FGF signalling from the lens being disrupted, but this would support a model where FGFs from the lens promote coordinated growth of the eye. Further work, targeting FGFs in the lens specifically would be needed to examine this. It is possible that the SU5402-induced microphthalmia is due to a non-specific toxic effect, which has been seen at high concentrations (Ma et al., 2007), however, as the eye continues growing and is able to recover from SU5402, this seems unlikely.

Removing the lens and replacing it with an exogenous source of FGFs bound to heparin beads did not rescue aphakia-induced microphthalmia. There are many reasons to explain this. Firstly, the FGFs may be too tightly bound to the beads, preventing sufficient secretion to have an affect on surrounding tissues. However, when implanted into the flank of an E3 chicken embryo, expression of a MAP kinase phosphatase, *pyst1,* known to be activated by FGFs (Eblaghie et al., 2003), is seen surrounding the bead. This, therefore, shows that the implanted beads can have an

affect on surrounding tissues and must be released from the beads. Secondly, FGFs are a large group of molecules, and it could be other family members which are the key molecules for maintaining coordinated growth of the eye. Furthermore, it may not be one single molecule acting alone, but a combination of FGFs or indeed other molecules which are needed.

### *5.3.3 Are signals from the lens having a direct or indirect affect?*

The lens is known to be important, not only for growth of the eye, but also for the development of anterior eye structures including the cornea, ciliary body, iris and anterior chamber (Genis-Galvez, 1966; Zinn, 1970; Kaur et al., 1989; Beebe and Coats, 2000; Thut et al., 2001). It is therefore possible that removal of the lens has an indirect affect on growth of the eye, by affecting development of these structures. In support of this, it is thought the ciliary body is needed for production of the vitreous (Bishop et al., 2002), and the vitreous has been shown to be important for growth of the eye (Coulombre, 1956). An alternative theory is the lens could have a direct affect by signalling to maintain proliferation, or by itself secreting vitreous components (Linsenmayer et al., 1990) and therefore promoting ocular growth.

### *5.3.4 What is the role of the vitreous?*

Is the vitreous exerting mechanical force to expand the eye, or does the vitreous allow the exchange of mitogenic signals across the eye? It is known the vitreous contains FGFs, along with other growth factors (Schulz et al., 1993; Sanders et al., 2003; Hartung et al., 2007), and that it is capable of signalling to structures within the eye including the lens, where it induces lens-fibre differentiation (Schulz et al., 1993). The original work by Coulombre et al., 1956, which first showed the vitreous is needed for growth of the eye, was performed by inserting a hollow tube into the eye to allow drainage of the vitreous (Coulombre, 1956). This would reduce mechanical forces which could induce growth of the eye. However, it would also remove any signals secreted by the lens into the vitreous that could signal to induce ocular growth. It is difficult to prove mechanical forces exerted by the vitreous

affect ocular growth, but if the signal from the lens could be found it would resolve this question.

# 6 Conclusions and Future work

## 6.1 Conclusions

RGCs extend axons away from the RGCL towards the vitreal surface of the retina, starting on the well-defined pathway towards their targets in the midbrain. Along this route there are many choice points were axons are steered precisely by an extensive range of axon guidance molecules. I have shown that Slit and Robo are key regulators of axon guidance in the visual system, not just at the optic chiasm (Plump et al., 2002), but at many points along this pathway. *In situ* hybridisation and immunostaining has revealed *slit1*, *slit2*, *robo1* and *robo2*, but not the other family members, are all expressed by RGCs and are all needed for axon pathfinding in the developing visual system. In the absence of Slit/Robo signalling axons project ectopically into outer regions of the retina, into the telencephalon, and the epithalamus and form an ectopic commissure at the ventral midline (Figure 6.1A). Slit2 is secreted from the lens to polarise the initial orientation of axons within the optic fibre layer. Previously, Slit was implicated as a key regulator of RGC axon fasciculation by acting as an inhibitory barrier along the length of the optic tract. Zebrafish *robo2/astray* mutants show RGC axon defasciculation, however this does not appear to be the case in mice. The extensive defasciculation predicted due to Slit expression patterns, does not occur. This is likely to be due to the presence of redundant mechanisms which are not found in zebrafish, but are present surrounding the optic tract in mice. This highlights the complexity of interactions needed for correct pathfinding. The function of Slit and Robo at the midline of the *Drosophila* nerve cord is to regulate which axons cross the midline, and allowing those that do cross to only do so once. The role of Slit/Robo signalling in the mouse visual system however is quite different. Robo is functional in commissural axons before and after crossing the midline, and Slit acts as an inhibitory barrier preventing axons extending into ectopic regions in the retina, chiasm and at key points along the optic tract.

Following removal of the lens *in ovo* of E4 chicken embryos growth of the eye is reduced, resulting in microphthalmia. I propose a model where the lens is acting as a signalling centre: initially patterning the optic cup into RPE and neural retina, then later inducing growth and guiding RGC axons (Figure 6.1B). This is analogous to the roof plate in the dorsal neural tube, a structure that early in development secretes Bmps and Wnts that act to pattern the developing dorsal neural tube (reviewed by Chizhikov and Millen, 2005). Later in development, the roof plate acts as a signalling centre, secreting Bmp family members to repel commissural interneurons away from dorsal regions (Augsburger et al., 1999). I have shown that Slit2 is one molecule secreted by the lens needed for intraretinal axon guidance; however, it is clear other inhibitory molecules remain to be elucidated. Furthermore, the secondary function of the lens as a coordinator of ocular growth suggests further signalling molecules are also expressed by the lens affecting surrounding tissues. The next challenge is to determine the identity of all these signalling factors, and elucidate how they function to coordinate growth of ocular tissues and guidance of RGC axons in a tightly controlled developing system.

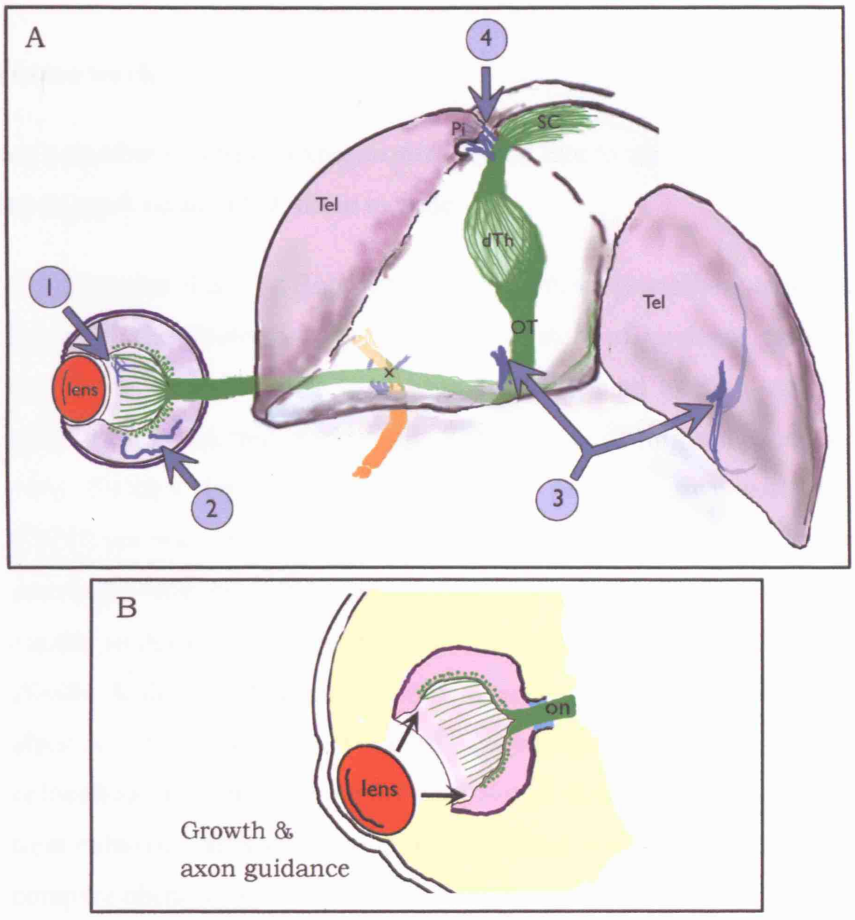


**Figure 6.1- Schematic summary diagrams**

(A) Diagram showing the path of RGC axons (green) through the visual system, indicating aberrant axons (blue) seen in *slit*- or *robo*- deficient embryos. Dorsal is up. (1) Dorsal RGC axons in the peripheral retina, initially project in aberrant trajectories away from the optic disc. (2) RGC axons are no longer seen restricted to the OFL, projecting into the outer layers of the retina, with more aberrant axons seen in the ventral retina. (3) RGC axons project into the telencephalon (purple). (4) RGC axons project into the epithalamus and pineal, crossing the dorsal midline. (B) Diagram showing the role of the lens on development of the eye; the lens is important for repelling RGC axons from the peripheral retina and for regulating growth of the eye. Tel, telencephalon; Pi, pineal; dTh, dorsal thalamus; x, chiasm; on, optic nerve; OT, optic tract; SC, superior colliculus.

## 6.2 Future work

There are a number of further experiments I would like to undertake, if I had another few years to work on my PhD, these include:

- To determine if Slit or Robo interact with other extracellular molecules apart from HSPGs. Proteoglycans are key regulators of guidance cue expression and function, and HSPGs have been found to bind to Slits and Robos and play an important role in regulating Slit/Robo signalling and axon guidance in vivo. Perhaps the same is true for other proteoglycans, such as CSPGs. CSPGs are expressed in the retina, at the chiasm and along the optic tract, and enzymatic removal of these molecules leads to RGC axon pathfinding defects similar to those seen in *slit*-deficient mice (Brittis et al., 1992; Chung et al., 2000b; Ichijo and Kawabata, 2001; Plump et al., 2002). To determine a physical interaction, I could use immunoprecipitation techniques or look for colocalisation when coexpressed with Slit or Robo in cell lines. I could also treat cultured wildtype or *slit*-deficient retinas with chondroitinase ABC and compare phenotypes.

- Determine Slit protein expression, which may explain the region-specific differences of phenotype seen in the retina in *slit*- or *robo*-deficient mice. The Slit antibodies I have already tested (Santa Cruz and Abcam) did not produce any specific staining. I could apply tagged secreted Robo to retinal sections and visualise the location of Slit proteins using anti-'tag' antibodies. In order to confirm Slit specificity, the *slit1/2*-deficient embryos would be used as controls. Alternatively, I could create the Slit antibodies myself.

- Determine if the pia around the diencephalon is altered in *slit*-deficient mice, which may allow RGC axons to leave the surface and cross over to the telencephalon. To achieve this I would look at the ultrastructure of the pia using electronmicroscopy.

- Robo/Robo interactions are thought to promote neurite outgrowth (Hivert et al., 2002), as seen in culture of rat retina and olfactory bulb cells. To examine this further, explants of wildtype retina cultured over Robo-expressing cells would be compared with *robo*-deficient mice retinal explants.

- Determine factors in the lens needed for RGC axon guidance within the retina and for coordinated growth of the eye. Firstly, continue looking for potential molecules within the lens in chick using RT-PCR and *in situ* hybridisation. Next, determine the best way to specifically transfect lens cells; either electroporation or lipofectin. Then using the best method, knock-down expression of any potential molecules alone or in combination, using siRNAs/ oligonucleotides *in ovo*. Finally, confirm the function of the discovered molecules by rescuing expression using protein-bound beads.

- Determine how lens removal affects the retina by looking for altered gene expression. For example, *chx10* is an early marker for neural retina which controls growth and differentiation (Nguyen and Arnheiter, 2000), and may be affected by lens removal. Also, looking at downstream molecules of FGF, Bmp and Shh activation would indicate if lens removal affects these signalling pathways. Finally, look for any alteration in the components of the vitreous. This may indicate if vitreous production has been altered, which may lead to reduced ocular growth. This would give a clearer picture of how the lens influences the eye.

- Do fate mapping using DiI to determine if progenitor cell dispersal is altered following lens removal, as this may explain the folded retinal structure and inhibited growth of the eye. Single cells or groups of cells can be labelled and their fate monitored after a defined period. This would also determine if growth is still concentrated in the ciliary margin.

# 7 References

Andrews W, Liapi A, Plachez C, Camurri L, Zhang J, Mori S, Murakami F, Parnavelas JG, Sundaresan V, Richards LJ (2006) Robo1 regulates the development of major axon tracts and interneuron migration in the forebrain. Development 133:2243-2252.

Ashery-Padan R, Marquardt T, Zhou X, Gruss P (2000) Pax6 activity in the lens primordium is required for lens formation and for correct placement of a single retina in the eye. Genes Dev 14:2701-2711.

Augsburger A, Schuchardt A, Hoskins S, Dodd J, Butler S (1999) BMPs as mediators of roof plate repulsion of commissural neurons. Neuron 24:127-141.

Avci HX, Zelina P, Thelen K, Pollerberg GE (2004) Role of cell adhesion molecule DM-GRASP in growth and orientation of retinal ganglion cell axons. Dev Biol 271:291-305.

Bagri A, Marin O, Plump AS, Mak J, Pleasure SJ, Rubenstein JL, Tessier-Lavigne M (2002) Slit proteins prevent midline crossing and determine the dorsoventral position of major axonal pathways in the mammalian forebrain. Neuron 33:233-248.

Barbieri AM, Lupo G, Bulfone A, Andreazzoli M, Mariani M, Fougerousse F, Consalez GG, Borsani G, Beckmann JS, Barsacchi G, Ballabio A, Banfi S (1999) A homeobox gene, vax2, controls the patterning of the eye dorsoventral axis. Proc Natl Acad Sci U S A 96:10729-10734.

Baron-Van Evercooren A, Kleinman HK, Ohno S, Marangos P, Schwartz JP, Dubois-Dalcq ME (1982) Nerve growth factor, laminin, and fibronectin promote neurite growth in human fetal sensory ganglia cultures. J Neurosci Res 8:179-193.

Bashaw GJ, Kidd T, Murray D, Pawson T, Goodman CS (2000) Repulsive axon guidance: Abelson and Enabled play opposing roles downstream of the roundabout receptor. Cell 101:703-715.

Battye R, Stevens A, Jacobs JR (1999) Axon repulsion from the midline of the Drosophila CNS requires slit function. Development 126:2475-2481.

Beebe DC, Coats JM (2000) The lens organizes the anterior segment: specification of neural crest cell differentiation in the avian eye. Dev Biol 220:424-431.

Birgbauer E, Cowan CA, Sretavan DW, Henkemeyer M (2000) Kinase independent function of EphB receptors in retinal axon pathfinding to the optic disc from dorsal but not ventral retina. Development 127:1231-1241.

Bishop PN, Takanosu M, Le Goff M, Mayne R (2002) The role of the posterior ciliary body in the biosynthesis of vitreous humour. Eye 16:454-460.

Blixt A, Mahlapuu M, Aitola M, Pelto-Huikko M, Enerback S, Carlsson P (2000) A forkhead gene, FoxE3, is essential for lens epithelial proliferation and closure of the lens vesicle. Genes Dev 14:245-254.

Bovolenta P, Fernaud-Espinosa I (2000) Nervous system proteoglycans as modulators of neurite outgrowth. Progress in Neurobiology 61:113-132.

Breitman ML, Clapoff S, Rossant J, Tsui LC, Glode LM, Maxwell IH, Bernstein A (1987) Genetic ablation: targeted expression of a toxin gene causes microphthalmia in transgenic mice. Science 238:1563-1565.

Breitman ML, Bryce DM, Giddens E, Clapoff S, Goring D, Tsui LC, Klintworth GK, Bernstein A (1989) Analysis of lens cell fate and eye morphogenesis in transgenic mice ablated for cells of the lens lineage. Development 106:457-463.

Brent AE, Schweitzer R, Tabin CJ (2003) A somitic compartment of tendon progenitors. Cell 113:235-248.

Brittis PA, Silver J (1995) Multiple factors govern intraretinal axon guidance: a time-lapse study. Mol Cell Neurosci 6:413-432.

Brittis PA, Canning DR, Silver J (1992) Chondroitin sulfate as a regulator of neuronal patterning in the retina. Science 255:733-736.

Brittis PA, Lemmon V, Rutishauser U, Silver J (1995) Unique changes of ganglion cell growth cone behavior following cell adhesion molecule perturbations: a time-lapse study of the living retina. Mol Cell Neurosci 6:433-449.

Brose K, Tessier-Lavigne M (2000) Slit proteins: key regulators of axon guidance, axonal branching, and cell migration. Curr Opin Neurobiol 10:95-102.

Brose K, Bland KS, Wang KH, Arnott D, Henzel W, Goodman CS, Tessier-Lavigne M, Kidd T (1999) Slit proteins bind Robo receptors and have an evolutionarily conserved role in repulsive axon guidance. Cell 96:795-806.

Brownell I, Dirksen M, Jamrich M (2000) Forkhead Foxe3 maps to the dysgenetic lens locus and is critical in lens development and differentiation. Genesis 27:81-93.

Brunet I, Weinl C, Piper M, Trembleau A, Volovitch M, Harris W, Prochiantz A, Holt C (2005) The transcription factor Engrailed-2 guides retinal axons. Nature 438:94-98.

Campbell DS, Holt CE (2001) Chemotropic responses of retinal growth cones mediated by rapid local protein synthesis and degradation. Neuron 32:1013-1026.

Campbell DS, Regan AG, Lopez JS, Tannahill D, Harris WA, Holt CE (2001) Semaphorin 3A elicits stage-dependent collapse, turning, and branching in Xenopus retinal growth cones. J Neurosci 21:8538-8547.

Campbell DS, Stringham SA, Timm A, Xiao T, Law MY, Baier H, Nonet ML, Chien CB (2007) Slit1a Inhibits Retinal Ganglion Cell Arborization and

Synaptogenesis via Robo2-Dependent and -Independent Pathways. Neuron 55:231-245.

Chalasani SH, Sabelko KA, Sunshine MJ, Littman DR, Raper JA (2003) A chemokine, SDF-1, reduces the effectiveness of multiple axonal repellents and is required for normal axon pathfinding. J Neurosci 23:1360-1371.

Chalasani SH, Sabol A, Xu H, Gyda MA, Rasband K, Granato M, Chien CB, Raper JA (2007) Stromal cell-derived factor-1 antagonizes slit/robo signaling in vivo. J Neurosci 27:973-980.

Charron F, Stein E, Jeong J, McMahon AP, Tessier-Lavigne M (2003) The morphogen sonic hedgehog is an axonal chemoattractant that collaborates with netrin-1 in midline axon guidance. Cell 113:11-23.

Chauhan BK, Reed NA, Zhang W, Duncan MK, Kilimann MW, Cvekl A (2002) Identification of genes downstream of Pax6 in the mouse lens using cDNA microarrays. J Biol Chem 277:11539-11548.

Chen H, Chedotal A, He Z, Goodman CS, Tessier-Lavigne M (1997) Neuropilin-2, a novel member of the neuropilin family, is a high affinity receptor for the semaphorins Sema E and Sema IV but not Sema III. Neuron 19:547-559.

Chen JH, Wen L, Dupuis S, Wu JY, Rao Y (2001) The N-terminal leucine-rich regions in Slit are sufficient to repel olfactory bulb axons and subventricular zone neurons. J Neurosci 21:1548-1556.

Chizhikov VV, Millen KJ (2005) Roof plate-dependent patterning of the vertebrate dorsal central nervous system. Dev Biol 277:287-295.

Chow RL, Lang RA (2001) Early eye development in vertebrates. Annu Rev Cell Dev Biol 17:255-296.

Chow RL, Altmann CR, Lang RA, Hemmati-Brivanlou A (1999) Pax6 induces ectopic eyes in a vertebrate. Development 126:4213-4222.

Chung KY, Shum DK, Chan SO (2000a) Expression of chondroitin sulfate proteoglycans in the chiasm of mouse embryos. J Comp Neurol 417:153-163.

Chung KY, Taylor JS, Shum DK, Chan SO (2000b) Axon routing at the optic chiasm after enzymatic removal of chondroitin sulfate in mouse embryos. Development 127:2673-2683.

Cohen J, Burne JF, McKinlay C, Winter J (1987) The role of laminin and the laminin/fibronectin receptor complex in the outgrowth of retinal ganglion cell axons. Dev Biol 122:407-418.

Colamarino SA, Tessier-Lavigne M (1995) The axonal chemoattractant netrin-1 is also a chemorepellent for trochlear motor axons. Cell 81:621-629.

Coulombre AJ (1956) The role of intraocular pressure in the development of the chick eye. J Exp Zool 133:211-225.

Coulombre AJ, Coulombre JL (1964) Lens Development. I. Role of the lens in eye growth. J Exp Zool 156:39-48.

De Bellard ME, Rao Y, Bronner-Fraser M (2003) Dual function of Slit2 in repulsion and enhanced migration of trunk, but not vagal, neural crest cells. J Cell Biol 162:269-279.

de la Torre JR, Hopker VH, Ming GL, Poo MM, Tessier-Lavigne M, Hemmati-Brivanlou A, Holt CE (1997) Turning of retinal growth cones in a netrin-1 gradient mediated by the netrin receptor DCC. Neuron 19:1211-1224.

Deiner MS, Sretavan DW (1999) Altered midline axon pathways and ectopic neurons in the developing hypothalamus of netrin-1- and DCC-deficient mice. J Neurosci 19:9900-9912.

Deiner MS, Kennedy TE, Fazeli A, Serafini T, Tessier-Lavigne M, Sretavan DW (1997) Netrin-1 and DCC mediate axon guidance locally at the optic disc: loss of function leads to optic nerve hypoplasia. Neuron 19:575-589.

Donner AL, Lachke SA, Maas RL (2006) Lens induction in vertebrates: variations on a conserved theme of signaling events. Semin Cell Dev Biol 17:676-685.

Drager UC (1985) Birth dates of retinal ganglion cells giving rise to the crossed and uncrossed optic projections in the mouse. Proc R Soc Lond B Biol Sci 224:57-77.

Eblaghie MC, Lunn JS, Dickinson RJ, Munsterberg AE, Sanz-Ezquerro JJ, Farrell ER, Mathers J, Keyse SM, Storey K, Tickle C (2003) Negative feedback regulation of FGF signaling levels by Pyst1/MKP3 in chick embryos. Curr Biol 13:1009-1018.

Englund C, Steneberg P, Falileeva L, Xylourgidis N, Samakovlis C (2002) Attractive and repulsive functions of Slit are mediated by different receptors in the Drosophila trachea. Development 129:4941-4951.

Erkman L, Yates PA, McLaughlin T, McEvilly RJ, Whisenhunt T, O'Connell SM, Krones AI, Kirby MA, Rapaport DH, Bermingham JR, O'Leary DD, Rosenfeld MG (2000) A POU domain transcription factor-dependent program regulates axon pathfinding in the vertebrate visual system. Neuron 28:779-792.

Erskine L, Patel K, Clarke JD (1998) Progenitor dispersal and the origin of early neuronal phenotypes in the chick embryo spinal cord. Dev Biol 199:26-41.

Erskine L, Williams SE, Brose K, Kidd T, Rachel RA, Goodman CS, Tessier-Lavigne M, Mason CA (2000) Retinal ganglion cell axon guidance in the mouse optic chiasm: expression and function of robos and slits. J Neurosci 20:4975-4982.

Fan J, Raper JA (1995) Localized collapsing cues can steer growth cones without inducing their full collapse. Neuron 14:263-274.

Fan X, Labrador JP, Hing H, Bashaw GJ (2003) Slit stimulation recruits Dock and Pak to the roundabout receptor and increases Rac activity to regulate axon repulsion at the CNS midline. Neuron 40:113-127.

Francis PH, Richardson MK, Brickell PM, Tickle C (1994) Bone morphogenetic proteins and a signalling pathway that controls patterning in the developing chick limb. Development 120:209-218.

Fricke C, Lee JS, Geiger-Rudolph S, Bonhoeffer F, Chien CB (2001) astray, a zebrafish roundabout homolog required for retinal axon guidance. Science 292:507-510.

Friedman GC, O'Leary DD (1996) Retroviral misexpression of engrailed genes in the chick optic tectum perturbs the topographic targeting of retinal axons. J Neurosci 16:5498-5509.

Furuta Y, Hogan BL (1998) BMP4 is essential for lens induction in the mouse embryo. Genes Dev 12:3764-3775.

Galko MJ, Tessier-Lavigne M (2000) Function of an axonal chemoattractant modulated by metalloprotease activity. Science 289:1365-1367.

Gardner CA, Darnell DK, Poole SJ, Ordahl CP, Barald KF (1988) Expression of an engrailed-like gene during development of the early embryonic chick nervous system. J Neurosci Res 21:426-437.

Genis-Galvez JM (1966) Role of the lens in the morphogenesis of the iris and cornea. Nature 210:209-210.

Georgiou M, Tear G (2002) Commissureless is required both in commissural neurones and midline cells for axon guidance across the midline. Development 129:2947-2956.

Georgiou M, Tear G (2003) The N-terminal and transmembrane domains of Commissureless are necessary for its function and trafficking within neurons. Mech Dev 120:1009-1019.

Godement P, Salaun J, Imbert M (1984) Prenatal and postnatal development of retinogeniculate and retinocollicular projections in the mouse. J Comp Neurol 230:552-575.

Grieshammer U, Le M, Plump AS, Wang F, Tessier-Lavigne M, Martin GR (2004) SLIT2-mediated ROBO2 signaling restricts kidney induction to a single site. Dev Cell 6:709-717.

Grimm C, Chatterjee B, Favor J, Immervoll T, Loster J, Klopp N, Sandulache R, Graw J (1998) Aphakia (ak), a mouse mutation affecting early eye development: fine mapping, consideration of candidate genes and altered Pax6 and Six3 gene expression pattern. Dev Genet 23:299-316.

Grindley JC, Davidson DR, Hill RE (1995) The role of Pax-6 in eye and nasal development. Development 121:1433-1442.

Guillemot F, Cepko CL (1992) Retinal fate and ganglion cell differentiation are potentiated by acidic FGF in an in vitro assay of early retinal development. Development 114:743-754.

Halder G, Callaerts P, Gehring WJ (1995) Induction of ectopic eyes by targeted expression of the eyeless gene in Drosophila. Science 267:1788-1792.

Halfter W (1996) Intraretinal grafting reveals growth requirements and guidance cues for optic axons in the developing avian retina. Dev Biol 177:160-177.

Halfter W, Deiss S, Schwarz U (1985) The formation of the axonal pattern in the embryonic avian retina. J Comp Neurol 232:466-480.

Hall A (1998) Rho GTPases and the actin cytoskeleton. Science 279:509-514.

Hall DE, Neugebauer KM, Reichardt LF (1987) Embryonic neural retinal cell response to extracellular matrix proteins: developmental changes and effects of the cell substratum attachment antibody (CSAT). J Cell Biol 104:623-634.

Hamburger V, Hamilton H (1951) A series of normal stages in the development of the chick embryo. Journal of Morphology 88:49-92.

Hamburger V, Hamilton HL (1992) A series of normal stages in the development of the chick embryo. 1951. Dev Dyn 195:231-272.

Hao JC, Yu TW, Fujisawa K, Culotti JG, Gengyo-Ando K, Mitani S, Moulder G, Barstead R, Tessier-Lavigne M, Bargmann CI (2001) C. elegans slit acts in midline, dorsal-ventral, and anterior-posterior guidance via the SAX-3/Robo receptor. Neuron 32:25-38.

Hartung R, Parapuram SK, Ganti R, Hunt DM, Chalam KV, Hunt RC (2007) Vitreous induces heme oxygenase-1 expression mediated by transforming growth factor-beta and reactive oxygen species generation in human retinal pigment epithelial cells. Mol Vis 13:66-78.

Harvey AR, Gan SK, Pauken JM (1987) Fetal tectal or cortical tissue transplanted into brachial lesion cavities in rats: influence on the regrowth of host retinal axons. J Comp Neurol 263:126-136.

He Z, Tessier-Lavigne M (1997) Neuropilin is a receptor for the axonal chemorepellent Semaphorin III. Cell 90:739-751.

Hehr CL, Hocking JC, McFarlane S (2005) Matrix metalloproteinases are required for retinal ganglion cell axon guidance at select decision points. Development 132:3371-3379.

Herrera E, Marcus R, Li S, Williams SE, Erskine L, Lai E, Mason C (2004) Foxd1 is required for proper formation of the optic chiasm. Development 131:5727-5739.

Herrera E, Brown L, Aruga J, Rachel RA, Dolen G, Mikoshiba K, Brown S, Mason CA (2003) Zic2 patterns binocular vision by specifying the uncrossed retinal projection. Cell 114:545-557.

Hill RE, Favor J, Hogan BL, Ton CC, Saunders GF, Hanson IM, Prosser J, Jordan T, Hastie ND, van Heyningen V (1991) Mouse small eye results from mutations in a paired-like homeobox-containing gene. Nature 354:522-525.

Hivert B, Liu Z, Chuang CY, Doherty P, Sundaresan V (2002) Robo1 and Robo2 are homophilic binding molecules that promote axonal growth. Mol Cell Neurosci 21:534-545.

Holland SJ, Gale NW, Mbamalu G, Yancopoulos GD, Henkemeyer M, Pawson T (1996) Bidirectional signalling through the EPH-family receptor Nuk and its transmembrane ligands. Nature 383:722-725.

Holmes GP, Negus K, Burridge L, Raman S, Algar E, Yamada T, Little MH (1998) Distinct but overlapping expression patterns of two vertebrate slit homologs implies functional roles in CNS development and organogenesis. Mech Dev 79:57-72.

Hong K, Nishiyama M, Henley J, Tessier-Lavigne M, Poo MM (2000) Calcium signalling in the guidance of nerve growth by netrin-1. Nature 403:93-98.

Hopker VH, Shewan D, Tessier-Lavigne M, Poo M, Holt C (1999) Growth-cone attraction to netrin-1 is converted to repulsion by laminin-1. Nature 401:69-73.

Hu H (1999) Chemorepulsion of neuronal migration by Slit2 in the developing mammalian forebrain. Neuron 23:703-711.

Hu H (2001) Cell-surface heparan sulfate is involved in the repulsive guidance activities of Slit2 protein. Nat Neurosci 4:695-701.

Hu H, Marton TF, Goodman CS (2001) Plexin B mediates axon guidance in Drosophila by simultaneously inhibiting active Rac and enhancing RhoA signaling. Neuron 32:39-51.

Hu H, Li M, Labrador JP, McEwen J, Lai EC, Goodman CS, Bashaw GJ (2005) Cross GTPase-activating protein (CrossGAP)/Vilse links the Roundabout receptor to Rac to regulate midline repulsion. Proc Natl Acad Sci U S A 102:4613-4618.

Huminiecki L, Bicknell R (2000) In silico cloning of novel endothelial-specific genes. Genome Res 10:1796-1806.

Huminiecki L, Gorn M, Suchting S, Poulsom R, Bicknell R (2002) Magic roundabout is a new member of the roundabout receptor family that is endothelial specific and expressed at sites of active angiogenesis. Genomics 79:547-552.

Hussain S-A, Piper M, Fukuhara N, Strochlic L, Cho G, Howitt JA, Ahmed Y, Powell AK, Turnbull JE, Holt CE, Hohenester E (2006) A Molecular Mechanism for the Heparan Sulfate Dependence of Slit-Robo Signaling. J Biol Chem 281:39693-39698.

Hutson LD, Chien CB (2002) Pathfinding and error correction by retinal axons: the role of astray/robo2. Neuron 33:205-217.

Hyer J, Mima T, Mikawa T (1998) FGF1 patterns the optic vesicle by directing the placement of the neural retina domain. Development 125:869-877.

Ichijo H, Kawabata I (2001) Roles of the telencephalic cells and their chondroitin sulfate proteoglycans in delimiting an anterior border of the retinal pathway. J Neurosci 21:9304-9314.

Inatani M, Irie F, Plump AS, Tessier-Lavigne M, Yamaguchi Y (2003) Mammalian brain morphogenesis and midline axon guidance require heparan sulfate. Science 302:1044-1046.

Irie A, Yates EA, Turnbull JE, Holt CE (2002) Specific heparan sulfate structures involved in retinal axon targeting. Development 129:61-70.

Irving C, Malhas A, Guthrie S, Mason I (2002) Establishing the trochlear motor axon trajectory: role of the isthmic organiser and Fgf8. Development 129:5389-5398.

Itoh A, Miyabayashi T, Ohno M, Sakano S (1998) Cloning and expressions of three mammalian homologues of Drosophila slit suggest possible roles for Slit in the formation and maintenance of the nervous system. Brain Res Mol Brain Res 62:175-186.

Jen JC, Chan WM, Bosley TM, Wan J, Carr JR, Rub U, Shattuck D, Salamon G, Kudo LC, Ou J, Lin DD, Salih MA, Kansu T, Al Dhalaan H, Al Zayed Z, MacDonald DB, Stigsby B, Plaitakis A, Dretakis EK, Gottlob I, Pieh C, Traboulsi EI, Wang Q, Wang L, Andrews C, Yamada K, Demer JL, Karim S, Alger JR, Geschwind DH, Deller T, Sicotte NL, Nelson SF, Baloh RW, Engle EC (2004) Mutations in a human ROBO gene disrupt hindbrain axon pathway crossing and morphogenesis. Science 304:1509-1513.

Jin Z, Zhang J, Klar A, Chedotal A, Rao Y, Cepko CL, Bao ZZ (2003) Irx4-mediated regulation of Slit1 expression contributes to the definition of early axonal paths inside the retina. Development 130:1037-1048.

Johnson KG, Ghose A, Epstein E, Lincecum J, O'Connor MB, Van Vactor D (2004) Axonal heparan sulfate proteoglycans regulate the distribution and efficiency of the repellent slit during midline axon guidance. Curr Biol 14:499-504.

Kamachi Y, Uchikawa M, Tanouchi A, Sekido R, Kondoh H (2001) Pax6 and SOX2 form a co-DNA-binding partner complex that regulates initiation of lens development. Genes Dev 15:1272-1286.

Karlstrom RO, Trowe T, Klostermann S, Baier H, Brand M, Crawford AD, Grunewald B, Haffter P, Hoffmann H, Meyer SU, Muller BK, Richter S, van Eeden FJ, Nusslein-Volhard C, Bonhoeffer F (1996) Zebrafish mutations affecting retinotectal axon pathfinding. Development 123:427-438.

Katz MJ (1985) How straight do axons grow? J Neurosci 5:589-595.

Kaur S, Key B, Stock J, McNeish JD, Akeson R, Potter SS (1989) Targeted ablation of alpha-crystallin-synthesizing cells produces lens-deficient eyes in transgenic mice. Development 105:613-619.

Keino-Masu K, Masu M, Hinck L, Leonardo ED, Chan SS, Culotti JG, Tessier-Lavigne M (1996) Deleted in Colorectal Cancer (DCC) encodes a netrin receptor. Cell 87:175-185.

Keleman K, Ribeiro C, Dickson BJ (2005) Comm function in commissural axon guidance: cell-autonomous sorting of Robo in vivo. Nat Neurosci 8:156-163.

Keleman K, Rajagopalan S, Cleppien D, Teis D, Paiha K, Huber LA, Technau GM, Dickson BJ (2002) Comm sorts robo to control axon guidance at the Drosophila midline. Cell 110:415-427.

Kennedy TE, Serafini T, de la Torre JR, Tessier-Lavigne M (1994) Netrins are diffusible chemotropic factors for commissural axons in the embryonic spinal cord. Cell 78:425-435.

Kidd T, Bland KS, Goodman CS (1999) Slit is the midline repellent for the robo receptor in Drosophila. Cell 96:785-794.

Kidd T, Russell C, Goodman CS, Tear G (1998a) Dosage-sensitive and complementary functions of roundabout and commissureless control axon crossing of the CNS midline. Neuron 20:25-33.

Kidd T, Brose K, Mitchell KJ, Fetter RD, Tessier-Lavigne M, Goodman CS, Tear G (1998b) Roundabout controls axon crossing of the CNS midline and defines a novel subfamily of evolutionarily conserved guidance receptors. Cell 92:205-215.

Kolpak A, Zhang J, Bao ZZ (2005) Sonic hedgehog has a dual effect on the growth of retinal ganglion axons depending on its concentration. J Neurosci 25:3432-3441.

Kozma R, Sarner S, Ahmed S, Lim L (1997) Rho family GTPases and neuronal growth cone remodelling: relationship between increased complexity induced by Cdc42Hs, Rac1, and acetylcholine and collapse induced by RhoA and lysophosphatidic acid. Mol Cell Biol 17:1201-1211.

Kramer SG, Kidd T, Simpson JH, Goodman CS (2001) Switching repulsion to attraction: changing responses to slit during transition in mesoderm migration. Science 292:737-740.

Landel CP, Zhao J, Bok D, Evans GA (1988) Lens-specific expression of recombinant ricin induces developmental defects in the eyes of transgenic mice. Genes Dev 2:1168-1178.

Lang RA (2004) Pathways regulating lens induction in the mouse. Int J Dev Biol 48:783-791.

Lee JS, Ray R, Chien CB (2001) Cloning and expression of three zebrafish roundabout homologs suggest roles in axon guidance and cell migration. Dev Dyn 221:216-230.

Lee JS, von der Hardt S, Rusch MA, Stringer SE, Stickney HL, Talbot WS, Geisler R, Nusslein-Volhard C, Selleck SB, Chien CB, Roehl H (2004) Axon sorting in the optic tract requires HSPG synthesis by ext2 (dackel) and extl3 (boxer). Neuron 44:947-960.

Leonardo ED, Hinck L, Masu M, Keino-Masu K, Ackerman SL, Tessier-Lavigne M (1997) Vertebrate homologues of C. elegans UNC-5 are candidate netrin receptors. Nature 386:833-838.

Leung KM, van Horck FP, Lin AC, Allison R, Standart N, Holt CE (2006) Asymmetrical beta-actin mRNA translation in growth cones mediates attractive turning to netrin-1. Nat Neurosci 9:1247-1256.

Li H, Wagner E, McCaffery P, Smith D, Andreadis A, Drager UC (2000) A retinoic acid synthesizing enzyme in ventral retina and telencephalon of the embryonic mouse. Mech Dev 95:283-289.

Li HS, Chen JH, Wu W, Fagaly T, Zhou L, Yuan W, Dupuis S, Jiang ZH, Nash W, Gick C, Ornitz DM, Wu JY, Rao Y (1999) Vertebrate slit, a secreted ligand for the transmembrane protein roundabout, is a repellent for olfactory bulb axons. Cell 96:807-818.

Li Q, Shirabe K, Thisse C, Thisse B, Okamoto H, Masai I, Kuwada JY (2005) Chemokine signaling guides axons within the retina in zebrafish. J Neurosci 25:1711-1717.

Liang Y, Annan RS, Carr SA, Popp S, Mevissen M, Margolis RK, Margolis RU (1999) Mammalian homologues of the Drosophila slit protein are ligands of the heparan sulfate proteoglycan glypican-1 in brain. J Biol Chem 274:17885-17892.

Lillien L, Cepko C (1992) Control of proliferation in the retina: temporal changes in responsiveness to FGF and TGF alpha. Development 115:253-266.

Lin X (2004) Functions of heparan sulfate proteoglycans in cell signaling during development. Development 131:6009-6021.

Linsenmayer TF, Gibney E, Gordon MK, Marchant JK, Hayashi M, Fitch JM (1990) Extracellular matrices of the developing chick retina and cornea. Localization of mRNAs for collagen types II and IX by in situ hybridization. Invest Ophthalmol Vis Sci 31:1271-1276.

Liu J, Wilson S, Reh T (2003) BMP receptor 1b is required for axon guidance and cell survival in the developing retina. Dev Biol 256:34-48.

Liu Y, Berndt J, Su F, Tawarayama H, Shoji W, Kuwada JY, Halloran MC (2004) Semaphorin3D guides retinal axons along the dorsoventral axis of the tectum. J Neurosci 24:310-318.

Logan M, Simon HG, Tabin C (1998) Differential regulation of T-box and homeobox transcription factors suggests roles in controlling chick limb-type identity. Development 125:2825-2835.

Lohof AM, Quillan M, Dan Y, Poo MM (1992) Asymmetric modulation of cytosolic cAMP activity induces growth cone turning. J Neurosci 12:1253-1261.

Long H, Sabatier C, Ma L, Plump A, Yuan W, Ornitz DM, Tamada A, Murakami F, Goodman CS, Tessier-Lavigne M (2004) Conserved roles for Slit and Robo proteins in midline commissural axon guidance. Neuron 42:213-223.

Lu W, van Eerde AM, Fan X, Quintero-Rivera F, Kulkarni S, Ferguson H, Kim HG, Fan Y, Xi Q, Li QG, Sanlaville D, Andrews W, Sundaresan V, Bi W, Yan J, Giltay JC, Wijmenga C, de Jong TP, Feather SA, Woolf AS, Rao Y, Lupski JR, Eccles MR, Quade BJ, Gusella JF, Morton CC, Maas RL (2007) Disruption of ROBO2 is associated with urinary tract anomalies and confers risk of vesicoureteral reflux. Am J Hum Genet 80:616-632.

Luo Y, Raible D, Raper JA (1993) Collapsin: a protein in brain that induces the collapse and paralysis of neuronal growth cones. Cell 75:217-227.

Lyuksyutova AI, Lu CC, Milanesio N, King LA, Guo N, Wang Y, Nathans J, Tessier-Lavigne M, Zou Y (2003) Anterior-posterior guidance of commissural axons by Wnt-frizzled signaling. Science 302:1984-1988.

Ma AC, Liang R, Leung AY (2007) The role of phospholipase C gamma 1 in primitive hematopoiesis during zebrafish development. Exp Hematol 35:368-373.

Ma L, Tessier-Lavigne M (2007) Dual branch-promoting and branch-repelling actions of Slit/Robo signaling on peripheral and central branches of developing sensory axons. J Neurosci 27:6843-6851.

Marcus RC, Matthews GA, Gale NW, Yancopoulos GD, Mason CA (2000) Axon guidance in the mouse optic chiasm: retinal neurite inhibition by ephrin "A"-expressing hypothalamic cells in vitro. Dev Biol 221:132-147.

Marillat V, Cases O, Nguyen-Ba-Charvet KT, Tessier-Lavigne M, Sotelo C, Chedotal A (2002) Spatiotemporal expression patterns of slit and robo genes in the rat brain. J Comp Neurol 442:130-155.

Marin O, Plump AS, Flames N, Sanchez-Camacho C, Tessier-Lavigne M, Rubenstein JL (2003) Directional guidance of interneuron migration to the cerebral cortex relies on subcortical Slit1/2-independent repulsion and cortical attraction. Development 130:1889-1901.

Martin GR (1998) The roles of FGFs in the early development of vertebrate limbs. Genes Dev 12:1571-1586.

Martinez-Morales JR, Del Bene F, Nica G, Hammerschmidt M, Bovolenta P, Wittbrodt J (2005) Differentiation of the vertebrate retina is coordinated by an FGF signaling center. Dev Cell 8:565-574.

McAdams BD, McLoon SC (1995) Expression of chondroitin sulfate and keratan sulfate proteoglycans in the path of growing retinal axons in the developing chick. J Comp Neurol 352:594-606.

McFarlane S (2003) Metalloproteases: carving out a role in axon guidance. Neuron 37:559-562.

McFarlane S, McNeill L, Holt CE (1995) FGF signaling and target recognition in the developing Xenopus visual system. Neuron 15:1017-1028.

McFarlane S, Cornel E, Amaya E, Holt CE (1996) Inhibition of FGF receptor activity in retinal ganglion cell axons causes errors in target recognition. Neuron 17:245-254.

McGovern VL, Seeger MA (2003) Mosaic analysis reveals a cell-autonomous, neuronal requirement for Commissureless in the Drosophila CNS. Dev Genes Evol 213:500-504.

McLaughlin T, O'Leary DD (2005) Molecular gradients and development of retinotopic maps. Annu Rev Neurosci 28:327-355.

Medina-Martinez O, Jamrich M (2007) Foxe view of lens development and disease. Development 134:1455-1463.

Medina-Martinez O, Brownell I, Amaya-Manzanares F, Hu Q, Behringer RR, Jamrich M (2005) Severe defects in proliferation and differentiation of lens cells in Foxe3 null mice. Mol Cell Biol 25:8854-8863.

Ming GL, Song HJ, Berninger B, Holt CE, Tessier-Lavigne M, Poo MM (1997) cAMP-dependent growth cone guidance by netrin-1. Neuron 19:1225-1235.

Mohammadi M, McMahon G, Sun L, Tang C, Hirth P, Yeh BK, Hubbard SR, Schlessinger J (1997) Structures of the tyrosine kinase domain of fibroblast growth factor receptor in complex with inhibitors. Science 276:955-960.

Monnier PP, Beck SG, Bolz J, Henke-Fahle S (2001) The polysialic acid moiety of the neural cell adhesion molecule is involved in intraretinal guidance of retinal ganglion cell axons. Dev Biol 229:1-14.

Myat A, Henry P, McCabe V, Flintoft L, Rotin D, Tear G (2002) Drosophila Nedd4, a ubiquitin ligase, is recruited by Commissureless to control cell surface levels of the roundabout receptor. Neuron 35:447-459.

Nakagawa S, Brennan C, Johnson KG, Shewan D, Harris WA, Holt CE (2000) Ephrin-B regulates the Ipsilateral routing of retinal axons at the optic chiasm. Neuron 25:599-610.

Nguyen-Ba-Charvet KT, Plump AS, Tessier-Lavigne M, Chedotal A (2002) Slit1 and slit2 proteins control the development of the lateral olfactory tract. J Neurosci 22:5473-5480.

Nguyen Ba-Charvet KT, Brose K, Marillat V, Kidd T, Goodman CS, Tessier-Lavigne M, Sotelo C, Chedotal A (1999) Slit2-Mediated chemorepulsion and collapse of developing forebrain axons. Neuron 22:463-473.

Nguyen Ba-Charvet KT, Brose K, Ma L, Wang KH, Marillat V, Sotelo C, Tessier-Lavigne M, Chedotal A (2001) Diversity and specificity of actions of Slit2 proteolytic fragments in axon guidance. J Neurosci 21:4281-4289.

Nguyen M, Arnheiter H (2000) Signaling and transcriptional regulation in early mammalian eye development: a link between FGF and MITF. Development 127:3581-3591.

Niclou SP, Jia L, Raper JA (2000) Slit2 is a repellent for retinal ganglion cell axons. J Neurosci 20:4962-4974.

Niswander L, Tickle C, Vogel A, Martin G (1994) Function of FGF-4 in limb development. Mol Reprod Dev 39:83-88; discussion 88-89.

O'Leary DD, Yates PA, McLaughlin T (1999) Molecular development of sensory maps: representing sights and smells in the brain. Cell 96:255-269.

Ohta K, Tannahill D, Yoshida K, Johnson AR, Cook GM, Keynes RJ (1999) Embryonic lens repels retinal ganglion cell axons. Dev Biol 211:124-132.

Ormestad M, Blixt A, Churchill A, Martinsson T, Enerback S, Carlsson P (2002) Foxe3 haploinsufficiency in mice: a model for Peters' anomaly. Invest Ophthalmol Vis Sci 43:1350-1357.

Oster SF, Bodeker MO, He F, Sretavan DW (2003) Invariant Sema5A inhibition serves an ensheathing function during optic nerve development. Development 130:775-784.

Ott H, Bastmeyer M, Stuermer CA (1998) Neurolin, the goldfish homolog of DM-GRASP, is involved in retinal axon pathfinding to the optic disk. J Neurosci 18:3363-3372.

Ozdinler PH, Erzurumlu RS (2002) Slit2, a branching-arborization factor for sensory axons in the Mammalian CNS. J Neurosci 22:4540-4549.

Pak W, Hindges R, Lim YS, Pfaff SL, O'Leary DD (2004) Magnitude of binocular vision controlled by islet-2 repression of a genetic program that specifies laterality of retinal axon pathfinding. Cell 119:567-578.

Park KW, Morrison CM, Sorensen LK, Jones CA, Rao Y, Chien CB, Wu JY, Urness LD, Li DY (2003) Robo4 is a vascular-specific receptor that inhibits endothelial migration. Dev Biol 261:251-267.

Piper M, Nurcombe V, Reid K, Bartlett P, Little M (2002) N-terminal Slit2 promotes survival and neurite extension in cultured peripheral neurons. Neuroreport 13:2375-2378.

Piper M, Anderson R, Dwivedy A, Weinl C, van Horck F, Leung KM, Cogill E, Holt C (2006) Signaling mechanisms underlying Slit2-induced collapse of Xenopus retinal growth cones. Neuron 49:215-228.

Plump AS, Erskine L, Sabatier C, Brose K, Epstein CJ, Goodman CS, Mason CA, Tessier-Lavigne M (2002) Slit1 and Slit2 cooperate to prevent premature midline crossing of retinal axons in the mouse visual system. Neuron 33:219-232.

Pollerberg GE, Beck-Sickinger A (1993) A functional role for the middle extracellular region of the neural cell adhesion molecule (NCAM) in axonal fasciculation and orientation. Dev Biol 156:324-340.

Polyak SL (1957) The Vertebrate Visual System. Universiy of Chicago Press, Chicago, Illinois.

Powers CJ, McLeskey SW, Wellstein A (2000) Fibroblast growth factors, their receptors and signaling. Endocr Relat Cancer 7:165-197.

Pratt T, Tian NM, Simpson TI, Mason JO, Price DJ (2004) The winged helix transcription factor Foxg1 facilitates retinal ganglion cell axon crossing of the ventral midline in the mouse. Development 131:3773-3784.

Pratt T, Conway CD, Tian NM, Price DJ, Mason JO (2006) Heparan sulphation patterns generated by specific heparan sulfotransferase enzymes direct distinct aspects of retinal axon guidance at the optic chiasm. J Neurosci 26:6911-6923.

Pratt T, Quinn JC, Simpson TI, West JD, Mason JO, Price DJ (2002) Disruption of early events in thalamocortical tract formation in mice lacking the transcription factors Pax6 or Foxg1. J Neurosci 22:8523-8531.

Rajagopalan S, Vivancos V, Nicolas E, Dickson BJ (2000a) Selecting a longitudinal pathway: Robo receptors specify the lateral position of axons in the Drosophila CNS. Cell 103:1033-1045.

Rajagopalan S, Nicolas E, Vivancos V, Berger J, Dickson BJ (2000b) Crossing the midline: roles and regulation of Robo receptors. Neuron 28:767-777.

~~Raper JA, Grunewald EB (1990) Temporal retinal growth cones collapse on contact with nasal retinal axons. Exp Neurol 109:70-74.~~

Rashid T, Upton AL, Blentic A, Ciossek T, Knoll B, Thompson ID, Drescher U (2005) Opposing gradients of ephrin-As and EphA7 in the superior colliculus are essential for topographic mapping in the mammalian visual system. Neuron 47:57-69.

Raymond SM, Jackson IJ (1995) The retinal pigmented epithelium is required for development and maintenance of the mouse neural retina. Curr Biol 5:1286-1295.

Rhee J, Buchan T, Zukerberg L, Lilien J, Balsamo J (2007) Cables links Robo-bound Abl kinase to N-cadherin-bound beta-catenin to mediate Slit-induced modulation of adhesion and transcription. Nat Cell Biol.

Rhee J, Mahfooz NS, Arregui C, Lilien J, Balsamo J, VanBerkum MF (2002) Activation of the repulsive receptor Roundabout inhibits N-cadherin-mediated cell adhesion. Nat Cell Biol 4:798-805.

Riddle RD, Johnson RL, Laufer E, Tabin C (1993) Sonic hedgehog mediates the polarizing activity of the ZPA. Cell 75:1401-1416.

Rieger DK, Reichenberger E, McLean W, Sidow A, Olsen BR (2001) A double-deletion mutation in the Pitx3 gene causes arrested lens development in aphakia mice. Genomics 72:61-72.

Ring C, Lemmon V, Halfter W (1995) Two chondroitin sulfate proteoglycans differentially expressed in the developing chick visual system. Dev Biol 168:11-27.

Ringstedt T, Braisted JE, Brose K, Kidd T, Goodman C, Tessier-Lavigne M, O'Leary DD (2000) Slit inhibition of retinal axon growth and its role in retinal axon pathfinding and innervation patterns in the diencephalon. J Neurosci 20:4983-4991.

Rothberg JM, Hartley DA, Walther Z, Artavanis-Tsakonas S (1988) slit: an EGF-homologous locus of D. melanogaster involved in the development of the embryonic central nervous system. Cell 55:1047-1059.

Rothberg JM, Jacobs JR, Goodman CS, Artavanis-Tsakonas S (1990) slit: an extracellular protein necessary for development of midline glia and commissural axon pathways contains both EGF and LRR domains. Genes Dev 4:2169-2187.

Sabatier C, Plump AS, Le M, Brose K, Tamada A, Murakami F, Lee EY, Tessier-Lavigne M (2004) The divergent Robo family protein rig-1/Robo3 is a negative regulator of slit responsiveness required for midline crossing by commissural axons. Cell 117:157-169.

Sanders EJ, Walter MA, Parker E, Aramburo C, Harvey S (2003) Opticin binds retinal growth hormone in the embryonic vitreous. Invest Ophthalmol Vis Sci 44:5404-5409.

Sang Q, Wu J, Rao Y, Hsueh YP, Tan SS (2002) Slit promotes branching and elongation of neurites of interneurons but not projection neurons from the developing telencephalon. Mol Cell Neurosci 21:250-265.

Sanyal S, Hawkins RK (1979) Dysgenetic lens (dyl)--a new gene in the mouse. Invest Ophthalmol Vis Sci 18:642-645.

Schmitt AM, Shi J, Wolf AM, Lu CC, King LA, Zou Y (2006) Wnt-Ryk signalling mediates medial-lateral retinotectal topographic mapping. Nature 439:31-37.

Schulz MW, Chamberlain CG, de Iongh RU, McAvoy JW (1993) Acidic and basic FGF in ocular media and lens: implications for lens polarity and growth patterns. Development 118:117-126.

Seeger M, Tear G, Ferres-Marco D, Goodman CS (1993) Mutations affecting growth cone guidance in Drosophila: genes necessary for guidance toward or away from the midline. Neuron 10:409-426.

Semina EV, Reiter RS, Murray JC (1997) Isolation of a new homeobox gene belonging to the Pitx/Rieg family: expression during lens development and mapping to the aphakia region on mouse chromosome 19. Hum Mol Genet 6:2109-2116.

Semina EV, Murray JC, Reiter R, Hrstka RF, Graw J (2000) Deletion in the promoter region and altered expression of Pitx3 homeobox gene in aphakia mice. Hum Mol Genet 9:1575-1585.

Semina EV, Brownell I, Mintz-Hittner HA, Murray JC, Jamrich M (2001) Mutations in the human forkhead transcription factor FOXE3 associated with anterior segment ocular dysgenesis and cataracts. Hum Mol Genet 10:231-236.

Serafini T, Kennedy TE, Galko MJ, Mirzayan C, Jessell TM, Tessier-Lavigne M (1994) The netrins define a family of axon outgrowth-promoting proteins homologous to C. elegans UNC-6. Cell 78:409-424.

Shi X, Bosenko DV, Zinkevich NS, Foley S, Hyde DR, Semina EV, Vihtelic TS (2005) Zebrafish *pitx3* is necessary for nomal lens and retinal development. Mechanisms of Development 122:513-527.

Shi X, Luo Y, Howley S, Dzialo A, Foley S, Hyde DR, Vihtelic TS (2006) Zebrafish foxe3: roles in ocular lens morphogenesis through interaction with pitx3. Mech Dev 123:761-782.

Sidman RL (1961) Histogenesis of Mouse Retina Studied with Thymidine-H3 (ed. G. K. Smelser). New York: Academic Press:487-506.

Silver J (1984) Studies on the factors that govern directionality of axonal growth in the embryonic optic nerve and at the chiasm of mice. J Comp Neurol 223:238-251.

Silver J, Sidman RL (1980) A mechanism for the guidance and topographic patterning of retinal ganglion cell axons. J Comp Neurol 189:101-111.

Simpson JH, Bland KS, Fetter RD, Goodman CS (2000a) Short-range and long-range guidance by Slit and its Robo receptors: a combinatorial code of Robo receptors controls lateral position. Cell 103:1019-1032.

Simpson JH, Kidd T, Bland KS, Goodman CS (2000b) Short-range and long-range guidance by slit and its Robo receptors. Robo and Robo2 play distinct roles in midline guidance. Neuron 28:753-766.

Snow DM, Watanabe M, Letourneau PC, Silver J (1991) A chondroitin sulfate proteoglycan may influence the direction of retinal ganglion cell outgrowth. Development 113:1473-1485.

Song HJ, Ming GL, Poo MM (1997) CAMP-induced switching in turning direction of nerve growth cones. Nature 388:275-279.

Song HJ, Ming G, He Z, Lehmann M, McKerracher L, Tessier-Lavigne M, Poo M (1998) Conversion of neuronal growth cone responses from repulsion to attraction by cyclic nucleotides. Science 281:1515-1518.

Sowden JC, Holt JK, Meins M, Smith HK, Bhattacharya SS (2001) Expression of Drosophila omb-related T-box genes in the developing human and mouse neural retina. Invest Ophthalmol Vis Sci 42:3095-3102.

Steigemann P, Molitor A, Fellert S, Jackle H, Vorbruggen G (2004) Heparan sulfate proteoglycan syndecan promotes axonal and myotube guidance by slit/robo signaling. Curr Biol 14:225-230.

Stein E, Tessier-Lavigne M (2001) Hierarchical organization of guidance receptors: silencing of netrin attraction by slit through a Robo/DCC receptor complex. Science 291:1928-1938.

Steinbach K, Volkmer H, Schlosshauer B (2002) Semaphorin 3E/collapsin-5 inhibits growing retinal axons. Exp Cell Res 279:52-61.

Stevens A, Jacobs JR (2002) Integrins regulate responsiveness to slit repellent signals. J Neurosci 22:4448-4455.

Stier H, Schlosshauer B (1995) Axonal guidance in the chicken retina. Development 121:1443-1454.

Stone KE, Sakaguchi DS (1996) Perturbation of the developing Xenopus retinotectal projection following injections of antibodies against beta1 integrin receptors and N-cadherin. Dev Biol 180:297-310.

Sundaresan V, Mambetisaeva E, Andrews W, Annan A, Knoll B, Tear G, Bannister L (2004) Dynamic expression patterns of Robo (Robo1 and Robo2) in the developing murine central nervous system. J Comp Neurol 468:467-481.

Tamagnone L, Artigiani S, Chen H, He Z, Ming GI, Song H, Chedotal A, Winberg ML, Goodman CS, Poo M, Tessier-Lavigne M, Comoglio PM (1999) Plexins are a large family of receptors for transmembrane, secreted, and GPI-anchored semaphorins in vertebrates. Cell 99:71-80.

Tear G, Harris R, Sutaria S, Kilomanski K, Goodman CS, Seeger MA (1996) commissureless controls growth cone guidance across the CNS midline in Drosophila and encodes a novel membrane protein. Neuron 16:501-514.

Thisse B, Thisse C (2005) Functions and regulations of fibroblast growth factor signaling during embryonic development. Dev Biol 287:390-402.

Thompson H, Camand O, Barker D, Erskine L (2006) Slit proteins regulate distinct aspects of retinal ganglion cell axon guidance within dorsal and ventral retina. J Neurosci 26:8082-8091.

Thut CJ, Rountree RB, Hwa M, Kingsley DM (2001) A large-scale in situ screen provides molecular evidence for the induction of eye anterior segment structures by the developing lens. Dev Biol 231:63-76.

Trousse F, Marti E, Gruss P, Torres M, Bovolenta P (2001) Control of retinal ganglion cell axon growth: a new role for Sonic hedgehog. Development 128:3927-3936.

Trowe T, Klostermann S, Baier H, Granato M, Crawford AD, Grunewald B, Hoffmann H, Karlstrom RO, Meyer SU, Muller B, Richter S, Nusslein-Volhard C, Bonhoeffer F (1996) Mutations disrupting the ordering and topographic mapping of axons in the retinotectal projection of the zebrafish, Danio rerio. Development 123:439-450.

Tuttle R, Braisted JE, Richards LJ, O'Leary DD (1998) Retinal axon guidance by region-specific cues in diencephalon. Development 125:791-801.

Varnum DS, Stevens LC (1968) Aphakia, a new mutation in the mouse. J Hered 59:147-150.

Vogel A, Rodriguez C, Izpisua-Belmonte JC (1996) Involvement of FGF-8 in initiation, outgrowth and patterning of the vertebrate limb. Development 122:1737-1750.

Wagner E, McCaffery P, Drager UC (2000) Retinoic acid in the formation of the dorsoventral retina and its central projections. Dev Biol 222:460-470.

Walz A, Anderson RB, Irie A, Chien CB, Holt CE (2002) Chondroitin sulfate disrupts axon pathfinding in the optic tract and alters growth cone dynamics. J Neurobiol 53:330-342.

Walz A, McFarlane S, Brickman YG, Nurcombe V, Bartlett PF, Holt CE (1997) Essential role of heparan sulfates in axon navigation and targeting in the developing visual system. Development 124:2421-2430.

Wang B, Xiao Y, Ding BB, Zhang N, Yuan X, Gui L, Qian KX, Duan S, Chen Z, Rao Y, Geng JG (2003) Induction of tumor angiogenesis by Slit-Robo signaling and inhibition of cancer growth by blocking Robo activity. Cancer Cell 4:19-29.

Wang KH, Brose K, Arnott D, Kidd T, Goodman CS, Henzel W, Tessier-Lavigne M (1999) Biochemical purification of a mammalian slit protein as a positive regulator of sensory axon elongation and branching. Cell 96:771-784.

Webber CA, Hyakutake MT, McFarlane S (2003) Fibroblast growth factors redirect retinal axons in vitro and in vivo. Dev Biol 263:24-34.

Webber CA, Hocking JC, Yong VW, Stange CL, McFarlane S (2002) Metalloproteases and guidance of retinal axons in the developing visual system. J Neurosci 22:8091-8100.

Weiner JA, Koo SJ, Nicolas S, Fraboulet S, Pfaff SL, Pourquie O, Sanes JR (2004) Axon fasciculation defects and retinal dysplasias in mice lacking the immunoglobulin superfamily adhesion molecule BEN/ALCAM/SC1. Mol Cell Neurosci 27:59-69.

Whitford KL, Marillat V, Stein E, Goodman CS, Tessier-Lavigne M, Chedotal A, Ghosh A (2002) Regulation of cortical dendrite development by Slit-Robo interactions. Neuron 33:47-61.

Williams SE, Mann F, Erskine L, Sakurai T, Wei S, Rossi DJ, Gale NW, Holt CE, Mason CA, Henkemeyer M (2003) Ephrin-B2 and EphB1 mediate retinal axon divergence at the optic chiasm. Neuron 39:919-935.

Wu JY, Feng L, Park HT, Havlioglu N, Wen L, Tang H, Bacon KB, Jiang Z, Zhang X, Rao Y (2001) The neuronal repellent Slit inhibits leukocyte chemotaxis induced by chemotactic factors. Nature 410:948-952.

Wu W, Wong K, Chen J, Jiang Z, Dupuis S, Wu JY, Rao Y (1999) Directional guidance of neuronal migration in the olfactory system by the protein Slit. Nature 400:331-336.

Yamamoto Y, Jeffery WR (2000) Central role for the lens in cave fish eye degeneration. Science 289:631-633.

Yamamoto Y, Stock DW, Jeffery WR (2004) Hedgehog signalling controls eye degeneration in blind cavefish. Nature 431:844-847.

Yao J, Sasaki Y, Wen Z, Bassell GJ, Zheng JQ (2006) An essential role for beta-actin mRNA localization and translation in Ca2+-dependent growth cone guidance. Nat Neurosci 9:1265-1273.

Yeo SY, Miyashita T, Fricke C, Little MH, Yamada T, Kuwada JY, Huh TL, Chien CB, Okamoto H (2004) Involvement of Islet-2 in the Slit signaling for axonal branching and defasciculation of the sensory neurons in embryonic zebrafish. Mech Dev 121:315-324.

Yoshikawa S, McKinnon RD, Kokel M, Thomas JB (2003) Wnt-mediated axon guidance via the Drosophila Derailed receptor. Nature 422:583-588.

Yuan SS, Cox LA, Dasika GK, Lee EY (1999a) Cloning and functional studies of a novel gene aberrantly expressed in RB-deficient embryos. Dev Biol 207:62-75.

Yuan W, Zhou L, Chen JH, Wu JY, Rao Y, Ornitz DM (1999b) The mouse SLIT family: secreted ligands for ROBO expressed in patterns that suggest a role in morphogenesis and axon guidance. Dev Biol 212:290-306.

Zallen JA, Yi BA, Bargmann CI (1998) The conserved immunoglobulin superfamily member SAX-3/Robo directs multiple aspects of axon guidance in C. elegans. Cell 92:217-227.

Zelina P, Avci HX, Thelen K, Pollerberg GE (2005) The cell adhesion molecule NrCAM is crucial for growth cone behaviour and pathfinding of retinal ganglion cell axons. Development 132:3609-3618.

Zhang F, Lu C, Severin C, Sretavan DW (2000) GAP-43 mediates retinal axon interaction with lateral diencephalon cells during optic tract formation. Development 127:969-980.

Zhang J, Jin Z, Bao ZZ (2004) Disruption of gradient expression of Zic3 resulted in abnormal intra-retinal axon projection. Development 131:1553-1562.

Zhao S, Chen Q, Hung FC, Overbeek PA (2002) BMP signaling is required for development of the ciliary body. Development 129:4435-4442.

Zheng JQ (2000) Turning of nerve growth cones induced by localized increases in intracellular calcium ions. Nature 403:89-93.

Zhu Y, Li H, Zhou L, Wu JY, Rao Y (1999) Cellular and molecular guidance of GABAergic neuronal migration from an extracortical origin to the neocortex. Neuron 23:473-485.

Zinn KM (1970) Changes in corneal ultrastructure resulting from early lens removal in the developing chick embryo. Invest Ophthalmol 9:165-182.

Zou Y, Lyuksyutova AI (2007) Morphogens as conserved axon guidance cues. Curr Opin Neurobiol 17:22-28.

Zou Y, Stoeckli E, Chen H, Tessier-Lavigne M (2000) Squeezing axons out of the gray matter: a role for slit and semaphorin proteins from midline and ventral spinal cord. Cell 102:363-375.

# 8 Publications resulting from this work

Thompson H, Barker D, Camand O, Erskine L (2006a) Slits contribute to the guidance of retinal ganglion cell axons in the mammalian optic tract. Dev Biol 296:476-484.

Thompson H, Camand O, Barker D, Erskine L (2006b) Slit proteins regulate distinct aspects of retinal ganglion cell axon guidance within dorsal and ventral retina. J Neurosci 26:8082-8091.